THE JOURNAL
OF
CHEMICAL PHYSICS

VOLUME 9 SEPTEMBER, 1941 NUMBER 9

The X-Ray Diffraction Pattern of Tricalcium Aluminate

LYNN J. BRADY AND WHEELER P. DAVEY
The Pennsylvania State College, State College, Pennsylvania

(Received May 13, 1941)

Using a new type of x-ray diffraction apparatus, the diffraction pattern of high purity tricalcium aluminate, ($3CaO \cdot Al_2O_3$), has been recorded automatically in the form of a graph of intensity *vs.* angle. The unit cube containing 264 atoms has an edge of 15.235A.

REPEATED attempts have been made to determine the crystal structure of tricalcium aluminate ($3CaO \cdot Al_2O_3$) (1–2–3–4–5). Its complete x-ray diffraction pattern is, therefore, of interest. It is known to be optically isotropic, so its crystals must have cubic symmetry. No method is known by which crystals can be made large enough to permit goniometric measurements. It is the purpose of this paper to give the diffraction pattern of tricalcium aluminate in a more complete form than seems to be given so far in the literature. This is necessary before a solution of its structure can be found.

Although previous workers have agreed on the position of the strongest lines in the diffraction pattern, no two workers have agreed on the intensity, the position, or the number of the weaker lines, nor have they agreed on the intensities of the stronger lines.

Harrington[1] found a number of lines in his powder photographs which could not be accounted for on the basis of a cubic crystal having an edge of 7.62A. He assumed, therefore, that this compound was only pseudo-cubic. Examination of his published data shows, however, that all his lines fit a cube whose edge is 15.24A.

Steele and Davey[2] found, in addition to the lines characteristic of a body-centered cube, three faint lines in their photographs which they were able to account for qualitatively on the basis of a unit cube of edge 7.62A. On this basis they proposed a structure which obviously cannot be correct if the edge of the unit cube is 15.24A.

Kondo and Yamauchi[3] and Solacolu[4] while proposing no structure agreed that the length of the edge of the unit crystal was approximately 15.2A.

Lagerqvist, Wallmark, and Westgren[5] found so many lines in their photographs that they had to assume the length of the unit cell to be 15.22A in order to account for all of them. They found their lines to match portions of a simple cubic pattern, but they have not, as yet, proposed a structure.

It is evident from the above that, if we are to arrive at a tenable solution of the structure of $3CaO \cdot Al_2O_3$, specimens must be of high enough

[1] E. A. Harrington, Am. J. Sci. **13**, 467 (1927).

[2] F. A. Steele and W. P. Davey, J. Am. Chem. Soc. **51**, 2283 (1929).

[3] S. Kondo and T. Yamauchi, J. Japan. Ceram. Assoc. **42**, 313 (1934).

[4] S. Solacolu, J. Japan. Ceram. Assoc. **42**, 319 (1934).

[5] K. Lagerqvist, S. Wallmark, and A. Westgren, Zeits f. anorg. allgem. Chemie **234**, 1 (1937).

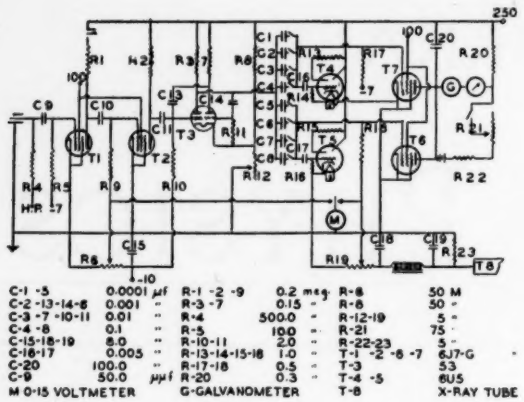

FIG. 1. Recorder circuit.

purity to justify precise determination of the diffraction patterns.

PREPARATION OF SAMPLES

Early in the course of this work attempts were made to make tricalcium aluminate using the technique of Lagerqvist, Wallmark, and Westgren. These workers fused 75 mole percent CaO and 25 mole percent Al_2O_3 together, using the oxyhydrogen blowpipe. The fused mass was then ground and heated at 1000°C for a period of ten days. Although their published procedure was followed carefully, the petrographic microscope showed that anisotropic material was present at the end of the twelfth day of heating at 1000°C.

Shepherd, Rankin, and Wright[6] showed that when $3CaO \cdot Al_2O_3$ is formed from the melt, crystals of the tricalcium aluminate frequently surround particles of CaO, with the consequent local formation of $5CaO \cdot 3Al_2O_3$. They further showed that a period of 21 days of heating at 1400°C is necessary to secure complete elimination of CaO and $5CaO \cdot 3Al_2O_3$.

In the present work, the starting materials for the formation of all the calcium aluminates were prepared by separately igniting precipitated chalk and "Bakers" analyzed aluminum oxide in platinum dishes at 1000°C for six hours. The resulting CaO and Al_2O_3 were ground and thoroughly mixed in the ratios of 3–1, 5–3, 1–1, and 3–5. These mixtures were fused at least once and were then ground to fine powders. Each of these specimens was subjected to several cycles of sintering and grinding, as in the work of Steele and Davey. A final purification was made on the basis of density, using methylene iodide and mesitilene. The resulting four purified products were examined for homogeneity under a petrographic microscope and their refractive indices determined. The identities of these specimens were considered to be established when they showed the accepted densities and refractive indices.

APPARATUS

The diffraction pattern was measured by means of a Geiger-Müller counter. The Geiger-Müller circuits such as Gingrich, Evans, and Edgerton[7] have developed are well adapted to x-ray measurements where the x-ray tube is operated under constant, or nearly constant, conditions. However, to make a circuit universally adaptable it should be made independent of fluctuations in the source due to changing line voltages on the x-ray filament transformer. Such a modified circuit, completely a.c. operated, was constructed which records the average intensities of the x-ray beams with a recording galvanometer.[8]

In this circuit pulses from the Geiger-Müller counter are amplified by two 6J7-G tubes in series to secure larger, more nearly uniform, pulses. These pulses are then converted to a uniform size by means of the relaxation oscillator type circuit. Pulses from the uniform pulse generator are amplified and fed into a so-called "tank" condenser having a fixed high resistance

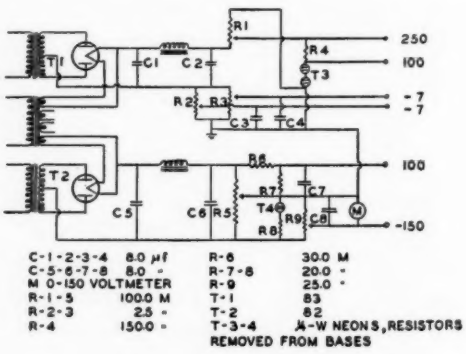

FIG. 2. Power circuits.

[6] E. S. Shepherd, G. A. Rankin, and F. E. Wright, Am. J. Sci. **28**, 293 (1909).

[7] N. S. Gingrich, R. D. Evans, and H. E. Edgerton, Rev. Sci. Inst. **7**, 451 (1936).

[8] L. J. Brady, Phys. Rev. **55**, 1133 (1939).

leak. The potential of the condenser is thus a measure of the average rate of arrival of x-ray quanta at the Geiger-Müller counter. This potential is then recorded by a recording galvanometer in terms of the current leaking off the condenser through the resistance.

The complete circuit is given in Fig. 1.

It will be seen that the circuit of Gingrich, Evans and Edgerton has been altered to include an additional tube, (T-6), in the vacuum tube voltmeter circuit. This is added to make the average output current independent of fluctuating line voltages on the x-ray filament transformer. It will be observed that, as the current through the x-ray tube increases, the grid bias on the tube (T-6) increases proportionally with a consequent decrease of current delivered per pulse by this tube to the electrical tank, (C-20). Since the rate of the Geiger-Müller pulses increases nearly linearly with increasing current through the x-ray tube it is apparent that by adjusting R-19, and by suitably choosing the sizes of the input condensers to the tube (T-6), and (T-7), a setting can be reached such that fluctuations of the x-ray filament transformer line voltages will not cause appreciable variations in the output current. Two electric "eyes" (T-4), and (T-5) have been placed in the circuit in the manner shown. These tubes serve as scales, so that settings of R-19 and the input condensers which have given the desired results can be duplicated at will.

The power circuits and the Lifschutz high potential circuit are shown in Fig. 2 and Fig. 3, respectively.

The fact that the output current has been made independent of the current through the x-ray tube removes the last objection to a completely automatic x-ray diffraction apparatus.

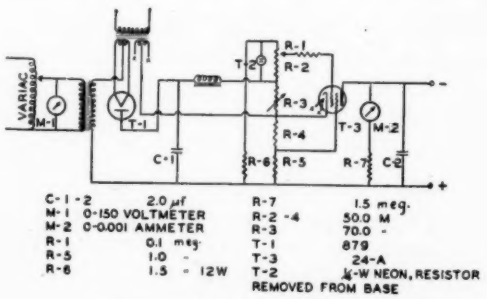

FIG. 3. High potential circuits.

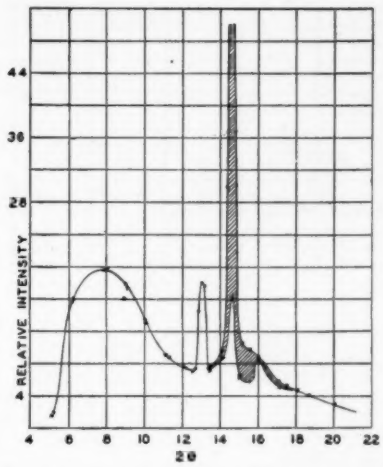

FIG. 4. Balanced filter diffraction—NaCl crystal. ●—ZrO_2; ×—SrO. Mo x-ray tube—43 kv peak, 10 ma.

The Geiger-Müller counter and the first amplifier are mounted on the movable arm of an x-ray spectrometer. This arm is driven over the desired range by means of a synchronous motor and a system of worm gears. This keeps the rotation of the arm rigorously in step with the recording galvanometer. Obviously, then, the galvanometer gives a record of x-ray intensities *vs.* angle.

Molybdenum $K\alpha$ radiation was used in conjunction with balanced filters of ZrO_2 and SrO. These filters were constructed jointly with P. H. Bell of The Pennsylvania State College. The close balance obtained is shown in Fig. 4, in which the shaded area represents the difference between the transmission of the two filters.

Six diffraction patterns of tricalcium aluminate were obtained using filters of ZrO_2 and SrO on alternate runs. Because of the randomness of the x-ray quanta registered by the counter, and because the apparatus used has an exponentially decaying memory, the galvanometer record of x-ray intensities shows considerable statistical deviations. To minimize this as far as is practical the width of the slit system might be increased. But previous workers have reported many lines relatively close together in the diffraction pattern, so it is obvious that the slit width should be kept as small as possible. If the number of readings at a given angle is increased, the actual intensity of the diffraction may be obtained by the method of averages. The same results may be obtained, however, if the angular rate of rotation of the spectrometer arm is made very

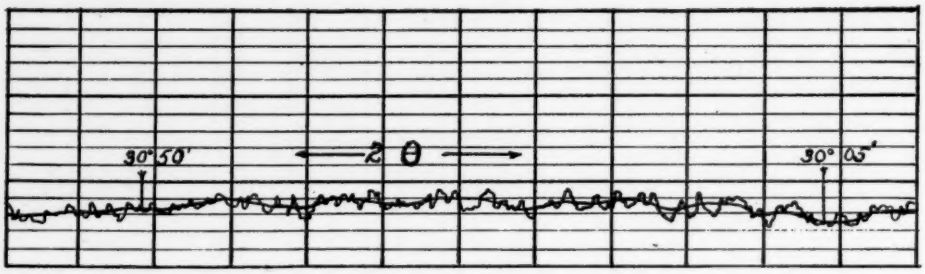

FIG. 5. A short portion of a typical diffraction record.

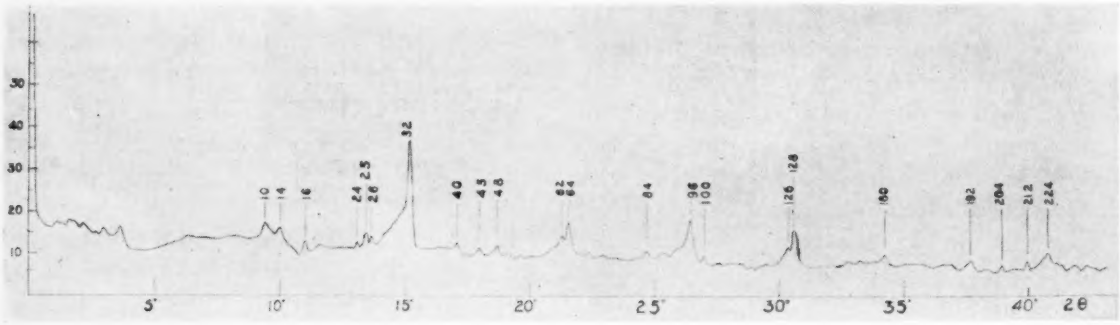

FIG. 6. The diffraction pattern of $3CaO \cdot Al_2O_3$. (The numbers directly above the peaks refer to $h^2+k^2+l^2$.)

slow and a smooth line drawn through the recorded diffraction pattern. It is this method which is used in this work.

A very short portion (angular length $2\theta=1$ degree) of a typical diffraction pattern is shown in Fig. 5. Reference to Fig. 6 shows that Fig. 5 actually represents portions of the diffraction peaks corresponding to $h^2+k^2+l^2=126$ and 128.

The average intensities, as measured by the heights of the diffraction record above the zero of ordinates, are determined for both sets of filters at intervals of one minute of arc 2θ. The differences of the averages are plotted point by point on a scale for 2θ much smaller than the original record and a smooth line is drawn through the points. On drawing this smooth line apparent "peaks" which obviously do not have the characteristics demanded by the slit widths are ignored.

The complete diffraction pattern is shown in Fig. 6. The left end of the pattern up to about $2\theta=4$ degrees shows the shadow effect of the slits. It is apparent that many portions of the pattern contain unresolved lines, the most notable of these being in the vicinity of $2\theta=14$ to 15 degrees. Similar studies of the diffraction patterns of the three other calcium aluminates shows that no peak in the diffraction pattern of Fig. 6 for tricalcium aluminate can possibly belong to the diffraction pattern of one of the other compounds. In addition to the unresolved and partly resolved lines just mentioned, Fig. 6 shows 22 clearly resolved lines within an angular range of $2\theta=42°$. A simple cubic structure would require, within an angular range of $2\theta=10°$, 12 additional lines. Any structure proposed for tricalcium aluminate must therefore account quantitatively for the absence of the 12 "forbidden" lines, as well as for the presence of the 22 lines of Fig. 6. The edge of the unit cube demanded by the lines shown in Fig. 6 is 15.235A. A smaller unit of structure cannot possibly account for a large number of the lines in the diffraction pattern, while no lines present require a larger unit cell. On the basis of its density and the size of the unit crystal the chemical formula of this compound is $(3CaO \cdot Al_2O_3)_{24}$. This means there are 72 Ca, 48 Al, and 144 O, a total of 264 atoms, in the unit cell.

A highly probable structure has been found which accounts for the x-ray dots and which predicts the peculiar properties of $3CaO \cdot Al_2O_3$. It will be published elsewhere.

The Raman Spectra of Mono- and Dichlorobenzenes†

H. SPONER AND J. S. KIRBY-SMITH*
Department of Physics, Duke University, Durham, North Carolina
(Received June 9, 1941)

Raman spectra were taken of gaseous mono- and dichlorobenzenes. Polarization measurements were made for the dichlorobenzenes in the liquid phase. Interpretations of the stronger lines are given in terms of modes of vibration. The experimental results and assignments of the frequencies are collected in Tables I–IV.

INTRODUCTION

THE Raman spectra of the different chlorobenzenes have been thoroughly studied in the liquid state by a number of investigators.[1] Polarization measurements have been carried out in the case of monochlorobenzene by Simons.[2] In the course of an analysis of the ultraviolet absorption spectra of mono-[3] and the dichlorobenzenes[4] it became desirable to have their vibrational frequencies in the gaseous phase. For this reason these compounds have been reinvestigated in the vapor phase. To facilitate interpretation of the observed frequencies polarization measurements were made for the dichlorobenzenes in the liquid state.

EXPERIMENTAL

A. Measurements in the gas

The substances used in this investigation, monochlorobenzene, ortho-, meta-, and para-dichlorobenzene, were kindly furnished by the Chemistry Department.‡ They were extremely pure, and were carefully introduced into the Raman tubes by vacuum distillation.

The apparatus used, except for modifications in the assembly of Raman tube and filter jacket, has been previously described.[5] Certain changes have been made necessary in order to attain the relatively high temperatures (200°C in the case of the dichlorobenzenes) needed to give sufficient vapor pressures for adequate scattered intensities, and at the same time permit suitable filters to be employed. This condition was attained by placing an extra glass cylinder between the filter jacket and Raman tube. Strong blasts of hot air were directed between this cylinder and the Raman tube and the scattering section of the tube was heated to the desired temperature. The space between the filter jacket and the wall of the extra cylinder served as an insulating air space and prohibited an excessive loss of heat to the circulating filter solution. The bottom section of the tube was heated by resistance coils which were wrapped around it. Temperatures were read with a thermocouple placed in contact with the coolest portion of the Raman tube. With this arrangement temperatures up to 220°C have been maintained at fairly constant values (±5°C) during all exposure times.

Twelve Hg arcs were used as the light source, excitation being by the 4047 and 4358A lines together as well as by 4358 alone. Filters were aqueous solutions of $CoCl_2$ when excitation by both lines was desired, and $CoCl_2$+quinine for the isolation of 4358. All spectra have been obtained upon antihalation Eastman Super Panchro Press or Ilford Hypersensitive Panchromatic plates. Exposure times have been from 6 to 24 hours. The spectrograph is the Zeiss 3 prism instrument used in previous work.

† Presented before the Division of Physical and Inorganic Chemistry of the American Chemical Society at Detroit, September, 1940.

* Present address: National Institute of Health, Bethesda, Maryland.

[1] A. Dadieu, A. Pongratz and K. W. F. Kohlrausch, Monats. f. Chem. **61**, 426 (1932); J. W. Murray and D. H. Andrews, J. Chem. Phys. **1**, 406 (1933). Complete references may be found in the second book of K. W. F. Kohlrausch, *Der Smekal-Raman Effekt*, Erg. Bd. (Julius Springer, Berlin, 1938), or in James H. Hibben, *The Raman Effect and its Chemical Applications* (Reinhold Publishing Corporation, New York, 1939).

[2] L. Simons, Soc. Sci. Fennica, Comm. Phys.-Math. **6**, No. 13 (1932).

[3] H. Sponer and S. H. Wollman, Phys. Rev. **57**, 1078A (1940).

[4] S. H. Wollman, unpublished results.

‡ We are indebted to Dr. Eunice Moore for the courtesy of providing us with the substances.

[5] J. S. Kirby-Smith and L. G. Bonner, J. Chem. Phys. **7**, 880 (1939).

TABLE I. C_6H_5Cl.

GAS	LIQUID (ANANTHAKRISHNAN)	DEPOLARIZATION FACTOR (SIMONS)	ASSIGNMENT
200 (*w*)	196 (6*b*)	0.87	(β_1)
	270 (1/2)		
	295 (2)	0.86	
416 (*m*)	420 (6)	0.32	α_1
608 (*w*)	615 (3)	0.89	β_1
703 (*m*)	702 (6)	0.13	α_1
	742 (0)		
	790 (0)		
	830 (0)		
	925 (0)		
	989 (0)		
1001 (*st*)	1003 (10*s*)	0.06	α_1
	1013 (00)		
1024 (*m*)	1024 (7)	0.19	α_1
1080 (*m*)	1084 (5)	0.10	α_1
1134 (*w*)	1121 (1/2)		(α_1)
1191 (*w*)	1158 (1/2)	0.88	(β_1)
	1176 (1/2)		
	1295 (0)		
	1321 (0)		
	1372 (0)		
	1443 (0)		
	1565 (0)		
1589 (*m*)	1584 (4)	0.87	β_1
	3008 (5)		
	3028 (0)		
3079 (*st b*)	3068 (10*b*)	0.32	α_1
	3140 (0)		
3180 (*w*)	3165 (1)		

TABLE II. *o*-$C_6H_4Cl_2$.

GAS	LIQUID (SWAINE AND MURRAY)	DEPOLARIZATION FACTOR	ASSIGNMENT
	154 (10)	0.8	
194 (*w*)	203 (3)	0.8	
	239 (1*b*)	0.8	
300 (*m*)	330 (0*b*)		
434 (*vw*)	430 (1)	0.8	
	469 (1)		
487 (*m*)	483 (2)	0.45	α_1
664 (*m*)	658 (5)	0.35	α_1
760 (*w*)	756 (0*b*)		
	860 (1*b*)		
	1020 (1)		
1035 (*st*)	1041 (10)	0.20	α_1
1133 (*st*)	1129 (5)	0.25	α_1
	1160 (1*b*)	dep	(β_1)
1271 (*w*)	1274 (1*b*)		
1598 (*w*)	1577 (4)	0.8	β_1
	1607 (0*b*)		
	2994 (1)		
3082 (*st*)	3073 (10)	0.40	α_1
3150 (*w*)	3146 (3)		

TABLE III. *m*-$C_6H_4Cl_2$.

GAS	LIQUID (SWAINE AND MURRAY)	DEPOLARIZATION FACTOR	ASSIGNMENT
	178 (3)	0.9	
205 (*wb*)	202 (3)	0.9	
	216 (2)		
356 (*w*)	366 (1)		
399 (*m*)	399 (4*b*)	0.10	α_1
	428 (2)	0.6	
613 (*vw*)	530 (0)		
665 (*m*)	666 (4)	0.25	α_1
998 (*st*)	999 (10)	0.20	α_1
	1018 (0)		
1056 (*m vb*)	1070 (3*b*)	0.30	
	1109 (2)		
1129 (*m*)	1126 (4)	0.10	α_1
	(1160 Kohlrausch)	dep	(β_1)
	1240 (0)		
	1425 (0)		
	1456 (0)		
	1544 (0)		
1590 (*m*)	1579 (5*b*)	0.8	β_1
	1625 (0)		
3090 (*st*)	3076 (10)	0.45	α_1
3169 (*w*)	3152 (2)		

B. Polarization measurements

The apparatus used here was of conventional type, using a sensibly parallel beam of unpolarized light as the incident radiation. The light source consisted of two small (15 cm long) Hg arcs similar in design to those used in the gas apparatus. Glass cylinders filled with filter solution focused and directed a strong beam of filtered light into the scattering tube. The source operated in a vertical position, and a totally reflecting glass prism was used to direct the scattered light into the polarizing system. This consisted of the usual Wollaston prism, a lens for focusing the two polarized components onto the spectrograph slit, and a half-wave plate. This arrangement gave good pictures in from 3 to 8 hours exposure time.

Under present conditions precise measurements have not been made. Density marks for the calibration of plates and the determination of relative intensities have not been put on all plates. The non-parallel character of the incident beam and imperfections in the half-wave plate are the other main sources of error.

RESULTS

The present results including the assignment of frequencies as well as previous liquid and polarization data are summarized in Tables I to IV. The most recently published values have been taken.[6] Intensities have been determined from microphotometer curves. However, due to the

[6] J. W. Swaine and J. W. Murray, J. Chem. Phys. **1**, 512 (1933); R. Ananthakrishnan, Proc. Ind. Acad. Sci. **3A**, 52 (1936).

relatively greater amount of Rayleigh scattering and general background inherent in gases these intensities are only estimated as strong (*st*), medium (*m*), weak (*w*) and very weak (*vw*).

While nothing has to be added to the tables for the dichlorobenzenes, it should be mentioned that for monochlorobenzene additional extremely weak, broad and diffuse lines have been observed at 275 and 500 cm^{-1}. These lines appear only on several plates, and then with such small intensity that they could be spurious.

The measurement of the frequency in the neighborhood of 200 cm^{-1} was taken as an anti-Stokes transition from Hg 4047. As a Stokes line from Hg 4047 it is masked by the strong Hg 4077 and from Hg 4358 by the Hg II line at 4398.6A. The 200 frequency is usually measured from the Hg 4358 line in the liquid, as under these conditions the spark line is too weak for detection.

A definite diffuse wing on the low frequency edge of the strong 3079 cm^{-1} line has been observed on all plates. Attempts to resolve any structure were unsuccessful.

Discussion of Results

For convenience in discussing the frequencies of the investigated benzene chlorides Fig. 1 has been included which represents the different types of vibration in the benzene molecule.[7] The symmetry D_{6h} of benzene is reduced to V_h in *p*-dichlorobenzene, and to C_{2v} in *o*- and *m*-dichlorobenzene and monochlorobenzene. The symmetries of the different vibrations of the substituted benzenes are represented in Tables V to VII.

The symmetry symbols are listed in Placzek's notation.[8] C_2^y, etc. refer to twofold axes in the *y*, etc., direction, σ_z denotes a plane of reflection perpendicular to the *z* axis (molecular plane), and *i* refers to the center of symmetry. The + and − signs indicate respectively that a given symmetry class is symmetric or antisymmetric to the noted symmetry element. The asterisk at the symbol of C_{2v} for the ortho-compound indicates that the twofold symmetry axis passes here between the two carbons having the substituents. Small Greek letters have been used for the symmetry symbols to distinguish them from the same symbols with capital Latin letters for elec-

Table IV. *p*-$C_6H_4Cl_2$.

Gas	Liquid (Swaine and Murray)	Depolarization Factor	Assignment
	302 (4)	0.8	β_{2g}
326 (*w*)	333 (8)	0.5	α_{1g}
386 (*w*)	355 (1)		
	627 (5)	0.8	β_{2g}
	710 (00)		
742 (*st*)	748 (10*b*)	0.2	α_{1g}
	885 (0)		
	942 (0)		
1050 (*m*)	1070 (3)	0.5	(α_{1g})
	1087 (2)		
1110 (*st*)	1109 (10)	0.4	α_{1g}
	1170 (1)		
	1217 (0)		
1300 (*vw b*)	1294 (0)		
	1331 (0)		
1440 (*vw b*)	1379 (0)		
1570 (*m*)	1576 (8)	0.8	β_{2g}
	1630 (1)		
	2953 (0)		
3090 (*st*)	3079 (10)	0.4	α_{1g}
	3153 (2)		

[7] Vibration types after Langseth and Lord, reference 9.

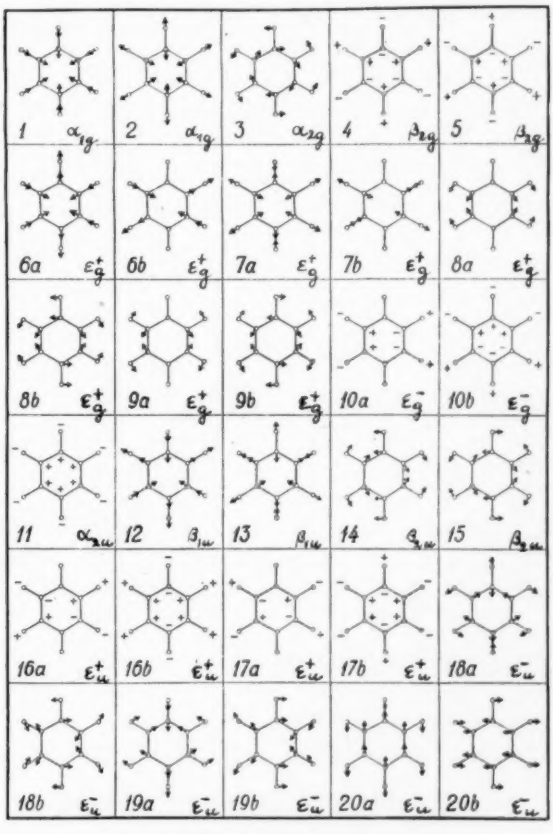

Fig. 1. Types of vibrations in benzene.

[8] G. Placzek, *Handbuch d. Radiologie*, Bd. **VI/2** (Leipzig, 1934), p. 283; L. Tisza, Zeits. f. Physik **82**, 285 (1932).

TABLE V. *Symmetries of vibrations for para-*$C_6H_4Cl_2$ *in group* V_h.

Symmetry	Essential Symmetry Elements C_{2y}	C_{2z}	i	Number of Vibrations	Selection Rules Raman	Infra-Red
α_{1g}	+	+	+	6	+	−
α_{1u}	+	+	−	2	−	−
β_{1g}	+	−	+	1	+	−
β_{1u}	+	−	−	5	−	+
β_{2g}	−	+	+	5	+	−
β_{2u}	−	+	−	3	−	+
β_{3g}	−	−	+	3	+	−
β_{3u}	−	−	−	5	−	+

tronic terms. Langseth and Lord[9] have discussed in the case of the deuterated benzenes which symmetry classes of the group D_{6h} go over into the respective classes of C_{2v} and V_h.

Monochlorobenzene

As can be seen from Table I, only the strong lines of the liquid have been observed in the gaseous phase. Most of them are totally symmetrical vibrations as is indicated in the last column under "Assignment."

The frequencies 416 and 608 correspond to the ϵ_g^+ vibration of 606 cm^{-1} in benzene[10] (No. 6 in Fig. 1). According to polarization measurements[2] the 416 is totally symmetrical and the 608 non-totally symmetrical. As already pointed out by Kohlrausch[11] the non-totally symmetrical vibration is very nearly independent of the substitution because here the motion of the carbon atom with the substituent is small and perpendicular to the C−Cl bond. The totally symmetric vibration, however, is strongly influenced because the carbon atom attached to the chlorine participates in the vibration.

The 703 represents the vibration of the chlorine atom towards the ring. It is totally symmetrical and originates out of the four 3000 cm^{-1} hydrogen vibrations in benzene α_{1g}, β_{1u}, ϵ^+_g and ϵ^-_u (Nos. 2, 13, 7, 20 in Fig. 1). The last two split in the monosubstituted benzenes into a totally symmetrical (α_1) and a non-totally symmetrical (β_1) part. We have, of course, to consider here only the α_1 vibrations. It has no meaning to correlate the 703 to a particular one of the four totally symmetrical vibrations since it will in reality have contributions from all of them. The observed frequency 3079 cm^{-1} has to be assigned to the remaining hydrogen vibrations. It is sharp on the short wave side and diffuse on the other, and may well cover two lines. The frequency of 3180 cm^{-1} is probably due to an overtone.

The strong lines at 1001, 1024, and 1080 cm^{-1} are all totally symmetrical according to polarization measurements.[2] They are believed to correspond to the carbon vibrations α_{1g}, β_{1u} and probably ϵ^-_u in benzene (Nos. 1, 12, 19 in Fig. 1). One should expect one of the three carbon frequencies β_{2u}, ϵ^+_g and ϵ^-_u (Nos. 14, 8 and 19 in Fig. 1) to decrease considerably in monochlorobenzene and this is probably the ϵ^-_u. A detailed correlation of the observed frequencies cannot be made because they will be linear combinations of all three modes of vibrations α_{1g}, β_{1u} and ϵ^-_u, particularly since the frequencies are almost identical.

The line at 1589 cm^{-1} is probably one of the components that arise from the carbon vibration $\epsilon^+_g = 1596$ in benzene (No. 8 in Fig. 1) when the degeneracy is released. As the line is found highly depolarized it must represent the non-totally symmetrical mode of vibration.

The line at 1134 cm^{-1} belongs quite likely to a hydrogen vibration, as does perhaps the 1191 line. The latter may correspond to the depolarized line 1158 or the 1176 in the liquid. To find an interpretation we consider the six hydrogen vibrations of benzene α_{2g}, β_{2u}, ϵ^+_g and ϵ^-_u (Nos. 3, 15, 9, 18 in Fig. 1). They all have frequencies between 1000 and 1200 cm^{-1}. In C_6H_5Cl one of them and in $C_6H_4Cl_2$ two of them must drop down to a very low value. In all compounds there must originate at least one totally symmetrical vibration around 1100 cm^{-1} and two non-totally

TABLE VI. *Symmetries of vibrations for* C_6H_5Cl *and meta-*$C_6H_4Cl_2$ *in group* C_{2v}.

Symmetry	Essential Symmetry Elements C_{2y}	σ_z	Number of Vibrations	Selection Rules Raman	Infra-Red
α_1	+	+	11	+	+
α_2	+	−	3	+	−
β_1	−	+	10	+	+
β_2	−	−	6	+	+

[9] A. Langseth and R. C. Lord, Kgl. Danske Vid. Sels. Math.-fys. Medd. **16**, No. 6 (1938).

[10] In his second volume, *Der Smekal-Raman Effekt*, Erg. Bd., 1938, p. 163, Kohlrausch correlates the Raman lines 416 and 470 with the 606 vibration in benzene. Our assignment corresponds to his previous one, cf. reference 11.

[11] K. W. F. Kohlrausch, Physik. Zeits. **37**, 58 (1936).

symmetrical vibrations in the same region. It is quite possible that in C_6H_5Cl the line at 1134 cm^{-1} is an α_1 (with large contribution from ϵ^+_g) and the 1190 cm^{-1} a β_1. The vibration with the low frequency mentioned above is perhaps the 200 cm^{-1}. It would be then a β_1 in accordance with the depolarization factor. Another possibility is that it is the 294 cm^{-1} observed in the liquid.

Dichlorobenzenes

Here too only the strong lines of the liquid have been found in the vapor. The 606 cm^{-1} ϵ^+_g vibration in benzene is split into $\alpha_1=416$ and $\beta_1=615$ cm^{-1} in monochlorobenzene. The same types occur in the meta- and ortho-derivatives, but here both will be influenced by the substitution, the values for the frequencies probably not being much apart from each other. Indeed, no line has been observed in the neighborhood of 600 cm^{-1} for meta- and ortho-$C_6H_4Cl_2$. There are several lines between 300 and 500 cm^{-1} in the meta- and ortho-compounds which may be chosen for the assignment in question. Polarization measurements indicate that the 399 in m-$C_6H_4Cl_2$ is totally symmetrical and hence quite likely is the α_1 in question. In o-$C_6H_4Cl_2$ the strong line at 483 has according to our measurements a rather low depolarization factor and therefore may be the corresponding α_1. Kohlrausch[11] has also made empirically a similar correlation. We make no proposal for the non-totally symmetrical component. In p-$C_6H_4Cl_2$ the 606 ϵ^+_g of benzene splits into an α_{1g} and a β_{2g} vibration. The results in the deutero-benzenes[9] make it probable that the α_{1g} is rather low, lower than in C_6H_5Cl. Hence the most reasonable assignment seems to be $\alpha_{1g}=326$ cm^{-1}. This is further confirmed by the polarization measurements. The β_{2g} should be higher and is perhaps similar to the corresponding β_1 in C_6H_5Cl which leads to the possible assignment $\beta_{2g}=627$ cm^{-1}, again in agreement with the depolarization factor.

The benzene hydrogen vibrations of high frequency α_{1g}, β_{1u}, ϵ^+_g and ϵ^-_u (Nos. 2, 13, 7, 20 in Fig. 1) which give rise in C_6H_5Cl to one chlorine valence vibration of 703 cm^{-1} produce two such vibrations in the di-derivatives. One of these has been observed with certainty in all three cases in the lines 742 (para), 665 (meta), and 664 cm^{-1} (ortho) as has been noticed by previous authors. Each line is polarized as it should be for a totally symmetrical vibration. The vibration has a larger contribution from ϵ^+_g for the para-compound.

TABLE VII. *Symmetries of vibrations for ortho-$C_6H_4Cl_2$ in group C^*_{2v}.*

Symmetry	Essential Symmetry Elements C_2^z	σ_z	Number of Vibrations	Selection Rules Raman	Infra-Red
α_1	+	+	11	+	+
α_2	+	−	5	+	−
β_1	−	+	10	+	+
β_2	−	−	4	+	+

The lines at 3082 (ortho), 3090 (meta), and 3090 cm^{-1} (para) have to be assigned, as in monochlorobenzene, to totally symmetric hydrogen vibrations. Polarization measurements support this conclusion. The frequencies of 3150 (ortho), 3169 (meta), and 3153 (para, observed in the liquid) probably represent overtones.

As in C_6H_5Cl the benzene carbon vibrations α_{1g} and β_{1u} (Nos. 1 and 12 in Fig. 1) should give frequencies in the neighborhood of 1000 cm^{-1}, the β_{1u} being Raman inactive in the para-compound. It is furthermore possible that the ϵ^-_u (No. 19 in Fig. 1) carbon vibration of benzene drops to a value in the 1000 cm^{-1} region. The six hydrogen vibrations of benzene α_{2g}, β_{2u}, ϵ^+_g and ϵ^-_u (Nos. 3, 15, 9, 18 in Fig. 1) will also give, besides two very low frequencies, four frequencies in the 1100 cm^{-1} region. In the case of p-$C_6H_4Cl_2$ two lines of appreciable intensity have been found in the gas at 1050 and 1110 cm^{-1}. The latter is the stronger of the two. It is very likely a totally symmetrical carbon vibration. This is supported by polarization measurements and the analysis of the ultraviolet spectrum.[4] The 1050 cm^{-1} line is probably also totally symmetric according to the fairly low depolarization factor. No preference can be offered as to the assignment to a carbon or hydrogen vibration. The 1170 cm^{-1} line is perhaps connected with the ϵ^+_g in benzene.

In meta-$C_6H_4Cl_2$ three fairly strong polarized lines have been observed with frequencies of 998, 1056, and 1129 cm^{-1}. We would like to consider the 998 and 1129 cm^{-1} as belonging to totally symmetrical carbon vibrations. This assignment

gets support again from the ultraviolet spectrum.[4] The explanation of the 1056 cm^{-1} line seems too indefinite at the moment although its low depolarization factor points to a totally symmetrical vibration.

In ortho-$C_6H_4Cl_2$ two lines were found at 1035 and 1133 and a weak one at 1271 cm^{-1}. We propose to ascribe the two strong polarized lines to totally symmetrical carbon vibrations, again in agreement with the analysis of the ultraviolet absorption spectrum.[4] The interpretation of the 1271 cm^{-1} seems ambiguous without additional information. We are, however, inclined to believe that the depolarized 1160 cm^{-1} line observed in the liquid[12] of ortho- and meta-$C_6H_4Cl_2$ corresponds to the depolarized line 1158 cm^{-1} in C_6H_5Cl and hence represents in both cases the non-totally symmetrical component originating mainly from the hydrogen bending vibration $\epsilon^+_g = 1178$ in benzene.

It has been mentioned before that out of the hydrogen vibrations α_{2g}, β_{2u}, ϵ^+_g and ϵ^-_u (Nos. 3, 15, 9, 18 in Fig. 1) there must originate two low frequencies which represent chlorine bending vibrations in the molecular plane. In the case of para-$C_6H_4Cl_2$ only one of them will be observable in the Raman effect which we believe to be $\beta_{2g} = 302$ cm^{-1} originating chiefly from ϵ^+_g and α_{2g} and found in the liquid. In meta-$C_6H_4Cl_2$ and in ortho-$C_6H_4Cl_2$ there have been observed in the liquid three low frequencies of 178, 202, 216 cm^{-1} and of 164, 203 and 239 cm^{-1}, respectively, while we could detect with certainty only one at 205 cm^{-1} (meta) and one at 194 cm^{-1} (ortho) in the gas. Since in the ortho- and meta-compounds one of the above-mentioned two low vibrations must be totally symmetrical (α_1) and the other one non-totally symmetrical (β_1), we were surprised to find only high depolarization factors for the observed low lines. A detailed assignment cannot be given.

In para-, meta-, and ortho-$C_6H_4Cl_2$ lines have been found at 1570, 1590, and 1598 cm^{-1}, respectively. As they are depolarized they correspond in all probability to the 1589 cm^{-1} in C_6H_5Cl and have likewise to be interpreted as the non-totally symmetric one of the two components into which the $\epsilon^+_g = 1596$ cm^{-1} in benzene (No. 8 in Fig. 1) splits in these molecules.

The vibrations which we have considered so far all take place in the molecular plane, either as valence or as bending vibrations. We have not mentioned any modes which occur perpendicular to the molecular plane. Of these the carbon vibrations β_{2g} and ϵ^+_u (Nos. 4 and 16 in Fig. 1) in benzene will be influenced only slightly by the substitution. They are both Raman inactive in benzene, and the ϵ^+_u is also forbidden in the para-derivative. They are allowed in the other derivatives considered here. Very few of them have been observed in the deuterobenzenes and these with very weak intensity. Weak lines in the neighborhood of 300 cm^{-1} in the corresponding chlorobenzenes could be due to these vibrations.

There are four hydrogen bending vibrations α_{2u}, β_{2g}, ϵ^+_u and ϵ^-_g perpendicular to the molecular plane in benzene (Nos. 11, 5, 17, 10 in Fig. 1). They lie between 670 and 1000 cm^{-1}. Out of these should result one low frequency for monochlorobenzene and two low ones for the dichlorobenzenes. The α_{2u} is Raman inactive in benzene but is known from the infra-red to occur at 670 cm^{-1}. In monochlorobenzene a strong band has been observed in the infra-red[13] at 680 cm^{-1} which is almost certainly the β_2 resulting mainly from α_{2u} in benzene. The ϵ^-_g gives weak to medium Raman lines in benzene and the deuterobenzenes. We suppose that one of the lowest frequencies, 200–294 cm^{-1} in C_6H_5Cl, and at least one of the three lowest in liquid *m*- and *o*-$C_6H_4Cl_2$ represent vibrations of the type discussed here.

The suggested assignments include most of the lines in the gas. Many more have been reported in the liquid phase. It seems too doubtful a procedure, however, to try an explanation of these. Some of the interpretations presented here have already been suggested by Kohlrausch,[11] while others differ from his. Since the whole problem is attacked here from a different point of view we believe it worth while to give our considerations and conclusions.

In conclusion we want to acknowledge a grant-in-aid from the Duke University Research Fund which made this research possible.

[12] This line has not been observed by Swaine and Murray in the meta-compound, but Kohlrausch and collaborators give it as a weak line. We have confirmed their observation.

[13] J. Lecomte, J. de Phys. et Rad. **8**, 489 (1937).

The Magnetic Susceptibility of Ti and Zr

C. F. SQUIRE AND A. R. KAUFMANN
Massachusetts Institute of Technology, Cambridge, Massachusetts

(Received June 3, 1941)

The paramagnetic susceptibilities of Ti and Zr have been found to increase linearly with increasing temperature from 20°K until a crystal structure change occurs at high temperatures. Electrical conductivity, specific heat, and thermal expansion studies were made on Zr and the evidence indicates a change in the electron configuration.

EVIDENCE for a phase transition in Ti, Zr, and Hf has been obtained by Zwikker,[1] Vogel and Tonn,[2] and by de Boer and his collaborators.[3] The x-ray evidence[4] shows that at low temperatures the Ti and Zr have a hexagonal close-packed lattice, and that above the transition they have a cubic body-centered lattice. Probably the same change in lattice structure occurs in Hf at its transition point. From our magnetic studies on Ti and Zr we believe the mechanism of the phase transition may be better understood.

EXPERIMENTAL

The chemical analysis of the Ti showed about 0.015 percent Fe (which means that the magnetic susceptibility should be unaffected) and about 2 percent silicon. The specimens used were solid slugs taken from the center of a large metallic-looking sample. The Zr analysis showed 0.11 percent Fe: This dissolved iron contributes to the paramagnetism of the Zr only at liquid-hydrogen temperatures. The sample was originally prepared by Professor J. H. de Boer[3] and consisted of large single crystals of ductile metal. Presumably there is 1 percent Hf dissolved in the Zr.

The magnetic susceptibility was determined by the well-known method of measuring the force which a non-homogeneous magnetic field exerts on a specimen.[5] The measurements were made with a Bitter type high field solenoid (magnet No. 1 of the M.I.T. magnet laboratory).[6] The adaptation for low temperature measurements is a modification of the apparatus developed at Leiden and elsewhere.[7] The measurements at high temperatures were carried out with the specimen enclosed in a small quartz capsule which had been previously evacuated and sealed off. The chamber in the solenoid into which the specimens were hung was continuously flushed with hydrogen gas. At liquid- and solid-hydrogen temperatures, helium was mixed with the hydrogen to prevent condensation.

Figure 1 shows the magnetic susceptibility per gram of Ti as a function of temperature. There are three unusual experimental facts to be observed from this curve: (1) There is a phase transition which appears to be completed at 1300°K, (2) the transition is continuous such as to suggest a "second-order" phase transition, (3) the temperature gradient of the susceptibility is not in accord with the existing theories of paramagnetic metals. The maximum error is estimated at 1.6 percent for our magnetic measurements. The transition temperature reported for Ti by de Boer is 1158°K and we concede that the 2 percent impurity of silicon could make our λ-point occur higher.

Figure 2 shows the magnetic susceptibility per gram of Zr as a function of temperature. The same unusual experimental evidence has been obtained as in Ti. The points observed were completely reproducible even in the transition region —i.e., no hysteresis with respect to temperature. The λ shape of the Zr curve appears more sharp than in the case of our Ti and the temperature at which the transition takes place agrees with other workers.[3] It will be noticed that in Zr our curve turns up again in the region of temperature

[1] C. Zwikker, Physica **6**, 361 (1926).
[2] R. Vogel and W. Tonn, Zeits. f. anorg. allgem. Chemie 202, 292 (1931).
[3] J. H. de Boer, P. Clausing, and J. D. Fast, Rec. Trav. Chim. **55**, 450 (1936). J. H. de Boer, W. G. Burgers, and J. D. Fast, Proc. Akad. Wet. Amst. **39**, 515 (1936).
[4] W. G. Burgers, Physica **1**, 561 (1934).
[5] F. Bitter and A. R. Kaufmann, Phys. Rev. **56**, 1044 (1939).
[6] F. Bitter, Rev. Sci. Inst. **10**, 373 (1939).
[7] M. and B. Ruhemann, *Low Temperature Physics* (Cambridge University Press, 1937).

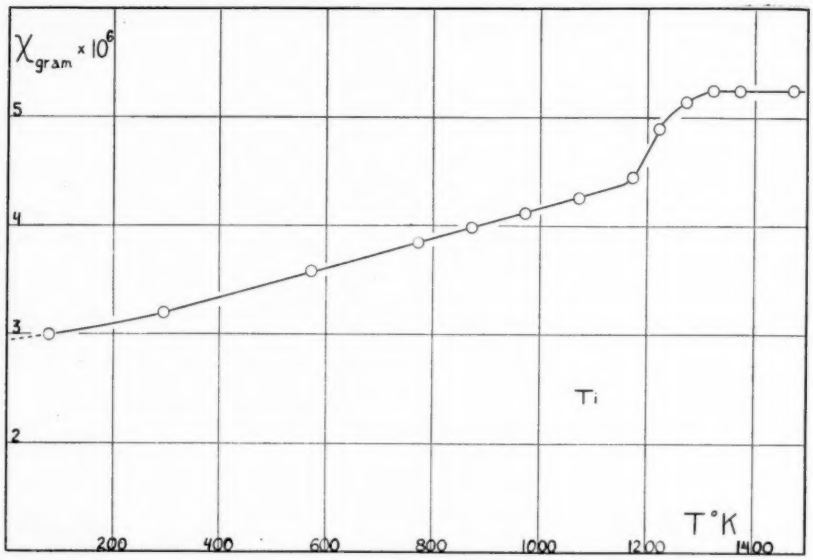

FIG. 1. Paramagnetic susceptibility of titanium as a function of temperature.

below 50°K, as the experimental points at 20°K and 14°K show. However, it is just at these low temperatures that the 0.11 percent Fe which our specimen contains has a paramagnetism sufficient to cause the susceptibility of the Zr to increase. Only at 14°K does the susceptibility show a significant field dependence. At all other higher temperatures, and in particular in the transition region, the susceptibility is independent of the field. We tried to retain some of the high temperature phase by quenching from high temperatures but the room temperature value of the susceptibility remained the same.

Figure 3 shows our results on the electrical resistance of Zr as a function of temperature (full line). The ductile Zr was swaged and then drawn into a wire about 25 cm in length and 0.38 mm in diameter. The wire was annealed in high vacuum to relieve strains between successive drawings. During the measurements the wire was in a high vacuum to prevent gas absorption at high temperatures. There are two unusual experimental facts to be observed from the curve: (1) The decrease in resistance becomes appreciable in just the region where the "second-order" phase transition sets in for Zr as observed in the magnetic studies, (2) the slope of the resistance curve changes well before the transition region. The minimum in the resistance corresponds to the peak of the λ-point in the susceptibility. The dashed curve in Fig. 3 shows the deviation of the resistance from a linear function extrapolated to high temperatures from the region below 500°K. Thus the decrease in resistance is not a sharp break but the result of a process going on well before the actual falling off occurs.

Figure 4 shows the specific heat as a function of temperature for Zr. The high temperature values are taken from Jaeger and Veenstra.[8] The low temperature values were taken by us in an attempt to find a hump in the specific heat of Zr which would be similar to that which Simon and Critescu[9] found in Hf at 85°K. We found no such hump at these low temperatures for Zr and our values are only good to ±0.2 cal./mole.[10] The high temperature results of Jaeger and Veenstra are interesting because they show an abnormally large specific heat in the region of the transition at 1115°K. Their technique consisted in heating the specimen to high temperature and then dropping it into a calorimeter. We have plotted their results on ductile Zr which they call specimen "*A*" and we refer the reader to their paper

[8] F. Jaeger and W. Veenstra, Rec. Trav. Chim. **53**, 922 (1934).

[9] F. Simon and S. Critescu, Zeits. f. physik. Chemie **B25**, 273 (1934).

[10] The hump in C_p which Simon observed for Hf has received considerable attention in recent books on the solid state. We believe that a small amount (1 percent) of Fe might show magnetic interaction at 85°K and so give the observed C_p hump. Another possibility would be the effect of dissolved hydrogen in the Hf (see K. K. Kelley, J. Chem. Phys. **8**, 316 (1940)).

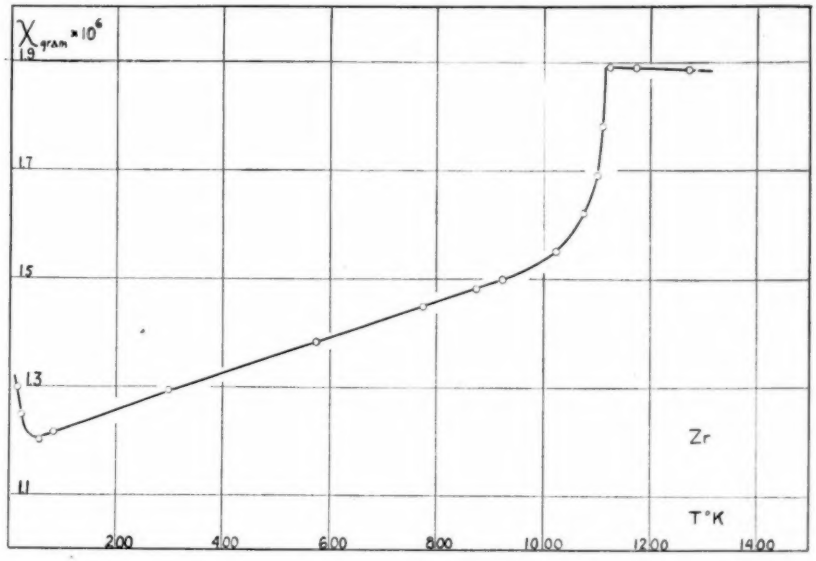

FIG. 2. Paramagnetic susceptibility of zirconium as a function of temperature.

concerning the uncertainty of the highest two values. Certainly there is a phase transition and at this temperature either the specific heat becomes infinite or has a hump in the neighborhood of the transition. That is, either it is a first- or a second-order transition. In view of our results in Figs. 2, 3, 5, we feel that, with our specimen, the specific heat curve should show a hump in the manner which we indicate with dashed lines. The question can only be settled by differential specific heat measurements in the transition region and preferably with specimens of higher purity than thus far reported.

Finally, we have measured the expansion of Zr as a function of temperature (Fig. 5). The normal linear expansion coefficient is about 6.5×10^{-6} per degree centigrade, and remains relatively normal up to the transition region. At this point the metal contracts on heating through the λ-point. This latter had been observed earlier in a qualitative way by Vogel and Tonn.[2] Our results are exploratory in nature and represent a maximum error of 3 percent. The ductile Zr resembles Cu in its elastic property so that we believe the large specific heat value at, say, 550°K, is not due entirely to the difference: $C_p-C_v=TV\alpha^2/X$, where $V=13.9\,\text{cm}^3$ per gram atom, $\alpha=19.5\times10^{-6}$ per degree as the volume thermal expansion coefficient, and $X=9\times10^{-13}$ cm²/dyne as the compressibility coefficient. For in the present case this difference is only about 0.1 cal./mole.

DISCUSSION

The electronic structure of Ti, Zr, and Hf is similar in that they each have four valence electrons with two in the *s* shell and two in the *d* shell. One would, therefore, expect their physical properties to be similar. All three form the hexagonal close-packed structure at low temperatures having lattice constants[11] which increase with the heavier atoms.

The magnetic property which we have observed is not only abnormal in the region of the transition but is unusual over the entire range of temperatures below the λ-point. The susceptibility resembles the situation which one finds for those paramagnetic salts exhibiting antiferromagnetism.[12] The susceptibility extrapolated to 0°K is nearly $\frac{2}{3}$ of the value at the λ-point which agrees qualitatively with the Van Vleck[13] theory of antiferromagnetism. The hexagonal close-packed crystal forms a layer lattice to conform with the requirements of antiferromagnetism. One big difference is that in these metals we have a crystal structure change, whilst in all cases of antiferromagnetism thus far studied there is no such change at the λ-point. Also, we do not find

[11] J. D. Fast, Rec. Trav. Chim. **58**, 972 (1939).
[12] H. Bizette, C. Squire, and B. Tsai, Comptes rendus **207**, 449 (1938). C. Squire, Phys. Rev. **56**, 922 (1939).
[13] J. H. Van Vleck, J. Chem. Phys. **9**, 85 (1941). See also: L. Neel, Ann. de physique **17**, 64 (1932); **5**, 256 (1936).

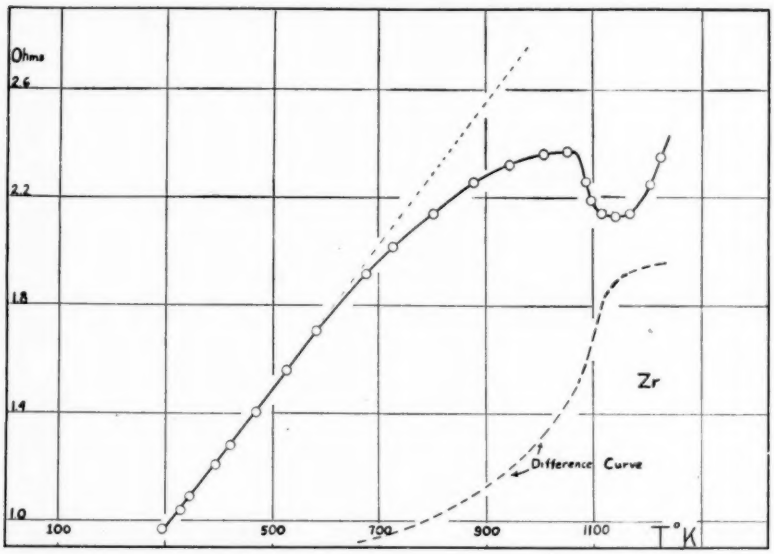

FIG. 3. Resistance of Zr against temperature and also the difference between the measured resistance and a linear resistance extrapolated to high temperatures.

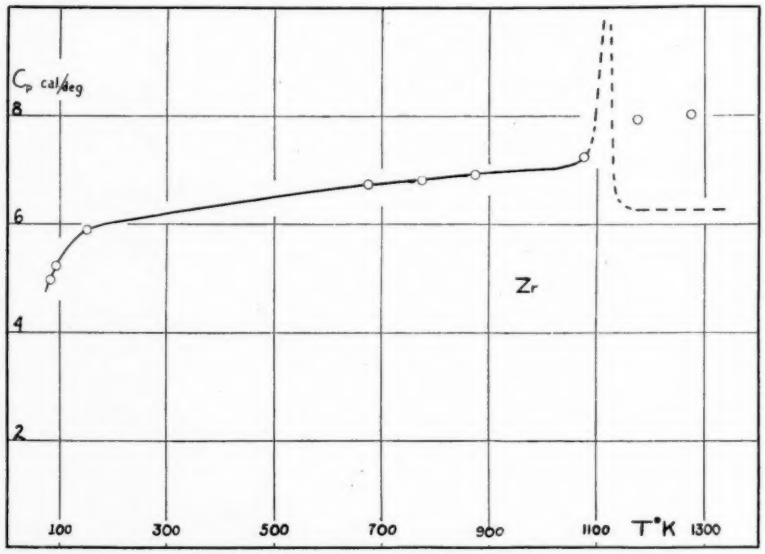

FIG. 4. Specific heat per mole of Zr. The high temperature values are taken from F. Jaeger and W. Veenstra (reference 8).

a field dependence of the susceptibility in contradiction to what the theory seems to predict.

There is an alternative viewpoint which we wish to propose. It would seem that the magnetic susceptibility as a function of temperature ought to be consistent with the electron theory of metals. Existing theory gives $\chi = 2\beta^2 N(\xi)[1+\cdots]$ where β is the Bohr magneton and $N(\xi)$ is the density of states at the top of the Fermi distribution. The higher terms in the series have the effect of slightly decreasing the susceptibility at higher temperatures. If we assume that, as the temperature increases, the function $N(\xi)$ increases—then the susceptibility would become larger. The extra specific heat associated with a change of $N(\xi)$ must be spread over the entire temperature range. Professor J. C. Slater has suggested to us the following possible mechanism which might give just the needed increase in $N(\xi)$: The "d" and "s" energy bands overlap in the solid but the d band might be split owing to the hexagonal crystalline electric field of the

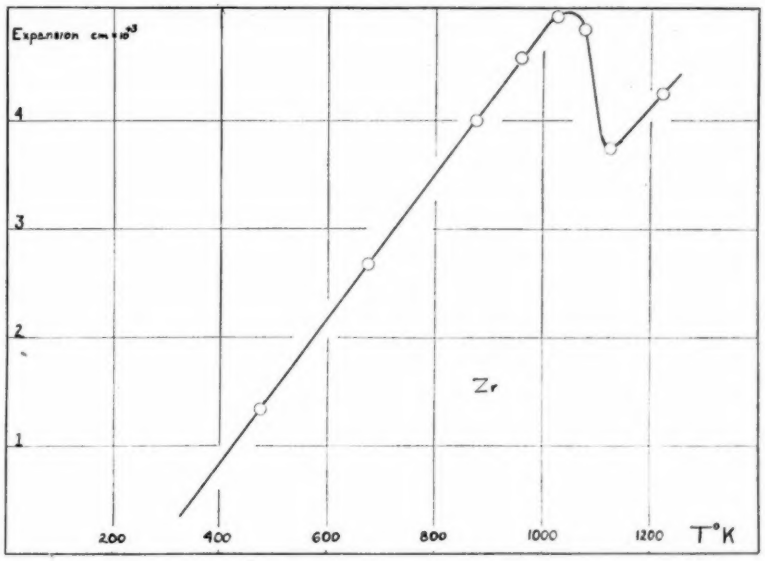

FIG. 5. Linear expansion per cm length of Zr.

atoms. At low temperatures, a plot of the density of energy states against energy will give $N(\xi)$ to be small owing to this splitting. If the splitting of the d band is sensitive to lattice spacing, which it may well be, then an increase of temperature might decrease the width of splitting and the magnitude of $N(\xi)$ should increase. We believe this would account for the decrease in resistance, as it means essentially the creation of a greater number of "free" electrons. We do not see any mechanism correlating the change of $N(\xi)$ with the existence of the phase transition.

It is difficult to understand why these metals should show a second-order phase transition instead of the normal first-order change to be expected with crystal structure change. Possibly the impurities present in our specimens caused the observed second-order transition. If our magnetic measurements are to be explained on the basis of antiferromagnetism, then we might expect a second-order phase transition. However, this requires an explanation of why there is a crystal structure change and why there is no field dependence of the susceptibility. If the magnetic results are to be explained on the basis of a change in the density of electron states, then we might expect only a first-order phase transition accompanying the crystal structure change.

One of us (A.R.K.) participated only in the magnetic and resistance studies. We hope to obtain some pure Hf at a later date and investigate its magnetic property. We wish to thank Mr. G. H. Chambers of the Foote Mineral Company, Philadelphia, for the specimens of Zr. We are indebted to Professor J. C. Slater for valuable criticism and to Professor F. G. Keyes and his associates for the liquid hydrogen.

Magnetic and X-Ray Studies on Ti and Zr with Dissolved Hydrogen

J. FITZWILLIAM, A. KAUFMANN, AND C. SQUIRE
Massachusetts Institute of Technology, Cambridge, Massachusetts

(Received June 3, 1941)

Dissolved hydrogen in Ti and Zr has the effect of changing the lattice of these metals from hexagonal close-packed to a nearly cubic face-centered lattice. The paramagnetic susceptibility of the system Ti-H and also Zr-H has a value at room temperature different from that of the respective pure metals. The dependence of susceptibility on the hydrogen concentration has been investigated for Zr in this article. A small trace of iron impurity which was dissolved in the Zr was found to precipitate out and regain its ferromagnetic property when the Zr was allowed to soak up hydrogen.

F. SIMON and J. Aharoni[1] have studied the magnetic susceptibility of the system Pd-H as a function of the concentration of the dissolved hydrogen and found a linear decrease of paramagnetism up to about 0.55 hydrogen atoms to each palladium atom. It has been deduced[2] that since the palladium shows 0.55 hole per atom in the *d* band, the dissolved hydrogen is completely ionized in the palladium lattice. It is known[3] that both Ti and Zr dissolve hydrogen up to quite large concentrations and we have, therefore, investigated the paramagnetism of the systems Ti-H and Zr-H. We have also studied the crystal structure change brought about by the addition of hydrogen to these metals and we have noted the magnetic behavior of a small amount of dissolved iron in the Zr-H system.

EXPERIMENTAL

The specimens of Ti and Zr metal which were used in the preceding paper[4] were allowed to soak up hydrogen by heating the specimens in a furnace with an atmosphere of hydrogen. It was found that a large amount of hydrogen could be dissolved in the Ti at 1000°K and that going to higher temperatures drove some of the hydrogen out.[5] Similarly, with the Zr, the specimen began to take on hydrogen at 900°K. The dissolved hydrogen could be readily removed from the metal by pumping at 900°K. We verified that the hydrogen did not form a compound but was, in reality, dissolved in the metal by determining the vapor pressure of hydrogen as a function of temperature. It was found that the vapor pressure was also a function of the concentration of the dissolved hydrogen. This means that one cannot employ the Clapeyron equation to determine the heat of adsorption. We did not attempt to run adsorption isotherms to obtain the true value of the heat of adsorption.

Normal pure Zr at room temperature has a hexagonal close-packed crystal structure ($c=5.137$A, and $a=3.227$A), but at 1115°K goes to cubic body-centered ($a=3.61$A).[6] In Fig. 1(a) our x-ray powder pattern of Zr at room temperature gives agreement with Burger.

The Zr was filled to approximately 66 atomic percent hydrogen, and at room temperature the powder pattern showed a tetragonal face-centered lattice ($c=4.58$A, $a=4.87$A). See Fig. 1(b). These constants are in good agreement with Hagg.[3] The introduction of the hydrogen into the specimen was accompanied by an 8.2 percent increase in volume. By pumping on the Zr-H system at 1000°K, the hydrogen was completely removed and x-ray studies showed a return of the metal to the original hexagonal close-packed structure. See Fig. 1(c). The lattice constants are the same within experimental error. The original Zr was a large single crystal and the treatment of adding and then subtracting the hydrogen caused the specimen to become quite polycrystalline.

With 1.2 atoms of hydrogen per atom of Ti, the

[1] F. Simon and J. Aharoni, Zeits. f. physik. Chemie **B4**, 175 (1929). See also B. Svensson, Ann. d. Physik **18**, 299 (1933).
[2] N. Mott and H. Jones, *Properties of Metals and Alloys* (Oxford University Press, 1936).
[3] G. Haag, Zeits. f. physik. Chemie **B11**, 433 (1931).
[4] C. Squire and A. Kaufmann, J. Chem. Phys. **9**, 673 (1941), this issue.
[5] A. Sievert and E. Roell, Zeits. f. anorg. Chemie **153**, 289 (1926).
[6] W. G. Burger, Physica **1**, 561 (1934).

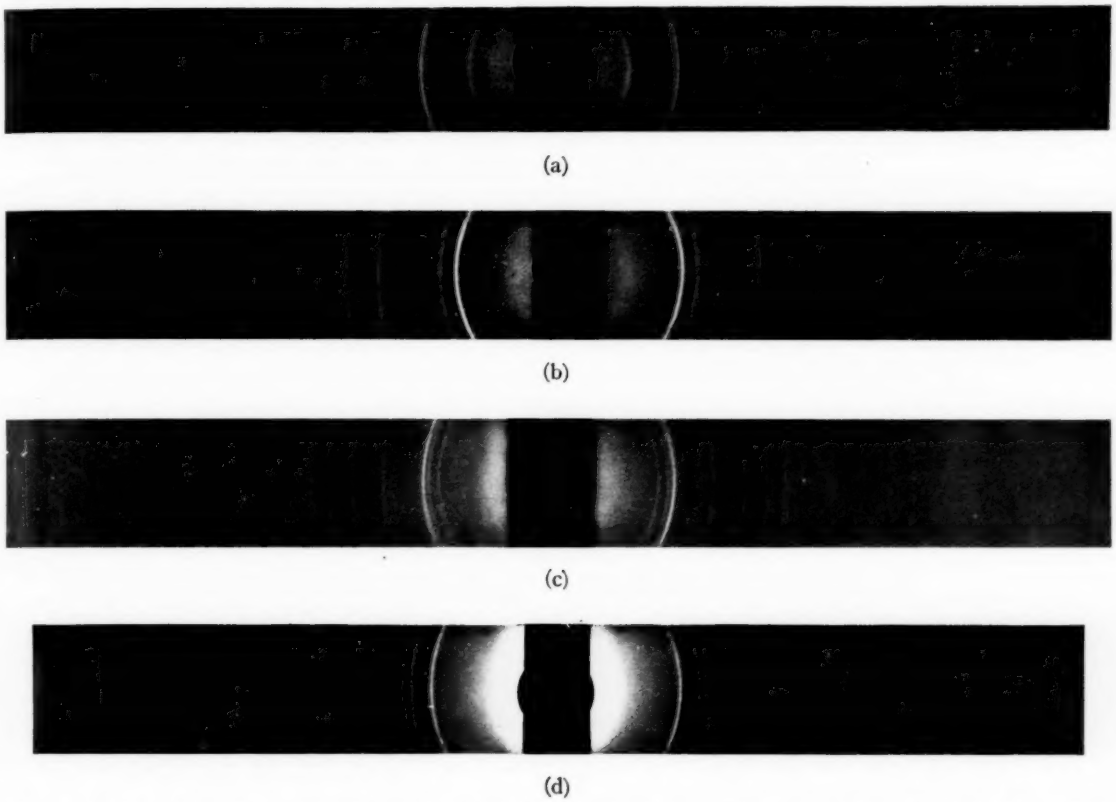

(a)

(b)

(c)

(d)

FIG. 1. (a) X-ray powder pattern of normal Zr showing hexagonal close-packed crystal structure. (b) X-ray powder pattern of the system Zr-H showing tetragonal face-centered lattice. (c) X-ray powder pattern of Zr after removal of dissolved hydrogen. (d) X-ray powder pattern of Ti-H showing a very nearly cubic face-centered structure.

system Ti-H was found to have a very nearly cubic face-centered structure with $a=4.45$A. See Fig. 1(d).

The x-ray powder patterns were taken in Debye cameras having diameters of approximately 57.5 mm. The Cu $K\alpha$ line was used (the other line was filtered out by Ni) and the tube carried 15 ma at 30 kv. No attempt was made to get high precision on lattice parameters.

Since both metal-hydrogen systems went to the face-centered forms rather than to the expected body-centered structures, it appears that the binding energy is higher in the face-centered form when hydrogen atoms are present.

MAGNETIC STUDIES

The pure Ti showed a susceptibility at 300°K of 3.2×10^{-6} per gram, and with 1.2 atoms of hydrogen per atom of Ti, the system showed an increase of susceptibility to 3.78×10^{-6}. The Ti-H system showed no magnetic field dependence of the susceptibility, and this should be carried in mind in understanding the difficulties which we encountered with our Zr-H system.

In the preceding paper we drew attention to the fact that our Zr specimen contained 0.11 percent Fe. This iron is dissolved in the Zr and at room temperature plays no role in the magnetic susceptibility. No amount of heat treatment and quenching could make this iron play an important role save at liquid-hydrogen temperatures (see Fig. 2 of reference 4). However, with hydrogen dissolved in the Zr and with suitable heat treatment, the iron appeared to precipitate out of solution with the Zr in that it gave a ferromagnetic component to the magnetization. Figure 2 shows a typical magnetization curve for a Zr-H specimen containing 0.015 gram of hydrogen per gram of Zr. It is evident that there are two components in the magnetization—one showing saturation after a few thousand gauss

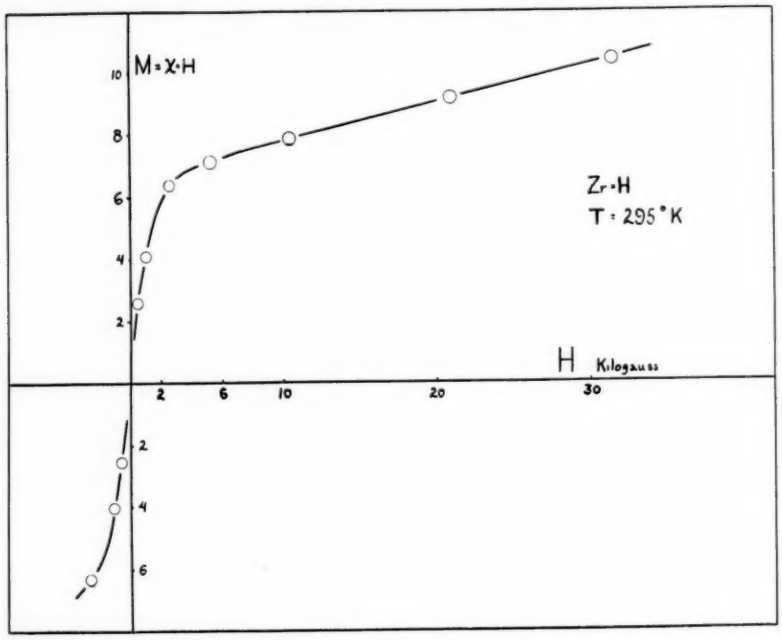

FIG. 2. Magnetization as a function of magnetic field for the system Zr-H.

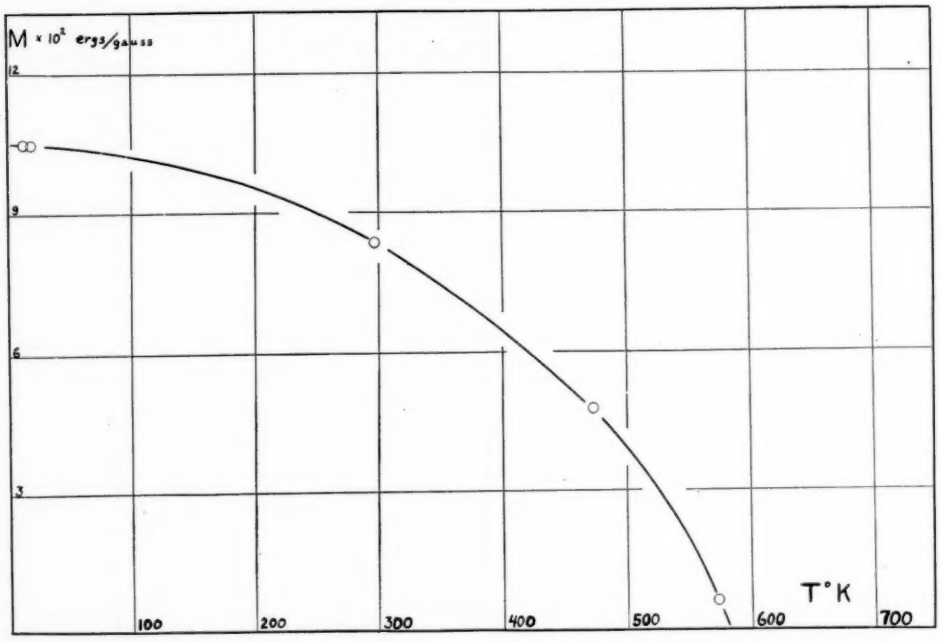

FIG. 3. Saturated magnetic moment of Fe impurity on the system Zr-H as a function of temperature.

(due to the 0.11 percent Fe) and another part showing a normal linear paramagnetic magnetization. There is no hysteresis loop as is found for pure iron, but the susceptibility of the specimen approaches infinity as the magnetic field approaches zero. Figure 3 shows the saturation magnetization of the Fe component as a function of temperature for a specimen which contained 0.022 gram of hydrogen per gram of Zr. The saturation magnetization at 0°K (extrapolated from the measurements at 14°K) is of the correct order of magnitude to be completely accounted for by the small iron content. All specimens containing hydrogen showed very

clearly a Curie point at 585°K. Above this temperature there was no saturation component. The Curie temperature for iron is much higher at 1000°K.

Whether or not the concentration of hydrogen plays a role other than that needed to change the crystal structure we cannot say. The predominating factor in causing the Fe to precipitate out was the holding of the hydrogen-filled specimen at 1000°K for a period of an hour. Phenomenologically, we feel that it is very interesting that the iron atoms, spaced some 10 atoms of Zr apart, can be made to precipitate out and restore their ferromagnetic characteristic. We believe that somehow the high temperature heat treatment must have allowed the iron actually to form clusters. In all specimens the ferromagnetism completely vanished when the hydrogen was removed by pumping at 900°K. This implies that the Fe has gone back into solution with the Zr. It occurred to us that the saturated moment might be due to the hydrogen—i.e., all protons aligned would give a magnetic moment of the order of magnitude which we observed. This is most unlikely unless one assumes an enormous internal Weiss field acting on the protons. We wish to emphasize that our Ti, having no Fe impurity, showed no such behavior on the addition of hydrogen.

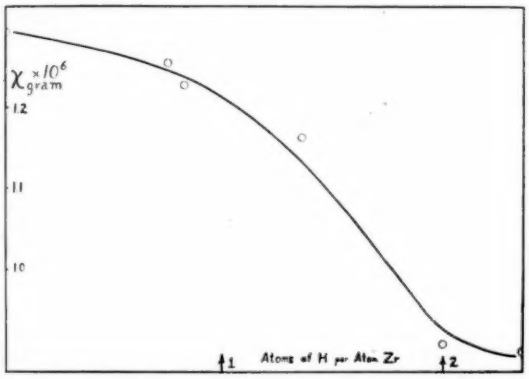

FIG. 4. Magnetic susceptibility of the system Zr-H as a function of hydrogen concentration at 295°K.

We have felt justified in subtracting off the saturated magnetic moment of the Fe at 300°K and calling what remained the magnetic moment of the Zr-H system. From this magnetic moment we compute the magnetic susceptibility and Fig. 4 shows the susceptibility per gram of Zr as a function of the concentration of dissolved hydrogen. There is some resemblance to the Pd-H system explored by Simon[1] in that here the susceptibility decreases and finally remains nearly constant at 2 atoms of H per atom of Zr. The change of lattice upon the addition of hydrogen makes us hesitate to draw theoretical conclusions

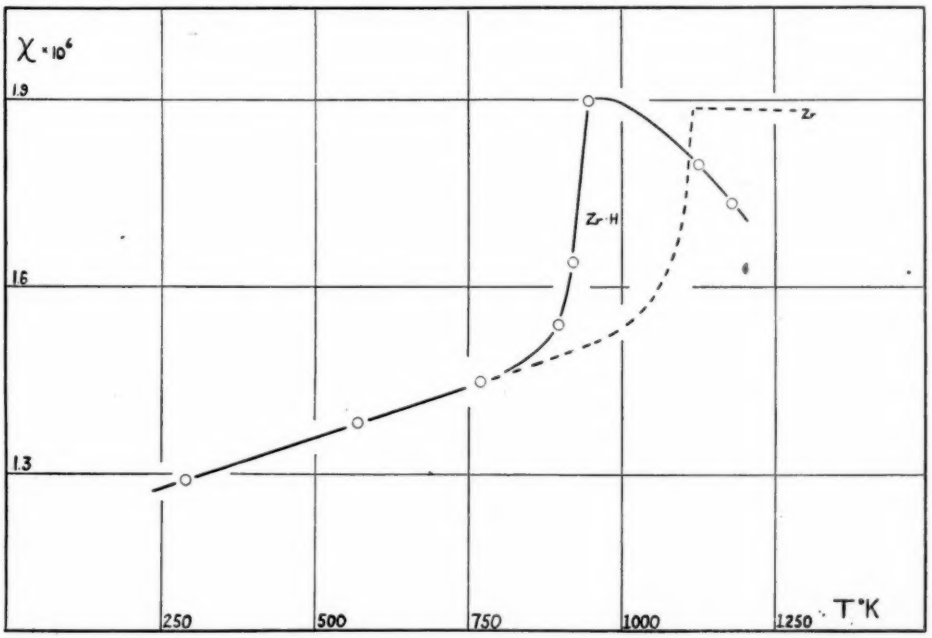

FIG. 5. Magnetic susceptibility of Zr as function of temperature showing effect of hydrogen dissolving at 900°K.

from the magnetic studies of either the Ti or the Zr.

Finally, we were interested in what happened to the magnetic susceptibility of Zr as the hydrogen began to enter the metal. Thus, starting with pure, ductile Zr, we began measuring the susceptibility as a function of temperature, while the specimen was exposed to an atmosphere of hydrogen. Figure 5 shows the results. Naturally, at low temperatures the values are exactly those of the pure metal. At 900°K the specimen began slowly to take on hydrogen and the susceptibility began to increase. Beyond the λ-point the specimen did not appear to gain or lose any appreciable quantity of hydrogen, and it is apparent that the susceptibility does not resemble that which the pure metal Zr shows in its high temperature phase. Comparing the λ-point with that found for pure Zr in reference 4 (here represented in dashed lines), it is seen that the transition occurs about 200° lower. The actual structure change is, however, entirely different, which is rather surprising. The measured curve in Fig. 5 is not reversible with temperature (unless one also pumps out the hydrogen) as the new phase is preserved on lowering the temperature.

ACKNOWLEDGMENTS

The authors are grateful for the interest and advice which Professor B. E. Warren has so kindly given and they also wish to acknowledge many stimulating discussions with Dr. C. Starr.

SEPTEMBER, 1941 JOURNAL OF CHEMICAL PHYSICS VOLUME 9

Velocity of Sound in Liquids and Chemical Constitution

M. RAMA RAO
Department of Physics, University of Mysore, Bangalore, India
(Received January 20, 1941)

A study of the recently obtained data on the velocity of sound and density in liquids reveals a simple relation between these quantities namely the law, $v^{\frac{1}{3}}M/\rho=R$ where v is the velocity of sound in the liquid, M the molecular weight, ρ the density and R a constant independent of temperature. It is shown that the velocity of sound cannot be a proper basis of comparison in any homologous series. The result of plotting the constant R against the molecular weight of members of homologous series leads to the equation $R=\alpha M+\beta$ where α is a general constant and β a characteristic constant for any one homologous series. The difference in R for successive members of homologous series is a constant independent of the series and R is an additive function of the chemical structure. Values of R for hydrogen, carbon, oxygen, bromine, and chlorine are tabulated.

A STUDY of recently obtained data[1] on the velocity of sound and density in liquids reveals a simple relation[2] between these quantities, namely the law,

$$v^{\frac{1}{3}}M/\rho=R,$$

where v is the velocity of sound in the liquid at the temperature θ, M the molecular weight, ρ the density of the liquid at the same temperature and R a constant independent of the temperature. Since M/ρ is equal to the molecular volume which is proportional to σ^3, where σ is the mean molecular distance, it follows[3] that the velocity of sound in the liquid at any temperature is inversely proportional to ninth power of the mean distance between the molecules at that temperature. As the temperature of the liquid increases, σ also increases, resulting in a decreased velocity of sound. When the pressure increases, σ decreases resulting in an increased

[1] Freyer, Hubbard, and Andrews, J. Am. Chem. Soc. **51**, 729 (1929); S. Parthasarathy, Proc. Ind. Acad. Sci. **2A**, 497 (1935); **4A**, 59 (1936); W. Schaafs, Zeits. f. Physik **105**, 658 (1937).

[2] M. Rama Rao, Ind. J. Phys. **14**, 109 (1940).

[3] M. Rama Rao, Curr. Sci. **8**, 510 (1939).

velocity of sound. These results[4] are true in the case of all non-associated liquids. Since R is independent of temperature, it follows that a change in the velocity of sound with temperature is determined by the dependence of the density on temperature. The law for the variation of v with temperature has been shown[5] to be

$$v=v_0(1-\theta/\theta_c)^{0.9},$$

where v_0 = velocity of sound when $\theta=0$, θ_c = critical temperature on the absolute temperature scale.

The chief importance of sound velocity measurements in liquids has so far been in their rendering possible a determination of the adiabatic compressibility. From this and the isothermal compressibility derived from static measurements, it is possible to calculate the ratio of the specific heats of the liquid. This then gives us the value of the specific heat at constant volume. The most extensive investigation, undertaken with the object of comparing the velocity of sound of members of homologous series, has been carried out by Parthasarathy.[6]

In general, aromatic compounds have higher velocity than the aliphatics. For the former the range is around 1300 m/sec., while for the latter 1300 m/sec. is about the upper limit. If we consider the velocity of sound to be the proper basis of comparison in homologous series, we find that in certain series the velocity increases with the increase in the length of the chain, in others it decreases with the increase in the length. In the benzene hydrocarbon series the velocity at first increases with the molecular weight and then decreases with the higher members of the series. The introduction of a heavier atom is found to bring down the velocity of sound. These qualitative observations are shown graphically in Fig. 1, where the variation of the velocity of sound of successive members of homologous series is studied by plotting the velocity of sound against the molecular weight. It is noticed that for the saturated hydrocarbons the velocity increases with the molecular weight, the increase being not proportional to increase in the molecular weight. In the case of esters there

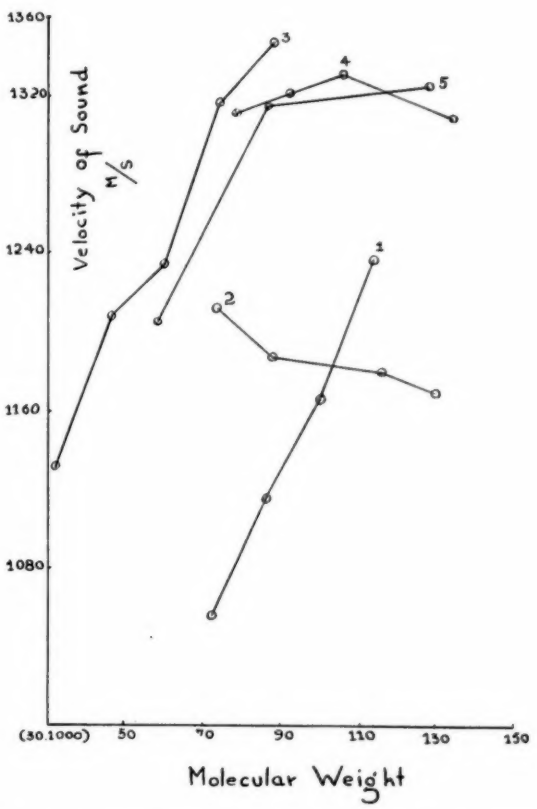

FIG. 1. 1—paraffins; 2—esters of acetic acid; 3—monohydric alcohols; 4—benzene hydrocarbons; 5—ketones.

is a diminution in the velocity with the increase in the molecular weight. In the case of monohydric alcohols and ketones it is found that the velocity increases but not regularly with the increase in molecular weight. In the case of benzene hydrocarbons there is a marked maximum of the velocity of sound for xylene. For higher members of the series, the velocity decreases but not regularly. The graph shown in Fig. 1 is drawn at one temperature for all the liquids. Hence it is not possible to get any insight into the chemical constitution of the substance having as our basis of comparison the velocity of sound.

The simple law between the velocity of sound in liquids and molecular volume $v^{\frac{1}{4}}M/\rho=R$, shows that a comparison of the values of R of two liquids is equivalent to the comparison of molecular volumes of these liquids at temperatures at which the acoustic velocity is the same in those liquids. The constant R for a liquid

[4] J. C. Swanson, J. Chem. Phys. **2**, 689 (1934).
[5] M. Rama Rao, Ind. J. Phys. **14**, 109 (1940).
[6] S. Parthasarathy, Curr. Sci. **5**, 11 (1937).

TABLE I.

SERIES	LIQUID	FORMULA	DENSITY	VELOCITY M/SEC.	R	R_{CH_2}
Paraffins	Pentane	C_5H_{12}	0.6320	1052	1160	
						196
	Hexane	C_6H_{14}	0.6580	1113	1356	
						189
	Heptane	C_7H_{16}	0.6812	1165	1545	
						201
	Octane	C_8H_{18}	0.7020	1238	1746	
Esters of acetic acid	Methyl	CH_3COOCH_3	0.9282	1211	851	
						186
	Ethyl	$CH_3COOC_2H_5$	0.8989	1187	1037	
						174
	Propyl	$CH_3COOC_3H_7$	0.8910	1182	1211	
						197
	Butyl	$CH_3COOC_4H_9$	0.8710	1179	1408	
						186
	Amyl	$CH_3COOC_5H_{11}$	0.8600	1168	1594	
Monohydric alcohols	Methyl	CH_3OH	0.7920	1130	421	
						203
	Ethyl	C_2H_5OH	0.7863	1207	624	
						182
	Propyl	C_3H_7OH	0.8010	1234	806	
						198
	Butyl	C_4H_9OH	0.8082	1315	1004	
						194
	Amyl	$C_5H_{11}OH$	0.8136	1347	1198	
Benzene hydrocarbons	Benzene	C_6H_6	0.8725	1310	979	
						191
	Toluene	C_7H_8	0.8631	1320	1170	
						192
	Xylene	C_8H_{10}	0.8580	1330	1362	
						2×185
	Cymene	$C_{10}H_{14}$	0.8470	1308	1731	
Ketones	Acetone	C_3H_6O	0.7910	1203	781	
						2×190
	Diethylketone	$C_5H_{10}O$	0.8132	1314	1161	
						3×187
	Methyl hexylketone	$C_8H_{16}O$	0.8170	1324	1720	
	Methylene chloride	CH_2Cl_2	1.3360	1064	649	
						197
	Ethylene chloride	$C_2H_4Cl_2$	1.2550	1240	846	

The average difference which corresponds to the value of R of the CH_2 group is found from the examination of several series to be 195.

may be regarded as the molecular volume of the liquid when the velocity of sound in it is unity. It is well known that molecular volumes of liquids at the boiling point are an additive function of the molecular volume. Since R can be regarded as a molecular volume when the velocity of sound in the liquid is unity, it is reasonable to suppose that the same additivity would apply to the constant R. This has proved to be definitely the case. In Table I are given values of R for members of homologous series. It is found that the difference in the value of R between successive members of a homologous series is a constant and independent of the type of compound.

In Fig. 2, values of R are plotted against the molecular weight of successive members of homologous series. It is seen that they are all straight lines having the same slope. In the first instance, the graph shows that for every addition of a CH_2 group the constant R increases by the same amount. Since all of them are a set of parallel lines, we can represent each one of them by the equation

$$R=\alpha M+\beta,$$

where α is a constant independent of the series

and β is a constant characteristic for any one homologous series. The relation holds well for a number of series. In Table II are given the values of α and β for a number of series.

By subtracting from the value of R for a paraffin (formula C_nH_{2n+2}) that for $n$$CH_2$ groups, i.e., $195n$, the value of R of two atoms of hydrogen can be found as in the case of the parachor[7] and the same considerations that apply to the case of the parachor also hold good for the case of R. The average difference for the series is thus found to be 185, and so the value of R for hydrogen is taken as 92.5. Since the value of R for CH_2 is 195, it follows that the value for the carbon atom is 10. Proceeding in this manner it is possible, from known values for carbon and hydrogen, to determine the values of R for other atoms. For example, that for oxygen is obtained as 74 from measurements on ethers. It will be observed that no value of R has been attributed to a single linkage. Although this is not necessarily correct, the atomic values of R given for hydrogen, carbon and oxygen really include the contribution of such a linkage. The single bond is taken as an arbitrary zero level from which the effect of other structures is reckoned. As with other additive properties, so with the constant R, constitutional factors must be taken into account. The same difference is obtained for all substances containing a double bond and a mean value of 110, for the contribution of R is attributed to the presence of such a bond. In Table III are given some of the values obtained for different atoms and structures. When more data on the velocity of sound are available, it is seen from the above considerations that it should be possible to extend these investigations to the problems of chemical structure.

TABLE II.

No.	SERIES	α	β
1	Paraffin	13.97	+155
2	Esters of acetic acid	14.01	−206
3	Monohydric alcohols	14.00	− 32
4	Benzene hydrocarbons	14.02	−120
5	Ketones	13.99	− 48

It is to be noticed from the above table that α is nearly the same for all the series examined with a mean value of 14, and β varies considerably from one series to the other. It is positive in the paraffin series but has a negative value in other series.

[7] Sugden, *The Parachor and Valency* (G. Routledge & Sons, London, 1930).

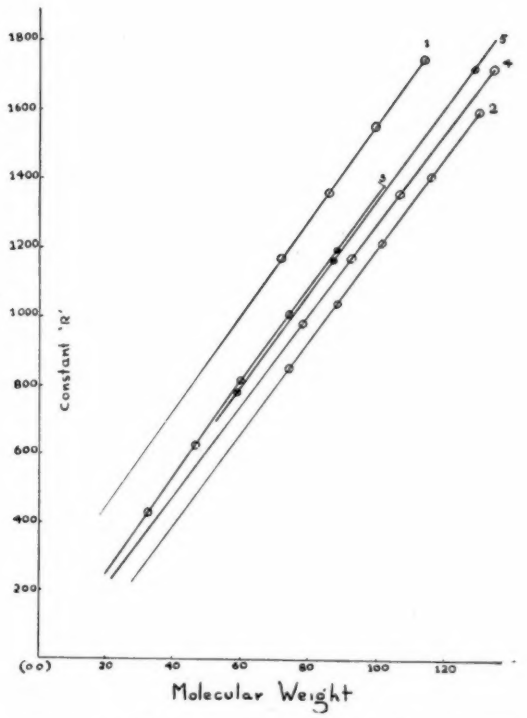

FIG. 2. 1—paraffins; 2—esters of acetic acid; 3—monohydric alcohols; 4—benzene hydrocarbons; 5—ketones.

TABLE III.

Element	R
Carbon	10
Hydrogen	92.5
Oxygen	74
Chlorine	227
Bromine	245
Double Bond	110

In conclusion it gives me great pleasure to record my thanks to Professor A. Venkata Rao Telang, for his encouragement throughout this investigation.

The Thickness of the Rigid Water Film at a Quartz-Water Interface from a Measurement of Newton's Rings

W. G. EVERSOLE AND PAUL H. LAHR
Division of Physical Chemistry, State University of Iowa, Iowa City, Iowa

(Received May 12, 1941)

The thickness of the water film between a quartz lens and disk was determined by measuring the radii of successive Newton's rings. The squares of these radii are a linear function of the order of the rings from the center, the intercept of the extrapolated graph of which is a function only of the radius of curvature of the lens and the vertical separation of the lens and plate. By comparing intercepts obtained from data taken before and after evaporation of a water layer, a value of the order of 100A was obtained for the thickness of the water film of each interface.

THE postulate of rigid water films, though frequently made, has not met with universal acceptance. However, J. M. Macauley[1] found a greater shear force for wet than for dry glass plates, 1.5×10^{-5} cm apart, which he attributed to rigidity in the water film. Also, B. Derjaguin[2] found a rigidity in water films as much as 1.5×10^{-5} cm thick. He determined the rigidity of the water layer by its effect on the period of a torsion pendulum. In a previous paper,[3] the authors showed that the assumption of a rigid water layer 9A to 63A thick at a solid-water interface could account for experimentally determined electrokinetic potential-concentration curves without assuming large specific adsorption potentials for the alkali and halide ions.

It was decided to investigate film thickness by a study of the interference rings formed in monochromatic light reflected from a flat disk resting on a convex lens. A rigid water film should support the small weight of the disk indefinitely, whereas a viscous film would not.

A few qualitative observations serve to illustrate some possibilities and limitations of this method of film measurement. The diameters of Newton's rings fluctuate greatly for small differences in the separation of the surfaces producing them. It was difficult to get dry, clean surfaces close enough together to produce a central dark spot. The upper disk would slide easily over the lens. A slight tapping on the lens support would cause the diameter of the central ring to increase or decrease in size or even disappear, indicating variations in height of the disk of the order of 1000A. These variations in ring size may have been due in part to dust particles, it being difficult to get a dust-free dry quartz surface; or to imperfections in the surfaces, 1000A being within the tolerance allowed in lenses.

Perhaps, also, an air cushion was present. If the lens and plate were assembled inside a glass tube and evacuated for 24 hours at 110° with a Hyvac and mercury vapor pump, no appreciable change could be observed in ring size. However, if water vapor was admitted to the tube, it would condense spontaneously between the quartz surfaces. On removal of the water by evacuation, the disk would make closer contact with the lens than before. It would no longer slide easily when the lens was jarred, even though exposed to the air. And only by forcibly separating the surfaces could the initial conditions be obtained. It was difficult to remove the water from between the lens and disk and it is not certain that the prolonged evacuation used resulted in removal of all the water.

An attempt to measure an air film thickness was discarded, since the change in ring diameters before and after wetting the lens was not consistent from one trial to the next. On the other hand, determination of a water film thickness by comparison of ring diameters before and after pumping off the water from the lens gave more consistent results.

The formula used follows simply from the optics of Newton's rings.[4] Thus:

$$e_n = n\lambda/2\mu\cos\theta, \qquad (1)$$

[1] J. M. Macauley, Nature **138**, 587L (1936).
[2] B. Derjaguin, Zeits. f. Physik **84**, 657 (1933).
[3] W. G. Eversole and Paul H. Lahr, J. Chem. Phys. **9**, 530 (1941).
[4] R. A. Houston, *A Treatise on Light* (Longmans, Green and Co., New York), pp. 144, 145.

where e_n is the vertical distance between a lens and plate at the nth ring, λ is the wave-length of light, μ is the index of refraction of the fluid between the surfaces, and θ is the angle of incidence of the light on the lens (in a plane at right angles to the plane of the diagram). (See Fig. 1.) Also:

$$a_n = r_n^2/2R, \tag{2}$$

where a_n is the height of the arc subtended by the chord, r_n, and R is the radius of curvature of the lens.

From the diagram it may be seen that the minimum separation of the lens and plate t is expressed by

$$t = e_n - a_n. \tag{3}$$

Substituting the values of e_n and a_n (Eqs. (1) and (2)) in Eq. (3) yields the formula

$$t = n\lambda/2\mu \cos\theta - r_n^2/2R$$

or

$$r_n^2 = n\lambda R/\mu \cos\theta - 2Rt. \tag{4}$$

From Eq. (4) it is evident that a graph of r_n^2 *vs.* n should give a straight line having an intercept on the $n=0$ axis of $(-2Rt)$. Thus t can be calculated independently of λ, θ and μ.

Both formulas (1) and (2) involve approximations which require that R be large compared to r_n and a_n. The fact that the points fall very nearly on a straight line for the first ten or fifteen rings is taken as sufficient evidence that the above conditions were met. Any optical errors introduced by irregularities in the lens or tube employed were eliminated or diminished by subtracting, from the t obtained for a water film, the t obtained over the same portion of the lens with the film removed.

The apparatus used is shown in Fig. 2. An optically polished flat quartz plate 25 mm in diameter and 5 mm thick rested on the convex

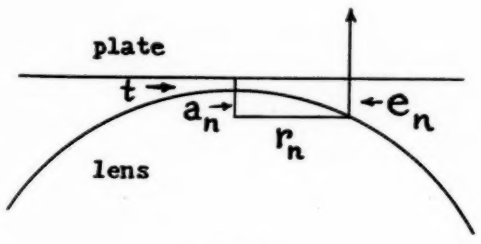

FIG. 1.

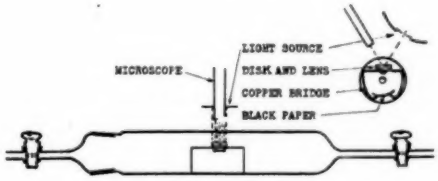

FIG. 2.

surface of a plano-convex lens of the same diameter, 2-meter radius of curvature, and 3 mm thick. A hemicylinder of glass was cemented with balsam to the bottom of the lens in order to deflect the undesirable light reflections from the lower surface of the lens. The lens and plate rested on a sheet copper bridge which could be slid into place in a Pyrex tube. The Pyrex tube or jacket could be opened at a ground glass joint, had a stopcock at one end for admitting water or dry air, and a stopcock at the other end which was connected to a Hyvac and mercury vapor pump capable of producing a vacuum of 10^{-6} cm. The tube rested horizontally across a heater element. A slit source of sodium vapor light was used to produce the Newton rings, diameters of which were measured with a low powered traveling microscope set at about a 30° angle with the axis of the lens. Dry air was admitted from a 5-foot $\frac{3}{4}$-inch glass tube filled with glass beads and P_2O_5. Water was admitted into the tube by a pipette drawn out to a capillary at its end so that it could be thrust through the open stopcock.

The general experimental procedure was to clean the lens, plate and tube, slide the lens into place in the Pyrex tube, admit a few cc of distilled water into the tube, evacuate most of the air and allow water to condense between the lens and plate. Although condensation of water between the lens and plate occurred spontaneously, the process could be hastened by suddenly heating the jacket (with the heater element and hot towels) to raise the vapor pressure. Once water condensed on the lens, the water was evaporated from the tube by prolonged pumping. Dry air was admitted from the P_2O_5 tube, the light and microscope were adjusted and the diameter of the first twenty rings recorded three times. Then the water was again admitted, the air evacuated and a water film allowed to condense. Air pressure was again brought to normal by carefully opening the stopcock and the diameter for the first twenty

TABLE I. *Calculation of Δt by the method of least squares.*

$$r^2_0=\frac{\Sigma(n)\Sigma(nr^2)-\Sigma(n^2)\Sigma(r^2)}{[\Sigma(n)]^2-N\Sigma(n^2)},$$

$$r^2_0=-2Rt, \quad R=200 \text{ cm}, \quad t=-r_0^2/400,$$

$$\Delta t=\frac{r^2_{0(\text{air})}-r^2_{0(\text{water})}}{400}, \quad \Delta t=3.3\times10^{-6} \text{ cm}.$$

n	$r^2_{(\text{water})}$	$nr^2_{(\text{water})}$	$r^2_{(\text{air})}$	$nr^2_{(\text{air})}$
2			0.0304	0.0607
3	0.0293	0.0879	.0429	.1288
4	.0382	.1529	.0560	.2241
5	.0473	.2366	.0688	.3438
6	.0562	.3373	.0818	.4908
7	.0650	.4548	.0945	.6615
8	.0735	.5880	.1072	.8576
9	.0821	.7387	.1199	1.0791
10	.0909	.9090	.1324	1.3240
11	.0995	1.0943		
12	.1085	1.3020		
13	.1172	1.5236		
14	.1254	1.7556		
Total	0.9331	9.1807	0.7339	5.1704

rings in the water film recorded three times. As a check, the water film was evacuated, air admitted and another recording made with the dried lens.

The values of r_n^2 obtained from the data when plotted against n, the number of the ring, gave very nearly straight lines. The points for the first few values of n were more variable due to the difficulty of measuring the more diffuse central rings. The line curved slightly toward the n axis for higher values of n due, perhaps, to the approximation involved in the formula $a=r^2/2R$ and to the fact that the rings were observed through a non-optical Pyrex tube. Therefore, t was determined by the method of least squares for the 2nd to the 10th ring for the air layer and for the 3rd to the 14th of the smaller water-layer rings. This involved readings taken over the same section of the lens. Values of Δt were obtained by subtracting t for the dry surfaces from the t obtained for the water film. The data and calculations for the first trial are shown in Table I. The results of five successive experiments are shown in Table II. The average Δt obtained was 230A. This involves two interfaces, so that the rigid film at a single interface would be $\Delta t/2$ or about 100A, subject of course to considerable experimental error. This value is to be compared with the films of 9 to 63A reported by the authors from a study of zeta potentials and with 750A or less reported by Derjaguin.[3] Figure 3 shows the appearance of the two curves of trial 5 when extrapolated to the $n=0$ axis.

Several factors were considered which were thought to have a possible bearing on the validity of the results. The intercepts representing r_0^2 were positive in all but one instance, indicating a negative value for the uncorrected t. Whatever the cause of these negative values (such as a flat spot on the lens or a slightly concave disk) it was assumed to affect t for the wet and dry lens equally and hence was eliminated in the values of Δt.

The surface tension of the water layer between the lens and disk is a factor which could not be similarly eliminated. However, it can be shown to be an influence opposing the formation of a rigid film. Water spreads spontaneously on a flat quartz surface even though such spreading requires an increase in the free energy of the air-water interface. The spreading of water between the lens and disk involved two quartz-water interfaces and a relatively smaller increase in the water-air surface. Consequently, the effect of surface tension was to augment the weight of the disk in compressing the water film.

According to Langmuir,[5] a repulsion would be expected between quartz surfaces in water due to the osmotic pressure of excess ions held between the surfaces by a potential resulting from "overlapping" of diffuse double layers. If the separation of the quartz surfaces t is a result of such repulsion, t should be a function of concentration of electrolyte. To test the effect of concentration on t, the lens and plate were mounted above a dark glass plate in a three-inch evaporating dish and conductivity water added until the meniscus nearly reached the top of the upper plate. Diameters of the first ten successive

TABLE II. *Results.*

TRIAL	$r^2_{0(\text{water})}$	$r^2_{0(\text{air})}$	$\Delta t\times10^6$ CM
1	0.00349 cm²	0.00482 cm²	3.3
2	.00318	.00381	1.6
3	−.00057	.00034	2.3
4	.00335	.00463	3.2
5	.00088	.00141	1.3
			Av. 2.3

[5] Irving Langmuir, J. Chem. Phys. **6**, 873 (1938).

Newton's rings were measured and solid potassium chloride added in sufficient quantity to raise the concentration of the solution above 0.1 molar. Readings were taken on successive days, care being taken to maintain the original water level by addition of distilled water. The only change after two to four days in each of five trials was a slight increase in t.

Because the diameters of the rings were dependent upon the level of the water in the dish, a slightly different procedure was tried. The lens and plate were mounted above a beaker and water solution was allowed to siphon through a capillary tube into a tiny wad of cotton which made contact with the water between the quartz surfaces. The rate of flow through the capillary was slightly greater than the evaporation rate so that excess solution dropped from the lens every few minutes. The lens and disk were pressed together while wet with conductivity water and placed in contact with 0.01 molar thorium nitrate solution from the siphon. The diameters of the first ten interference rings were measured daily for four days. A slight increase instead of a decrease in t was observed, although evaporation of the solution no doubt increased the concentration of the solution many times. Since no decrease in t was found, it is assumed that the plates were held apart by other than the "Langmuir effect."

Several observations add weight to a hypothesis of a water film between the quartz surfaces. The midpoint of the central dark spot in the Newton ring pattern is dark gray when water wets the surfaces. When the water is pumped off, the center of the dark spot becomes very black as though a true quartz to quartz contact were obtained. Also, when the two disks rest in a dish of water, the diameter of the observed rings is

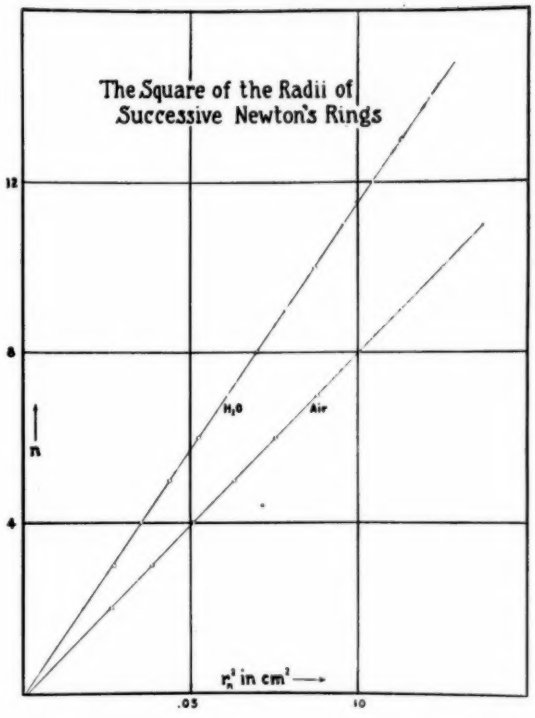

FIG. 3.

quite sensitively dependent upon the depth of the water, and hence upon the buoyant effect and surface tension of the water on the upper disk. As the water in the dish becomes deeper, the rings get smaller, indicating a greater separation of the lens and plate.

It appears from the results of this experiment that water adsorbs on quartz in a rigid multilayer the minimum thickness of which is of the order of 100A. Perhaps surface forces and the potential gradient at a quartz-water interface acting on water dipoles are sufficient to give rigidity to the structure of water in this region.

The Production of Concentrated Carbon (13) by Thermal Diffusion

ALFRED O. NIER AND JOHN BARDEEN
Department of Physics, University of Minnesota, Minneapolis, Minnesota
(Received June 27, 1941)

A thermal diffusion column 74 feet long and employing methane is being used for the concentration of C^{13}. Every 48 hours 308 milligrams of methane are removed in which the C^{13}/C^{12} ratio has been increased 11.5 times. The power consumption is 6490 watts and six liters/minute of cooling water is used. An expenditure of 156 kw-hr. of energy thus results in a transport of 13.5 mg of C^{13} per 24 hours. The measured output is in good agreement with the value computed from the theory.

THE thermal diffusion method of Clusius and Dickel[1] has been used in a number of cases[2] to produce methane in which the C^{13} content was increased. Two years ago a 24-foot column was constructed in this laboratory with which it was possible to obtain a satisfactory check[3,4] of the theory of operation proposed by Furry, Jones and Onsager.[5]

The question arose as to how this column might be extended to become useful for the production of methane in which the C^{13} content had been increased from a normal 1.1 percent to at least 10 times this value. The fact that brass tubing is made in lengths of approximately 12 feet and that there was available a vertical space of approximately 36 feet suggested the use of a 72-foot column broken into two parts.

Furry, Jones and Onsager[5] have shown that if τ represents the transport of gas along the tube and if C_1 is the concentration of $C^{13}H_4$ at any point along the tube and if the rate of removal of $C^{13}H_4$ from the lower end of the column is $C_1{}^L\tau$ one may write

$$C_1{}^L\tau = H\left[C_1(1-C_1) - \frac{1}{2A}\frac{dC_1}{dz}\right] + C_1\tau, \quad (1)$$

where A and H can be computed in terms of various constants for the gas, and the pressure, temperature and dimensions of the column.

The solution of (1) subject to the condition that C_1 is small is

$$C_1{}^L/C_1{}^0 = (1+n)/\{n+\exp[-(1+n)2AL]\}, \quad (2)$$

where $n=\tau/H$ and L is the length of the column.

Table I gives the computed concentration and transport under various operating conditions for a 72-foot column similar to the 24-foot one previously investigated.

In substituting in Eq. (2) $2AL$ was taken as

$$(6.58/p^2)/(1.63+0.208/p^4), \quad (3)$$

where p is in atmospheres pressure. This value is three times the empirically measured value[3] for the 24-foot section. H was computed from Eq. (30) of reference 5.

The concentrations given are all somewhat high as they are based upon the assumption that $C_1 \leqq C_1(1-C_1)$. Only in the cases of the high concentrations would this discrepancy be serious. It appears that operation at a pressure of one atmosphere with a drain of 0.150 g of CH_4 per 24 hours would give sufficient concentration with reasonable economy. Moreover operation at a pressure of one atmosphere or slightly over would minimize difficulties should the system have any small leaks.

TABLE I. *Approximate separation factor* $\frac{C_1{}^L}{C_1{}^0}$ *for* C^{13} *and transport in mg of* C^{13} *per day for average* $C_1{}^0 = 0.01$.

PRESSURE (ATMOS.)	0.6		0.8		1.0		1.2	
g CH_4 removal per day	$\frac{C_1{}^L}{C_1{}^0}$	Transport	$\frac{C_1{}^L}{C_1{}^0}$	Transport	$\frac{C_1{}^L}{C_1{}^0}$	Transport	$\frac{C_1{}^L}{C_1{}^0}$	Transport
0.05	16.9	5.4	28.1	8.2	22.4	6.9	12.0	4.0
0.10	9.1	6.2	16.3	10.5	15.7	10.2	10.6	7.2
0.15	6.53	6.9	10.3	10.5	12.2	12.2	9.58	9.8
0.30	3.76	8.2	5.82	12.4	7.65	16.0	6.93	14.6
0.45	2.85	9.3	4.22	13.6	5.70	18.2	6.11	19.4

[1] K. Clusius and G. Dickel, Nature **26**, 546 (1938); **27**, 148 (1939).
[2] H. S. Taylor, Nature **144**, 8 (1939); T. I. Taylor and G. Glockler, J. Chem. Phys. **7**, 851 (1939); **8**, 843 (1940); W. W. Watson, Phys. Rev. **56**, 703 (1939); **57**, 899 (1940).
[3] A. O. Nier, Phys. Rev. **57**, 30 (1940).
[4] J. Bardeen, Phys. Rev. **57**, 35 (1940).
[5] W. H. Furry, R. C. Jones and L. Onsager, Phys. Rev. **55**, 1083 (1939).

From the standpoint of maximum power economy it would be desirable to use a column for which the average circumference of the annular gas-containing space varied approximately inversely with the concentration along the column.[5,6] Such a column would not be practical to build so one would reduce the size by a number of stages having progressively smaller cross sections from top to bottom. Such an arrangement would not give quite the output of a continuous large column but would require considerably less power.

The arrangement used in the present work is shown in Fig. 1. Table II gives the dimensions and other pertinent data concerning the several sections. Section 1 is the original one[3] and section 2 was an extension added later. The combination operated at a pressure of 0.8 atmosphere with the hot walls at 300°C and produced 170 milligrams of CH_4 per 24 hours in which the C^{13} content had been increased by a factor of 6.0. In the fall of 1940 section 3 was added, the temperatures of the hot walls raised to approximately 380°C and the pressure to 1 atmosphere.

Section 1 is connected to the 150-liter reservoir by means of two leads of ordinary $\frac{1}{4}$-inch copper refrigerator tubing. A pump P_1 circulates the gas. This consists merely of an iron cylinder which moves up and down with a period of approximately one second in a brass tube surrounded by solenoid actuated by a multivibrator oscillator. A small piece of rubber dam over a hole in the iron cylinder and a similar valve in an obstruction in the brass tube insure the unidirectional flow of gas in the tube. The pumping speed of several cc per second is sufficient to maintain equilibrium between the column and reservoir.

TABLE II. *Data on the three sections of column.*

	No. 1	No. 2	No. 3
Length (ft.)	24	14	36
(cm)	730	427	1100
Diameters (inches)			
Steel heated surface			
O. D.	1.375	0.750	0.375
I. D.	1.305	0.312	0.277
Brass cooled surfoce			
O. D.	2.000	1.375	1.000
I. D.	1.936	1.291	0.928
Spacing "d" between hot and cold walls (cm)	0.712	0.69	0.71
Average circumference "B" of annular space (cm)	12.5	8.13	5.23
Size Nichrome V heating wire (B. and S. gauge)	8	14	14
Voltage	61.6	61.6	109
Current (amp.)	55.2	21.9	15.9
Power (watts)	3400	1350	1740
Temp. °C. Hot wall	380	385	367
Cold wall	~27	~27	~27
$2AL$	1.21	0.78	1.82
H (g/sec. of CH_4)	3.24×10^{-5}	1.89×10^{-5}	1.36×10^{-5}
Volume of upper reservoir	150 liters		
Volume of lower reservoir	500 cc		

[6] W. Krasny-Ergen, Phys. Rev. **58**, 1078 (1940).

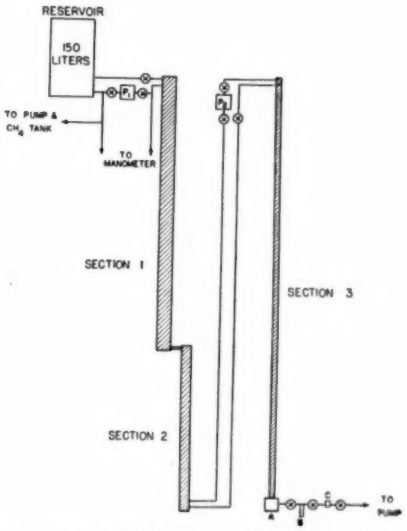

FIG. 1. Schematic drawing showing arrangement of sections of column.

Section 2 is connected directly to section 1 by means of a short brass tube (length = 5 cm, diameter = 1.8 cm). Because of the limited vertical space available section 3 is set next to 1 and 2 and is connected to 2 by two leads of $\frac{1}{4}$-inch copper refrigerator tubing one of which contains a pump P_2 similar to P_1.

The construction of sections 2 and 3 was similar to that of 1 except that the steel tubing constituting the hot walls had sufficient thickness to eliminate the necessity for the extra tube used in section 1 to center the heating wire.

The methane is kindly supplied by the Southern California Gas Company and is over 99 percent pure. Every 48 hours 550 cc of gas is removed from the bottom by attaching a bulb at the point marked C between the valves. B is a small appendage which contains KOH pellets for the removal of CO_2. As the column is extremely efficient in separating heavy impurities in the methane the output is only approximately 75 percent methane. The equivalent steady drain of concentrated methane is thus 6.4 mg/hr. The C^{13}/C^{12} ratio in this is 11.8 percent. Every 8 days the contents of the upper reservoir are

changed after closing the valves between column and reservoir. The C^{13} in the reservoir is never depleted by more than 15 percent. The average C^{13}/C^{12} ratio in the reservoir is thus 0.0103. The average concentration produced by the column is hence 11.5 times.

The C^{13}/C^{12} ratio at the top of section 3 is 0.030. Sections 1 and 2 together change the concentration by a factor of 2.9 whereas section 3 produces a change of 4.0 times.

These data are not sufficient to determine empirically both the separation factor exp $(2AL)$ and the transport (H) for the different sections of the column. It is of interest, however, to compare the observed changes in concentration with those expected from theoretical considerations. The separation factor for the 24-foot section can be estimated from the empirical expression found earlier, i.e. $\frac{1}{3}$ of (3).

This expression was obtained when the temperature difference between the walls was 300°C. Since the operating temperature difference is now about 350° a slight change is necessary. The numerator and the first term in the denominator should be more or less independent of temperature, while the second term in the denominator should vary roughly as $(T/\Delta T)^2$, where T is the mean temperature and ΔT the temperature difference. The value of $2A_1L_1$ obtained from (3) with this correction from the change in temperature is noted in Table I. The same expression has been used to estimate the expected values for $2A_2L_2$ and $2A_3L_3$ for the second and third sections. The value of A for the third section was taken to be the same as the A for the first section. A correction for the difference in spacing (d) was made in obtaining $2A_2L_2$ for the second section. These estimates assume that the correction for asymmetry in the temperature distribution is the same for all three columns. Without further information about the operation of the columns, this is probably as good a guess as any. The transport coefficients, H, as computed from the theoretical expression[7] of Furry, Jones and Onsager, are also listed for the three sections.

It is not difficult to compute from these values and a combine formula similar to (2) the concentration to be expected for any given rate of drain. If methane is drawn at a steady rate of 6.4 mg/hr., the calculations yield a concentration of 12.5 times for the whole column and of 3.0 for the first two sections, as compared with the observed 11.5 and 2.9, respectively. The calculated values are thus a little higher than those obtained in practice.

The discrepancy between practice and theory could be due to a number of factors. The rate of drain is not constant but intermittent. This means that each time a sample is removed the lower end of section 3 is disturbed abruptly. This disturbance is transmitted through the entire system. Also, no doubt, due to the action of the pumps there is a certain amount of remixing at the ends of the columns, a factor which would cut down the effective over-all length. In the previous work it was shown that in section 1 there was some remixing due to some asymmetry. It might well be true that this is different for 2 and 3 than for 1. The existing line voltage fluctuation of 4 percent would also contribute to the remixing. No account has been taken in the computations of the impurities.

This apparatus has been in continuous use since the fall of 1940 and has required practically no attention aside from time spent in removing the samples from the bottom and replenishing the gas at the top. It would thus be fair to state that including what little maintenance there is, not over $1\frac{1}{2}$ hours per week of a man's time was needed.

Starting from scratch, it would probably be easier to build up the column by connecting standard sections in series and parallel. The third section which is 36 feet long may be a convenient choice. With two of these sections in parallel feeding a third in series, we compute a multiplication of 11.2 times for the same rate of drain as used above. With three sections in parallel feeding one in series the factor is 14 times. Probably the values obtained in practice would be somewhat less than these theoretical values as was true in the case investigated.

In the design of any new column one would, of course, choose the heating wires of such a size that an autotransformer would not be necessary as was the case for sections 1 and 2 of our set-up.

The authors are indebted to Mr. Rudolph Thorness for his skill in constructing and assembling the columns.

[7] Because of the numerous approximations made, it was not felt justified to correct H, A, and K_D/K to allow for the cylindrical construction of columns. See W. H. Furry and R. C. Jones, Phys. Rev. **57**, 561 (1940).

The Heat Capacities of Molecular Lattices

I. Introduction

R. C. LORD, JR.
Department of Chemistry, The Johns Hopkins University, Baltimore, Maryland

(Received June 5, 1941)

The interpretation of the heat capacities of molecular crystals is discussed. The assumption is made that the lattice part of the molecular heat capacity can be represented by a single Debye function with the appropriate number of degrees of freedom. The reasons for supposing that this assumption is valid are considered, and it is shown that one can reasonably expect its validity except at temperatures low in comparison with the characteristic temperature θ of the Debye function. It is proposed to apply this point of view to the interpretation of the heat capacity curves of a number of molecules. The conversion of C_v to C_p is discussed for molecular lattices.

IT has been widely recognized that the theory of specific heats developed by Debye for atomic lattices has its shortcomings. Nonetheless it has been attended with much success from an empirical point of view. The number of examples of atomic specific heats which depart markedly from the Debye curve because of the inexactness of the Debye theory is small. Moreover, the development of a more exact theory has been precluded up to the present by the inherent difficulties of the problem, and it seems hardly probable that an improved theory is going to better the concordance between theory and experiment to any great extent.

In the last twenty years or so a considerable body of accurate heat capacity measurements on molecular crystals has accumulated. It appears quite likely that a satisfactory analysis of these measurements will yield valuable information about molecular structures in the same fashion that analysis of atomic heat capacities has led, in the past, to increased knowledge of atomic and lattice structure. Analysis of molecular heat capacities in the solid state, of course, must rest on some theory of lattice heat capacity. Pending the development of a tractable theory to supplant Debye's for atomic lattices, it seems desirable to carry out this analysis as far as possible on the basis of the Debye theory. It is the purpose of the present series of papers to make such an analysis of the heat capacity data for a number of molecular crystals, and to point out examples of the sort of information on molecular and lattice structure which can accrue from study of heat capacities in the solid state.

BRIEF SURVEY OF HEAT CAPACITY THEORY

A crystal composed of N atoms has $3N$ degrees of freedom. If we suppose the interatomic forces to be purely harmonic ones, that is to say, Hooke's law forces, all $3N$ degrees of freedom[1] are associated with harmonic vibrations. If we know the interatomic force constants and the atomic masses we can then, in principle, calculate the $3N$ normal coordinates and their vibrational frequencies. Once these latter are known, the heat capacity of the lattice at constant volume C_v can be immediately calculated from the expression

$$C_v = k \sum_{i=1}^{3N} \frac{x_i^2 \exp(x_i)}{(\exp(x_i)-1)^2}, \tag{1}$$

where k is Boltzmann's constant and $x_i = h\nu_i/kT$. The ν_i are the various frequency values.

The problem of finding C_v thus reduces to that of finding the ν_i. The simplest assumption, made by Einstein in his original theory of C_v, is that all the ν_i are equal, in which case

$$C_v = 3R[x^2e^x/(e^x-1)^2]. \tag{2}$$

The C_v-temperature curve given by (2) deviates from observation at low temperatures, but agrees not too badly, considering the crudity of the assumption, with the general form of the observed curve. Much better agreement is found if one makes the assumption of Debye that the number of degrees of freedom N_i having frequency ν_i is given by

$$N_i = \alpha\nu_i^2, \tag{3}$$

[1] We must except the six degrees of translational and rotational freedom of the crystal as a whole, but these six are negligible in comparison with the other $3N-6$.

α being a proportionality constant. This assumption is based on an analogy of the vibrations of a discrete lattice with those of an isotropic continuum. The principle difference between the two cases is that the continuum has an infinite, the lattice a finite (i.e., $3N$), number of normal vibrations. The distribution of frequencies given by (3) is therefore cut off at that ν value, $\nu_{\max}$, which gives a total of $3N$ ν values between zero and $\nu_{\max}$. The C_v due to this set of frequencies is

$$C_v = 3R\left[\frac{3}{x_{\max}}\int_0^{x_{\max}} \frac{x^4 e^x dx}{(e^x-1)^2}\right]. \qquad (4)$$

Detailed dynamical treatment of lattices in an attempt to find a rigorous distribution function to replace (3) which could be expressed in terms of the independently measurable elastic constants of the crystal has been carried out by Born[2] and more recently by Blackman.[3] Such studies show that the real distribution function may deviate widely from (3), but attempts to determine a more exact frequency distribution law which yields a workable C_v equation have thus far been unsuccessful. One reason for this lack of success is the difficulty of solving the dynamical problem of finding the distribution law. A second is the unfortunate one that even when the distribution law is known, the integration of Eq. (1) offers further trouble. Because of these difficulties and of the empirical successes of the Debye theory, the Debye equation remains the only generally useful one for the interpretation of lattice C_v in atomic crystals.

The first step in the extension of the lattice theory of specific heats to molecular crystals is to suppose that the N atoms of the lattice are grouped into molecules of S atoms each in such a way that the extramolecular forces are much weaker than the intramolecular. As a result of this disparity, the $3N$ degrees of freedom can be classified conveniently into $6N/S$ extramolecular and $(3S-6)N/S$ intramolecular degrees.[4] Two assumptions are now made: (1) The frequencies corresponding to the $(3S-6)N/S$ intramolecular degrees of freedom are (N/S)-fold degenerate; (2) these (N/S)-fold degenerate frequencies have values quite close to the $3S-6$ frequencies of the S-atomic molecule in the gas phase. Under these assumptions that part of C_v due to the intramolecular frequencies is given by Eq. (1), in which the summation runs over the $3S-6$ frequencies, the entire sum being multiplied by N/S. When a knowledge of these frequencies is at hand, from spectroscopic sources for example, the intramolecular part of C_v can be calculated without difficulty.

To obtain the extramolecular part of C_v (hereafter called "lattice C_v") we need the $6N/S$ frequency values associated with the extramolecular degrees of freedom. Experience with atomic lattices has shown that we cannot expect to find these frequencies in any direct fashion. It is necessary to make assumptions about the apportionment of the $6N/S$ degrees of freedom among various frequency values. The distribution schemes are naturally more varied for the molecular lattice than for the atomic:

(1) One can make the assumption, analogous to that of Einstein for atomic solids, that all $6N/S$ ν values are the same. The lattice C_v is then given by the simple Einstein formula (Eq. (2) with $6R$ in place of $3R$). The agreement between calculated and observed temperature dependence of C_v under this assumption is little better than that exhibited by the Einstein equation for atomic lattices.

(2) The $6N/S$ degrees of freedom can be classified into $3N/S$ degrees associated with the motion of the center of gravity of the molecule and $3N/6$ with angular displacements about the center of gravity. The former degrees of freedom (the "translational") may be assumed to have frequencies distributed in the Debye fashion and thus to have a C_v given by the Debye function. The $3N/S$ angular degrees of freedom (the "rotational"), on the other hand, may be supposed, as was first suggested by Born[5] to possess frequencies nearly alike. An Einstein function will represent, in that case, the C_v due to the angular vibrations. To calculate the lattice C_v, then, two frequency values are needed: the $\nu_{\max}$

[2] M. Born, "Atomtheorie des festen Zustandes," Encyl. Math. Wiss., Vol. 5, part 3. M. Born and M. Goeppert-Mayer, "Dynamische Gittertheorie der Kristalle," *Handbuch der Physik*, Vol. 24, Part 2.

[3] M. Blackman, Proc. Roy. Soc. **A148**, 365 (1934) *et seq.*

[4] For linear molecules these figures are respectively $5N/S$ and $(3S-5)N/S$. *Mutatis mutandis*, everything said in the text for non-linear molecules applies equally well to linear ones.

[5] M. Born, *Dynamik der Kristallgitter* (Teubner, Leipzig, 1915). See particularly Eq. (200), p. 77.

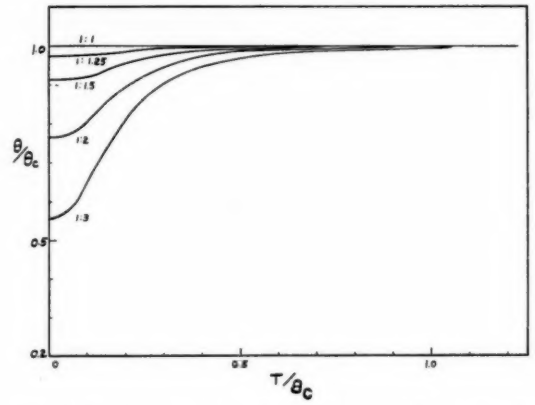

FIG. 1. Temperature trend of apparent θ for molecular lattices. Rotational degrees of freedom assumed to follow a Debye curve.

for the Debye distribution and the average ν, ν_{rot}, for the angular vibrations. The requisite information for the dynamical calculation of the θ values corresponding to $\nu_{\max}$ and ν_{rot} is ordinarily not available and there is no direct way of finding them independently of thermal measurements. *A priori* calculation of the lattice C_v on the foregoing basis is, therefore, not possible. By trial and error, however, one can find those values of $\theta_{\max}$ and θ_{rot} which give the closest representation of C_v. It is found, in practice, as shown, for instance, by Eucken and his coworkers,[6] that the representation so obtained is often very good.

(3) A third classification assumes that the $3N/S$ angular degrees of freedom have frequencies distributed in the Debye fashion.[7] This distribution is known when the $\nu_{\max}$ is known, and the calculation of the lattice C_v then involves a knowledge of two $\theta_{\max}$ values. Since this information is no more obtainable on *a priori* grounds than were the θ values of the previous classification, one cannot do more than compare the lattice part of the observed C_v with that calculated from two Debye functions using arbitrary θ values. The representation of the observed C_v in this function is just as good as that obtained with the assumptions of (2).

The two preceding assumptions undoubtedly are overly simple and are only a rough approximation to the actual frequency distribution for the extramolecular degrees of freedom. That both of them reproduce the lattice C_v rather accurately is attributable to two causes: (a) Even if a frequency distribution function is only approximately correct, the C_v calculated from the distribution may often be very close to the true C_v.[8] (b) The liberty of choice of two parameters (the two θ's) clearly makes possible the better matching of calculation with observation.

The usefulness of crystalline heat capacity data in aiding the solution of molecular structural problems is enhanced if we can find a simple and satisfactory way of allowing for the lattice C_v. It seems to the writer preferable to adopt *for this purpose* the assumption (3), with the further restriction that the $\theta_{\max}$ for the rotational degrees of freedom be assumed equal to the $\theta_{\max}$ for the translational ones.[9] Such a simplification reduces to a minimum the number of parameters in terms of which the lattice C_v is expressed. When the θ values for the translational and rotational degrees of freedom are equal, the $6N/S$ extramolecular frequencies give rise to a specific heat expressed by the usual Debye equation (4) except that the $3R$ of that equation is replaced by $6R$.

At first sight it may seem completely unjustifiable to make such a restrictive *a priori* assumption about the relative sizes of the $\theta_{\max}$. It is shown below, however, that as long as the two θ's are not drastically different, the lattice C_v is rather accurately representable by a Debye function in which a kind of mean $\theta_{\max}$ is used. The two values in many actual molecular crystals turn out empirically to be close together. This is not surprising when we consider that molecules of relatively high molecular weight, on which $\theta_{\max}$ for the translational degrees of freedom

[6] See, for example, A. Eucken and E. Schröder, Zeits. f. physik. Chemie **B41**, 307 (1938).

[7] This classification was first proposed by D. H. Andrews, Proc. K. Akad. Amst. **29**, 744 (1926).

[8] This fact probably accounts for much of the success of the Debye theory. It is interesting to note that those authors who wish to emphasize the virtues of the Debye theory do so by comparing calculated and observed C_v (e.g., E. Schrödinger, *Handbuch der Physik*, Vol. X, p. 305 ff.). Those who are more concerned with its shortcomings (Blackman, reference 3; R. H. Fowler, *Statistical Mechanics* (Cambridge University Press, 1936), second edition, p. 131; W. H. Keesom and C. W. Clark, Physica **2**, 698 (1935), etc.) compare θ values obtained from C_v at various temperatures with the theoretically constant θ demanded by Debye theory.

[9] This additional restriction was first made by Andrews (reference 7), in his original treatment of C_v for crystalline benzene. It is particularly valid for that crystal.

depends, ordinarily have correspondingly high moments of inertia, which determine the rotational θ_{max}. The most important exception to this generalization is the class of molecules whose molecular weights are made up mostly of atomic weights much heavier than hydrogen but whose moments of inertia are determined chiefly by hydrogen atoms. The hydrogen halides, water, ammonia and methane are good examples of the class. For them, however, our fundamental assumption of harmonic extramolecular forces is very bad and we could scarcely expect to understand their heat capacities on the basis of any theory restricted to harmonic vibrations. Accordingly, we shall make no attempt, in the present group of articles, to consider any molecular crystal whose C_v depends on higher terms than the quadratic in the power series expressing intermolecular potential as a function of intermolecular distance.

The accuracy with which the lattice C_v of a molecular crystal can be represented by a six-degree Debye function involving a single θ_{max} may be shown as follows. Suppose, for a given crystal, the θ_{max} for the translational and rotational degrees of freedom are equal. If the lattice C_v of this crystal be utilized to find the value of the Debye θ at various temperatures, θ will, of course, be found to have a fixed value independent of T. A plot of θ *versus* T will show a horizontal straight line. If the two θ_{max} have slightly different values, however, the resultant lattice C_v, when utilized to find θ as a function of T, will give a θ value which is not constant but which has a temperature-dependent trend. The nature of this trend is illustrated in Fig. 1. The ordinate gives the value of the apparent θ obtained at any temperature by substituting the lattice C_v in the Debye equation. The lattice C_v at any T is found by adding the C_v due to the translational degrees of freedom and the C_v due to the rotational degrees. These C_v values are found from the Debye equation in which assumed values of θ_{max} for the respective degrees of freedom have been used.

For example, if a hypothetical molecular crystal has a θ_{max} for translation of 150° and θ_{max} for rotation of 300°, it will have a lattice C_v given by the sum of two Debye equations [Eq. (4)] in which the respective θ's have been

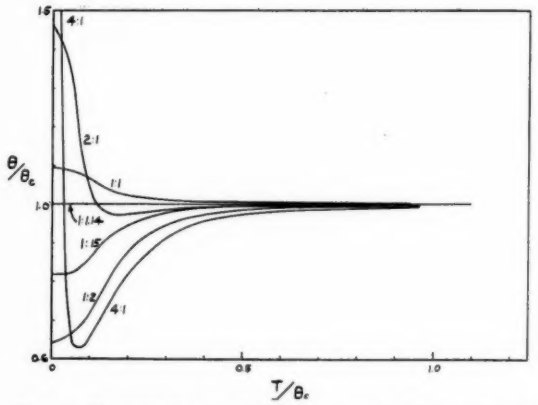

FIG. 2. Temperature trend of apparent θ for molecular lattices. Rotational degrees of freedom assumed to follow an Einstein curve.

used. This lattice C_v may be used in conjunction with a six-degree Debye equation [Eq. (4) in which $6R$ replaces $3R$] to calculate an apparent θ. The apparent θ will be somewhere between the two original θ values at all temperatures, but will exhibit the above-mentioned trend. What we want to investigate is the quantitative character of this trend for hypothetical values of the θ's in order that we may interpret the trends observed in the apparent θ's in actual molecular crystals.

In order to make the curves in Fig. 1 somewhat more general, the θ values are plotted as fractions of the constant θ value (referred to as θ_c), which they ultimately reach at high temperatures. The temperature scale is correspondingly generalized by plotting temperature as a fraction of θ_c. This generalization enables the comparison of the temperature dependence of the apparent θ for various real crystals, regardless of whether the actual θ values are large or small. That the apparent θ's do approach a limiting high temperature value can readily be shown by using the form for the Debye equation at high temperatures:

$$C_v = 3R\left(1-\frac{1}{20}\frac{\theta^2}{T^2}\right). \tag{5}$$

By adding together the C_v terms given by two of these equations, each with its own θ, and equating the sum to a six-degree function [Eq. (5) in which $6R$ replaces $3R$], the limiting high temperature θ value in the latter may be found. It is

$$\theta_c = [(r^2+1)/2]^{\frac{1}{2}}\theta_{trans}, \tag{6}$$

in which θ_{trans} is the θ value assumed for the translational degrees of freedom and $r=\theta_{rot}/\theta_{trans}$. θ_{rot} is the other θ value.

In plotting the curves of Fig. 1, various ratios of translational to rotational θ values have been used. These ratios are indicated on the respective curves. Thus the curve marked "1 : 2" represents the apparent θ trend for a crystal whose respective translational and rotational θ's are, say, 100 and 200. The θ_c for these two values is somewhere in the neighborhood of 150, to be exact at 158. To obtain the ordinate points, then, every apparent θ was divided by 158, and the temperature scale was altered similarly by dividing each temperature by 158. In this way a curve is obtained which is independent of the initial θ values; precisely the same curve would have been found if the initial θ's had been chosen, for example, as 500 and 1000.

The curves of Fig. 1 show clearly that a single θ value (corresponding to θ_c) can be used to represent the lattice C_v curve with accuracy comparable to that of experiment at temperatures above 0.3–$0.4\theta_c$, even though the translational and rotational θ values may differ considerably. Of course, when the two θ's are not far apart, the representation is accurate to much lower temperatures. We can, therefore, express the lattice C_v in terms of a single θ with sufficient accuracy in that temperature range where the *intramolecular* C_v usually becomes of interest, namely from 0.3–$0.4\theta_c$ up to a few degrees short of the melting point. In the latter neighborhood the anharmonicity of the lattice frequencies becomes important and no theory based solely on harmonic vibrations holds good.

In addition to calculating the θ *vs.* T curves on the basis of Debye theory (Fig. 1), curves were calculated also on the assumption that the rotational degrees of extramolecular freedom had only one frequency, i.e., that the rotational degrees contributed to C_v according to the Einstein equation. These curves are given in Fig. 2. In order to calculate the limiting value of θ when the rotational C_v follows an Einstein curve, it is, of course, necessary to use the high temperature Einstein equation analogous to Eq. (5). It is

$$C_v=3R\left(1-\frac{1}{12}\frac{\theta^2}{T^2}\right). \tag{7}$$

This equation, coupled with the Debye equation for the translational degrees of freedom, leads to

$$\theta_c=[(5r^2+3)/6]^{\frac{1}{2}}\theta_{trans}. \tag{8}$$

The general form of the curves in Fig. 2 is not much different from that of the curves in Fig. 1 so long as we consider only $\theta_{rot}/\theta_{trans}$ ratios larger than 1.14. When the ratio is smaller, the apparent θ curve rises above the θ_c asymptote at sufficiently low temperatures. As can be seen from Fig. 1, such a rise does not occur, regardless of the relative values of the θ's, when both translational and rotational degrees of freedom follow a Debye frequency distribution. Figure 2 shows that when the rotational θ is well below that for translation, a pronounced minimum develops in the apparent θ curve. As one proceeds to sufficiently low temperatures, however, the Debye heat capacity will ultimately become larger than the Einstein, and the apparent θ curve will, in the end, always rise above the θ_c value.

The close similarity between the curves in Fig. 1 and those of Fig. 2 whose ratios are less than 1 : 1.14 means that an apparent θ *vs.* T plot for a real crystal will not make clear whether the rotational degrees of freedom give rise to a Debye or an Einstein specific heat contribution. Of course, if, for a real crystal, the Einstein θ were smaller than the Debye θ and heat capacity data were available to sufficiently low temperatures, one might be able to decide by the upturn in the curve at low temperatures that the rotational degrees have Einstein heat capacity. It does not, however, seem probable physically that the rotational θ should be much, if at all, lower than the translational θ. Indeed, in the molecular crystals so far studied, the curves follow the form of those in Fig. 1. The only conclusion to be drawn from Fig. 2 for our purpose is that the lattice C_v can be represented at temperatures above 0.3–$0.4\ \theta_c$ by a single six-degree Debye function, even when the rotational degrees of freedom contribute to the lattice C_v according to the Einstein equation.

Curves analogous to those of Figs. 1 and 2 can be drawn for molecular crystals whose molecules have only two degrees of rotational freedom. These curves differ not at all qualitatively, and very little quantitatively, from those of Figs. 1

and 2. It can be easily shown that the equations for linear molecules analogous to (6) and (8) are, respectively:

$$\theta_c=[(2r^2+3)/5]^{\frac{1}{2}}\theta_{\text{trans}} \tag{9}$$

and

$$\theta_c=[(10r^2+9)/15]^{\frac{1}{2}}\theta_{\text{trans}}. \tag{10}$$

In the papers following this Introduction, the heat capacities of a number of molecular crystals will be interpreted by assuming that the lattice part of the C_v can be represented by a Debye function with a single θ, and the appropriate number of degrees of freedom. When the lattice C_v has been subtracted from the total, the remainder will be used as a source of information concerning other degrees of freedom of the molecule. The kinds of information obtainable are varied and of considerable interest in connection with questions of molecular structure. For instance, the location with fair accuracy of low molecular frequencies which are, for one reason or another, spectroscopically inaccessible can often be accomplished. The structure of molecules in the solid state can sometimes be determined—for example, the linearity or nonlinearity of a molecule can be established. It may also prove possible to determine the energy of a low-lying electronic level, or the frequency of a molecular vibration associated with restricted rotation within the molecule.

The paper following this one will deal with a case in which the temperature trend of the Debye θ for a presumably atomic lattice can be reduced considerably by assuming an association of atoms into diatomic molecules. We will then consider a number of simple molecules for which both the specific heat[10] and the molecular energy levels are accurately known, to illustrate the accuracy with which C_v can be calculated when all the molecular information is available. Among these molecules are Cl_2, CO_2, benzene and benzene-d_6. Following this demonstration of the applicability of the method, consideration will be given to certain molecules whose heat capacities yield hitherto unavailable information.

[10] It has been our experience in these calculations that accurate specific heat data are quite essential. Fortunately, the accuracy of much of present-day thermal data on molecules, particularly those studied by Giauque and his collaborators, is ample for our purposes.

The Determination of C_v from C_p

The greatest difficulty in the utilization of heat capacity data for molecular crystals arises in the conversion of experimentally measured C_p to C_v. This conversion can be accomplished at any temperature by means of the thermodynamic formula

$$C_p-C_v=\alpha^2VT/\beta. \tag{11}$$

Use of Eq. (11), however, requires a knowledge of α, the coefficient of thermal expansion, β, the coefficient of compressibility, and V, the molar volume, all of which are functions of temperature. The necessary information is often available for atomic lattices[11] but rarely is for molecular crystals. Some modification is, therefore, required of Eq. (11) which will enable one to use it in the absence of complete knowledge of the T dependence of α, β and V.

The important factor in the right-hand member of Eq. (11) is α^2, since the temperature dependences of both β and V are small and to a large extent compensatory. The thermal expansion of a crystal whose atoms are held in their equilibrium positions by *purely harmonic* forces is zero. The expansion observed in actual crystals is due to the anharmonic character of these forces. Grüneisen,[12] has developed an equation for the temperature dependence of α which shows this explicitly. Extension of Grüneisen's reasoning to molecular lattices can be made in the following way.

It can be shown[13] by thermodynamic argument, combined with the theory of quasi-harmonic lattice vibrations, that the thermal expansion of a crystal is given by

$$\alpha=\frac{\beta}{V}k\sum_{i=1}^{3N}f_E\left(\frac{\theta_i}{T}\right)\left(\frac{\partial \ln \theta_i}{\partial \ln V}\right), \tag{12}$$

where f_E is the Einstein function given in Eq. (1) and the summation extends, as it does in Eq. (1),

[11] See, for example, R. C. Lord, Jr., J. Chem. Phys. **9**, 700 (1941) (this issue).

[12] E. Grüneisen, *Handbuch der Physik*, Vol. X, p. 22 ff.

[13] Cf. Grüneisen (reference 12); see also A. Eucken, *Handbuch der Experimentalphysik*, Vol. VIII, part 1, p. 281. The discussion here given of the C_p-C_v formula for molecular crystals was indicated in outline in Lord, Andrews, and Ahlberg, J. Chem. Phys. **5**, 651 (1937). A lucid discussion of thermal expansion and the equation of state of solids will be found in J. C. Slater, *Introduction to Chemical Physics* (McGraw-Hill, 1939), Chapter XIII Slater derives Eq. (12) (p. 219, Eq. (4.13)).

over the $3N$ vibrational degrees of freedom of the crystal. The factor $(\partial \ln \theta_i)/(\partial \ln V)$ gives the dependence of the vibrational frequencies on the volume of the crystal. For strictly harmonic vibrations this factor is zero. For quasi-harmonic vibrations it is an index to the relationship between the amplitude of the atomic vibrations and the volume of the crystal. The f_E-factor gives the temperature-rate at which the crystal takes up energy, i.e., increases amplitude of vibration. The product of these two factors is then an index of the temperature-rate of volume change. As we have mentioned above, the T dependence of β and V is not great, and we will regard their quotient as a T-independent constant. We will, in addition, assume that each $(\partial \ln \theta_i)/(\partial \ln V)$ is a T-independent constant. This approximation is good as long as the anharmonicity is small.

To find a workable expression for α, (12) can be simplified with the help of our discussion of the classification of the $3N$ vibrations of a molecular crystal. The sum in (12) can be broken up in the following way:

$$\sum_{j=1}^{6N/S} f_E\left(\frac{\theta_j}{T}\right)\left(\frac{\partial \ln \theta_j}{\partial \ln V}\right)+\frac{N}{S}\sum_{k=1}^{3S-6} f_E\left(\frac{\theta_k}{T}\right)\left(\frac{\partial \ln \theta_k}{\partial \ln V}\right). \quad (13)$$

The $6N/S$ extramolecular vibrations have been postulated to follow a Debye distribution. The implication of this distribution is that all the frequencies show the same volume dependence, i.e., that the factor $(\partial \ln \theta_j)/(\partial \ln V)$ is the same for all of the $6N/S$ frequencies. The factor can thus be removed from the summation sign, leaving a sum which is just the Debye C_v.

The right-hand member of (13) gives the contribution of the intramolecular vibrations to the thermal expansion. The sharper the separation between these frequencies and those of the crystal lattice, the less likely it is that there will be any similarity in the values of $(\partial \ln \theta)/(\partial \ln V)$ for the intra- and extramolecular frequencies. Moreover, the intramolecular vibrations themselves differ widely in character, and their anharmonicities may be supposed to differ just as widely. For this reason no further simplification of Eq. (13) is possible without the help of additional assumptions. In order to effect this simplification, we make the *ad hoc* assumption that all $(3S-6)$ values of $(\partial \ln \theta_k)/(\partial \ln V)$ are the same. It is presumed, also, that they are temperature independent. When this common coefficient is removed from the summation, the remaining sum is simply the total internal C_v of the molecule.

Equation (12) thus reduces to:

$$\alpha V/\beta = a' C_v(\text{lattice}) + b' C_v(\text{internal}), \quad (14)$$

where

$$a' = (\partial \ln \theta_j)/(\partial \ln V) \text{ and } b' = (\partial \ln \theta_k)/(\partial \ln V).$$

Substituting for α in Eq. (11) and making our usual assumption of the constancy of β/V, we find

$$C_p - C_v = [aC_v(\text{lattice}) + bC_v(\text{internal})]^2 T. \quad (15)$$

If some independent way existed for finding the a and b constants, our conversion of C_v to C_p could be readily accomplished. Unfortunately, there appears, at present, to be no way of obtaining them. Equation (15) can, therefore, be used only as an extrapolation formula. In case the α and β values are available in a limited temperature range, the a and b constants may be evaluated inside this range and $C_p - C_v$ then calculated for temperatures outside it. If even this information is lacking, Eq. (15) can be used in a purely empirical fashion by evaluating a and b from the observed $C_p - C_v$ differences in a temperature range over which the calculation of C_v is free from doubt. $C_p - C_v$ can then be calculated, for purposes of comparing observed and calculated C_p, in temperature regions where the calculation of C_v is dependent on assumptions.

In the following papers, $C_p - C_v$ will, of course, be evaluated by means of the thermodynamic Eq. (11) whenever the data are available. It will frequently happen, however, that purely empirical use of Eq. (15) must be made. Fortunately, the $C_p - C_v$ difference is often so small that even rather large percentage error in it does not interfere with straightforward interpretation of C_p. The only effect is a decrease in the closeness of the quantitative agreement between theory and experiment.

The Heat Capacities of Molecular Lattices

II. The Structure of Metallic Lithium

R. C. Lord, Jr.
Department of Chemistry, The Johns Hopkins University, Baltimore, Maryland
(Received June 5, 1941)

The failure of the Debye equation for atomic lattices to hold for the heat capacity of metallic lithium is attributed to the association of lithium atoms in the crystal into diatomic ions. It is then shown, with the help of a reasonable assumption as to the value of the diatomic vibration frequency, that the heat capacity of lithium can be understood without postulating a breakdown of the Debye theory. Some implications of this point of view for the theory of the metallic properties of lithium are pointed out and further experimental work to decide the question proposed.

METALLIC lithium provides an interesting example of the helpfulness of specific heat studies in suggesting solutions to problems of structure in solids. In 1935 Simon and Swain[1] reported an accurate investigation of the heat capacity of lithium in the range 15°–300°K. They recognized that an anomaly of some sort existed in solid lithium, because the heat capacity failed to follow a Debye curve and did not have the usual simple relationship to the coefficient of thermal expansion.[2] Simon and Swain interpreted the observed specific heat as made up of two components. The first of these was the normal lattice specific heat, which was assumed to be given by the usual Debye equation ($\theta=505°$), and to which the thermal expansion bore its usual approximate relation of simple proportionality. The second was attributed to the presence, in the atoms composing the lattice, of a single electronic energy level which lay some 140 cm^{-1} above the ground level. The sum of the contributions from the two sources agreed nicely with observed C_v over the entire range of the measurements.

This sort of interpretation had been used previously[3] to explain pronounced departures of metallic and other specific heats from the Debye curve and would have occasioned no surprise except for two difficulties. In the first place, the lithium atoms in the lattice should presumably be in the form of Li^+ ions and the existence of a sharp electronic energy level of the value postulated conflicts with our ideas of the structure of Li^+. Secondly, the Debye θ needed to reproduce the lattice portion of the specific heat curve is surprisingly high in comparison with θ's for the other alkali metals. It conflicts, moreover, with the θ value found for lithium from the temperature dependence of electrical resistance and from the temperature dependence of x-ray scattering (*vide infra*), the latter two methods giving about the same value.

For these and other reasons the suggestion of Simon and Swain is probably to be rejected, despite the satisfactory quantitative agreement between theory and experiment to which it leads. It is rejected by Fowler,[4] for example, who cites lithium as an "excellent example of a simple substance with a C_v which departs markedly from Debye's curve" because of the incorrectness of Debye's frequency-distribution function. If this be the real reason for the departure, we have no alternative but to accept the discrepancy without further comment until such time as a more satisfactory theory than Debye's is proposed. The nature of the departure, however, as shown by the decided temperature trend in the Debye θ,[5] gives us a clue to a possible means of reconciling the Debye theory with the C_v curve for lithium. Of more importance, it

[1] F. Simon and R. C. Swain, Zeits. f. physik. Chemie **B28**, 189 (1935).
[2] F. Simon and R. Bergmann, Zeits. f. physik. Chemie **B8**, 255 (1930).
[3] Cf. the review by F. Simon, Ergeb. d. exakt. Naturwiss. **9**, 253 (1930).
[4] R. H. Fowler, *Statistical Mechanics* (Cambridge University Press, 1936), second edition, pp. 131–2.
[5] See Fowler, reference 4, p. 131, Table 10.1, or Simon and Swain, reference 1, p. 190, Table 1.

leads us to an interesting conception of the structure of metallic lithium.

Suppose that we were to assume, for lack of knowledge to the contrary, that a substance such as crystalline chlorine is an atomic solid. We should then expect to find that the lattice C_v of the crystal is representable by the usual Debye equation for atomic lattices. If we substitute in this equation the observed C_v values for solid chlorine at low temperatures, we find, however, that the θ given by the C_v exhibits a marked temperature trend, increasing considerably with increasing temperature. If we have faith in the Debye equation for atomic lattices, we then infer that, for some reason, we cannot apply it to crystalline chlorine. If the reason be that solid chlorine is a *molecular* crystal, we can apply the Debye equation for *molecular* lattices as outlined in the previous paper.

In actuality, of course, the evidence is that the chlorine atoms in crystalline chlorine are in the form of diatomic molecules. We should, therefore, expect that the above temperature trend in θ would be eliminated if we remove from C_v the component due to the internal degree of freedom and use the remainder to calculate θ from a 5-degree Debye equation. A small temperature trend in θ at very low temperatures should remain, for reasons discussed in the previous paper and illustrated there by Fig. 1.

The temperature trends are plotted for monatomic and diatomic chlorine in Fig. 1. On the same axes is plotted the temperature trend for the atomic lithium θ, θ_c being set at 430. It will be seen at once that the trend in θ is similar to, but not so marked as, that found when crystalline chlorine was assumed to have an atomic lattice. If one infers from this similarity that lithium is not a monatomic solid but is diatomic, one should compute from C_v the Debye θ for *five* degrees of freedom per gram molecular weight of Li_2. We expect, then, to find a constant θ, save at very low temperatures and at high temperatures where the sixth, or internal, degree of freedom begins to contribute. The $\theta - T$ curve for Li_2 is also shown in Fig. 1.

The assumption of the existence of diatomic molecules in metallic lithium clearly carries with it serious implications with respect to the properties of the metal. First of all, because lithium *is*

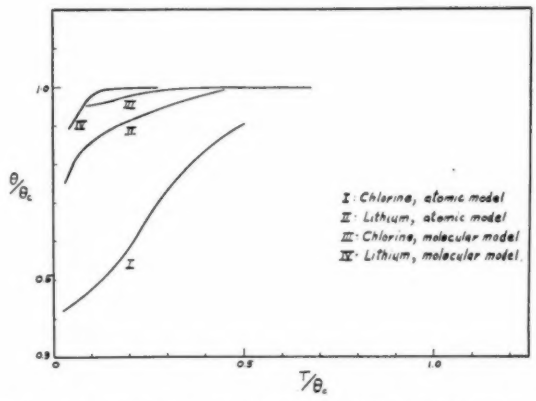

FIG. 1. Temperature trend of apparent θ's for lithium and chlorine crystals.

a metal, the form of the diatomic molecule is hardly likely to be neutral Li_2. We must presume that the molecules are ions, most probably with an electronic structure closely related to Li_2^+. The chemical binding in the latter in the gaseous state has been computed by accurate wave-mechanical methods[6] to be slightly stronger than that in neutral Li_2. The free electrons necessary for the metallic properties of lithium are thus available, although the number of them is in principle reduced by a factor of two.[7]

A question which is of immediate importance for heat capacity theory is that of the numerical value of the internal vibration frequency which is the molecule's sixth degree of freedom. Since the binding energy of Li_2^+ is only slightly greater than that of Li_2, it may be supposed that the force constant for Li_2^+ is not drastically different from that of Li_2. The latter is known from band spectra. Making the two assumptions that the force constants are about the same and are not altered in passing from gas to solid, we have at our disposal an approximate value of the vibrational frequency of Li_2^+. The contribution of the internal degree of freedom to C_v can thus be readily computed.

The frequency of Li_2 has been observed[8] as

[6] H. M. James, J. Chem. Phys. **3**, 9 (1935).

[7] One might regard lithium, if the diatomic model is correct, as a crystal intermediate in character between the pure molecular, non-metallic lattice of solid H_2 and the atomic and metallic lattice of Na. Cf. the interesting speculations of E. Wigner and H. B. Huntington on the possibility of a metallic modification of solid hydrogen at extremely high pressures: J. Chem. Phys. **3**, 764 (1935).

[8] F. W. Loomis and R. E. Nusbaum, Phys. Rev. **38**, 1447 (1931); G. M. Almy and G. R. Irvin, Phys. Rev. **49**, 72 (1936).

TABLE I. *Heat capacity of lithium. Diatomic model*: $\theta=345$, $\tilde{\nu}=420$ cm^{-1}.

T°K	C_v (LATTICE)	C_v (INTERNAL)	C_v (TOTAL)	C_v (OBS.)	C_p (CALC.)	C_p (OBS.)
15	0.06		0.06	0.09	0.06	0.09
20	0.15		0.15	0.19	0.15	0.19
30	0.51		0.51	0.55	0.51	0.55
40	1.13		1.13	1.15	1.13	1.15
50	1.97		1.97	1.99	1.97	1.99
60	2.86	0.01	2.87	2.84	2.88	2.86
70	3.74	0.02	3.76	3.74	3.78	3.76
80	4.55	0.06	4.61	4.62	4.64	4.64
90	5.25	0.10	5.35	5.34	5.39	5.38
100	5.85	0.17	6.02	6.04	6.08	6.10
120	6.80	0.32	7.12	7.18	7.22	7.28
140	7.48	0.49	7.97	8.02	8.13	8.16
160	7.97	0.67	8.64	8.68	8.84	8.86
180	8.32	0.82	9.14	9.14	9.40	9.36
200	8.59	0.96	9.55	9.56	9.86	9.84
220	8.81	1.09	9.90	9.88	10.27	10.30
240	8.98	1.19	10.17	10.18	10.59	10.56
260	9.10	1.28	10.38	10.44	10.86	10.88
280	9.21	1.36	10.57	10.62	11.10	11.12
300	9.30	1.43	10.73	10.78	11.32	11.32
320	9.38	1.48	10.86		11.50	
340	9.44	1.53	10.97		11.67	
360	9.49	1.57	11.06		11.81	
380	9.53	1.61	11.14		11.95	
400	9.57	1.64	11.21		12.07	
420	9.60	1.67	11.27		12.18	
440	9.63	1.70	11.33		12.30	

350 cm^{-1}, and by using this value in conjunction with a five-degree Debye function ($\theta=355$) to calculate C_v, fairly satisfactory agreement with experiment is obtained at temperatures above 30°K. The numerical agreement can be somewhat improved if the frequency value is taken as 420 cm^{-1} rather than 350. One would scarcely expect the 350 value to carry over exactly, and the 420 cm^{-1} figure probably represents a more nearly correct value for the Li_2^+ frequency in the solid.[9] For this reason we present in Table I the values of C_v and C_p for lithium calculated by setting $\theta_D=345$ and $\tilde{\nu}=420$ cm^{-1}. The calculated C_v is compared with a so-called "observed" C_v obtained by converting the C_p measurements with the help of the thermodynamic equation involving the coefficients of compression and thermal expansion. The latter of these quantities has been measured by Simon and Bergmann[10] over the entire temperature range in which C_p-C_v is appreciable, and the value of C_v, since it is computed from C_p by a thermodynamic expression, may fairly be considered as "observed." The experimental C_p values are listed beside a set of C_p's calculated from the expression

$$C_p=C_v+aC_v^2T, \tag{1}$$

in which a, the empirical constant, is equal to 1.71×10^{-5} reciprocal calorie. The sort of agreement given by an approximate expression like Eq. (1) may be seen by comparing columns 6 and 7, Table I.

From their study of the thermal expansion, α, of lithium, Simon and Bergmann[11] found that no simple proportionality exists between C_v and α. Indeed, it was this fact as much as the failure of the Debye law which led them to postulate the existence of an electronic level as a contributor to C_v. Since such a level should presumably make no contribution to α, its share of the heat capacity must, perforce, be removed from C_v before seeking a relationship between C_v and α. Simon and Bergmann found an accurate proportionality between α and the residual heat capacity as given by a Debye curve with $\theta=505$.

For molecular lattices, however, the theory does not forecast so simple a relationship between C_v and α. In fact, for a diatomic lattice the relation should be [12]

$$\alpha=k_1C_{vL}+k_2C_{vI}, \tag{2}$$

where k_1 and k_2 are constants, and C_{vL} and C_{vI} are the lattice and internal components of C_v, respectively. Only in the event that $k_1=k_2$ will simple proportionality obtain, and, as we know from the C_p-C_v values of such a diatomic molecule as Cl_2, the two constants can have quite different values.

If we assume the thermal expansion of lithium to be resolvable into two components, the two constants k_1 and k_2 can be evaluated from C_{vL}, C_{vI} and α at any two temperatures. It should then be possible to represent α as a function of temperature over the whole range of the crystal. The values of α calculated in this way in the range 15–300°K are listed in Table II. It will be seen that from 100° to 260°, the range in which data are available, the agreement with experiment is fair. The values calculated by simple

[9] It is of interest to note that, in the analogous molecules H_2 and H_2^+ the chemical binding is much stronger in the *former* (4.48 *vs.* 2.65 ev) and the frequency decidedly *higher* (4160 *vs.* 2170 cm^{-1}).

[10] F. Simon and Bergmann, Zeits. f. physik. Chemie **B8**, 255 (1930).

[11] Cf. (a) Eq. (12) and (b) references 13 of previous paper (R. C. Lord, Jr., J. Chem. Phys. **9**, 693 (1941) (this issue).

[12] Cf. Eq. (14) of reference 11.

proportion from a Debye θ of 515 [13] are listed for comparison. Since the two methods give divergent results below 100°, it would be interesting to have at hand expansion data in that region.

Evaluation of θ by Other Methods

While the agreement is satisfactory between experimental values of heat capacity and of thermal expansion and those calculated on the basis of the diatomic model, something more than this numerical coincidence is needed to inspire confidence in the model. As we have mentioned previously, one of the reasons for doubting Simon and Swain's original interpretation was the disagreement between the θ found by them and that obtained from a study of the temperature dependence of the electrical resistance of lithium. This study was made by Grüneisen.[14] He investigated the numerical values of a parameter θ which appears in an equation portraying the temperature dependence of resistance. Since this equation rests on similar foundations and has a similar mathematical form to the Debye equation, Grüneisen expected and found experimentally for a number of metals, that the θ values obtained from electrical studies and from specific heats are very nearly the same. At the time of his work[14] the specific heat of lithium had not been measured at low temperatures, and he was thus unable to compare a Debye θ with the θ value he obtained, namely 363.

The disagreement between this figure and that of Simon and Bergmann[2] led Pankow and Scherrer[15] to an investigation of the temperature dependence of the relative intensities of various lines in the x-ray pattern of lithium. Here again the theory involves a parameter θ in a fashion similar to the Debye theory, and opportunity is at hand to obtain a numerical value of θ. From intensity measurements at 90° and 293°K, Pankow and Scherrer, found a θ value of 352 (± 12).

Table II. *Temperature dependence of thermal expansion.* $k_1 = 2.9 \times 10^{-6}$, $k_2 = 15 \times 10^{-6}$ *reciprocal calorie.*

T°K	α(LATTICE)	α(INTERNAL)	α(CALC.)	α(OBS.)	α(CALC. $\theta = 515$)
15	0.17		0.17		0.09
20	0.44		0.44		0.27
30	1.47		1.47		0.91
40	3.28		3.28		2.01
50	5.71		5.71		3.79
60	8.29	0.15	8.44		6.21
70	10.85	0.30	11.15		9.27
80	13.20	0.90	14.10		12.5
90	15.23	1.50	16.73		15.9
100	16.97	2.55	19.52	18.5	19.1
120	19.72	4.80	24.52	24.45	25.1
140	21.69	7.35	29.04	29.6	30.0
160	23.11	10.05	33.16	33.7	34.0
180	24.13	12.30	36.43	37.0	37.4
200	24.91	14.40	39.31	39.7	40.0
220	25.55	16.35	41.90	41.9	42.0
240	26.04	17.85	43.89	43.6	43.7
260	26.39	19.20	45.59	45.0	45.1
280	26.71	20.40	47.11	46.2	46.2
300	26.97	21.45	28.42		

Table III. θ *values for lithium from various sources.*

SOURCE	VALUE OF θ
Temperature dependence of:	
Specific heat, monatomic model	328–420
Specific heat, diatomic model	345
Electrical conductivity	363
X-ray intensities	352
Einstein formula	365
Lindemann formula:	
1. Constant = 135	470
2. Constant = 115	400
Elastic constants (theor.)	339
Elastic constants (est.)	336

The agreement of these two θ values with that found from specific heats with the help of the diatomic model makes us look into the various other means of calculating θ. There are two equations of semi-empirical character, the Einstein[16] and the Lindemann[17] which are, respectively,

$$\theta = 1.76 \times 10^{-4} \beta^{-\frac{1}{2}} M^{-\frac{1}{2}} V^{-1/6}, \quad (3)$$

$$\theta = 135 T_m^{\frac{1}{2}} M^{-\frac{1}{2}} V^{-\frac{1}{2}}, \quad (4)$$

in which β is the compressibility, M the atomic weight, V the atomic volume, and T_m the melting point. These equations were intended to apply to atomic lattices and their extension to molecular lattices is a procedure of unknown validity. With regard to the diatomic model for lithium, there arises the question of what values to use for M and V. If we consider the diatomic molecule as a single mass unit, formally we should use twice the atomic

[13] See reference 1, p. 191.
[14] E. Grüneisen, Ann. d. Physik **16**, 530 (1933).
[15] G. W. Pankow and P. Scherrer, Helv. Phys. Acta **7**, 644 (1934). G. W. Pankow, *ibid.* **9**, 87 (1936).
[16] A. Einstein, Ann. der Physik **34**, 170 (1911). The constant in Einstein's equation has been corrected by the factor 4/3 to make the equation yield a θ suitable for use with the Debye equation rather than with the original Einstein C_v equation. See N. F. Mott and H. Jones, *Properties of Metals and Alloys* (Oxford University Press, 1936), p. 8.
[17] F. A. Lindemann, Physik. Zeits. **11**, 609 (1910). In order to obtain agreement with the observed θ's for sodium and potassium, the constant of the Lindemann equation needs to be reduced from 135 to 115.

weight for M. Since the intermolecular forces, as indicated by compressibility or melting temperature, are approximately twice as great, however, on a diatomic molecule as on a single atom, the observed θ should be roughly the same whether or not the atoms are dimerized into molecules. It thus seems appropriate in applying these more or less empirical relationships to use atomic values for M and V for the diatomic model.

Another procedure for finding θ, based on the theory of elastic solids[18] makes use of β and of Poisson's ratio. Although Poisson's ratio appears not to have been measured for lithium or the other alkali metals, an approximate calculation of θ may be made by estimating Poisson's ratio as $\frac{1}{3}$, a value which is probably not far from correct. The formula of Born leads to $\theta=336$. Here, as in the Lindemann and Einstein equations, the *atomic* weight and volume of lithium have been used.

An equivalent calculation of θ has been made by Fuchs[19] in the course of a theoretical study of the elastic constants of lithium. He does not explicitly calculate Poisson's ratio, but the method of obtaining θ is that of Born. Fuchs finds $\theta=339$.

The θ's obtained by the several methods are assembled in Table III. It may readily be appreciated from this table that the various θ values hardly can be used to confirm or disprove the diatomic model. They do indicate, however, that θ is quite unlikely to have a value so high as 500.

X-Ray Structural Studies of Lithium

Until very recently all investigators of the structure of lithium by x-ray methods[20] agreed that the patterns obtained indicate clearly a body-centered structure, which has also been found for sodium and potassium. There was no difficulty with the interpretation of the x-ray spectra, and on the basis of this evidence alone the structure of lithium seems clearly to be atomic rather than molecular. Precise study[21] of the intensities of x-rays scattered by metallic lithium powder at various temperatures shows, however, that there are complicated features of the x-ray spectrum which cannot be explained on the basis of a two-atom body-centered structure involving scattering centers with spherical symmetry. While a unique interpretation of the experimental data has not yet been demonstrated, it appears[22] that a $T_v^6(c)$ structure[23] which has 16 Li atoms per unit cell gives a better agreement with the x-ray intensities, which were measured by means of an ionization chamber. In this structure the lithium atoms are associated in pairs, a situation entirely compatible with the diatomic model. A detailed analysis and discussion of these x-ray results is to be published by Professor Harris and Dr. Griffith in the near future.

TABLE IV. *Low frequency limit of ultraviolet transmission.*

Element	Atomic Number	ν_0(obs.)	ν_0(calc.)
Cs	55	6.8×10^{14}	8.3×10^{14}
Rb	37	8.3	9.4
K	19	9.6	10.3
Na	11	14.3	14.3
Li	3	14.6	19.3
			13.7 (Li_2^+)

Properties of Lithium Metal

Apart from the foregoing thermal and x-ray evidence, there is additional experimental material which appears to support the diatomic model. One clear implication of the diatomic model is a reduction of the number of free electrons in the metal. If all the atoms are combined into Li_2^+ ions, the number of free electrons is reduced by a factor of 2. Thus any metallic property depending on the number of free electrons per unit volume would have an anomalous value for lithium in comparison, let us say, with the other alkali metals, which presumably have their full complement of free electrons.

An example of such a property is the transmission of ultraviolet radiation by films of the alkali metals.[24] There is some definite frequency in the ultraviolet region at which each of these metals, in thin films, becomes transparent to

[18] M. Born, "Atomtheorie des festen Zustandes," Encyc. Math. Wiss., Vol. 5, Part 3 (1923), pp. 642–43. Born's discussion is summarized in Fowler (reference 4, p. 127), where the equations for the calculation of θ will be found.

[19] K. Fuchs, Proc. Roy. Soc. **A153**, 622 (1936).

[20] A. W. Hull, Phys. Rev. **10**, 661 (1917); J. M. Bijvoet and A. Karssen, Proc. K. Akad. Amst. **23**, 1365 (1922); **29**, 1286 (1926); F. Simon and E. Vohsen, Zeits. f. Physik. Chemie **A133**, 165 (1928); P. Scherrer and B. Arakatzu, Helv. Phys. Acta **3**, 48 (1930). See also reference 15.

[21] R. L. Griffith and P. M. Harris, Phys. Rev. **59**, 110A (1941).

[22] Private communication from Professor P. M. Harris. I am greatly indebted to Professor Harris for the privilege of hearing of these x-ray results in advance of their publication and for interesting discussion of their correlation with the heat capacity data.

[23] *Int. Tab. zur Best. von Kristallstrukturen*, Vol. I, p. 333.

[24] R. W. Wood, *Physical Optics* (Macmillan, New York, 1934), third edition, pp. 558–560.

radiation. The frequency depends on the number of free electrons per cc.[25] We can calculate ν_0, the frequency at which transmission sets in, by means of the formula given by Zener

$$\nu_0^2 = Ne^2/\pi m_0. \quad (5)$$

Here N is the number of electrons per cc, and e and m_0 are the electronic charge and mass. Comparison of calculated frequencies with those observed by Wood shows satisfactory agreement except for lithium (Table IV). When we use for N, however, a value corresponding to the diatomic model, agreement comparable to that found for the other metals is obtained. The theoretical and experimental values are plotted as functions of atomic number in Fig. 2. It will be seen that the plots follow one another nicely provided the diatomic model is assumed for lithium.[26]

There are various other properties of metals which are dependent on the number of free electrons in unit volume, but for none of these does comparison of theory with experiment appear to offer a clear-cut decision concerning the diatomic model. In general, the properties of lithium are out of line with those of the other alkalis but calculation based on the theory of metals is not precise enough to show what the source of the anomalies is. As good examples of these properties one can cite the energy widths of the soft x-ray emission bands,[27] the paramagnetic susceptibility[28] and the pressure coefficient of electrical resistance.[29] The anomalous behavior of these properties of lithium in reference to the other alkalis has been explained separately and on various grounds for each of them, but it seems reasonable to suppose that if the theoretical calculations could be repeated on the basis of the diatomic model, they would lead to the same sort of agreement with experiment as has been found for the other alkali metals.

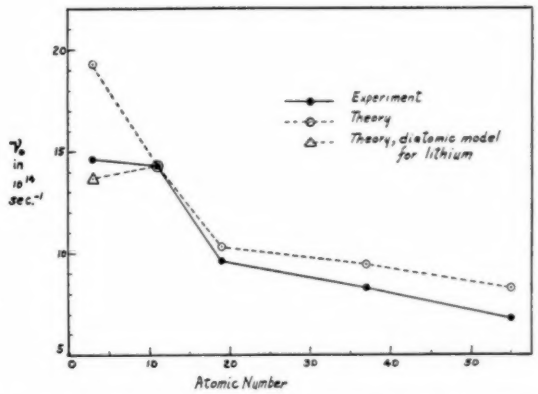

FIG. 2. Low frequency limit of transmission of ultraviolet radiation by the alkali metals.

FURTHER EXPERIMENTAL WORK

There are several experiments which might enable a decision of the question. One of these has already been suggested by Simon and Swain,[30] namely the extension of the thermal expansion data to 15°K or lower. A comparision of the values listed in Table II, columns 4 and 6, with the experimental α's in the low temperature range would be illuminating. It would also be helpful to have accurate C_v data from 300°K to the melting point. At present, neither α nor C_p is known very accurately in this range.[31]

In this connection it would also be valuable for comparative purposes to have α over the entire temperature range for which C_p is known for sodium and potassium. Simon[32] has suggested that the heat capacity data for these metals also can best be interpreted with the help of an electronic level. Here, however, the Debye curve seems to fit fairly well at low temperatures and the necessity for assuming other components of C_v not at all convincing.

[25] C. Zener, Nature **132**, 968 (1934); N. F. Mott and C. Zener, Proc. Camb. Phil. Soc. **30**, 249 (1934). See also A. H. Wilson, *Theory of Metals* (Cambridge University Press, 1936), pp. 125–126.

[26] It has been suggested by Wilson, (reference 25, p. 126), that the discrepancies in Table IV might well be attributed to the effective mass. If we use an effective mass of 1.4 m_0 the agreement improves for Cs and Rb and very decidedly for Li. However, it gets worse for Na and K, and, more important, there is still no break in the value for Li as compared with Na. On the whole it seems to us that little improvement is made by using an effective mass in place of m_0.

[27] See H. W. B. Skinner, *Reports on Progress in Physics* (Cambridge, 1939), Vol. V, p. 257, and references there cited.

[28] J. B. Sampson and F. Seitz, Phys. Rev. **58**, 633 (1940).

[29] Experimental: P. W. Bridgman, Proc. Am. Acad. **72**, 157 (1938); theoretical: N. H. Frank, Phys. Rev. **47**, 282 (1935).

[30] Reference 1, p. 192.

[31] See, however, C. C. Bidwell, Phys. Rev. **28**, 584 (1926).

[32] F. Simon, Ber. Berlin. Akad. **33**, 483 (1926).

Statistical Mechanics of Nearest Neighbor Systems

ELLIOTT W. MONTROLL*
Sterling Chemistry Laboratory, Yale University, New Haven, Connecticut
(Received June 6, 1941)

In many solids the intermolecular forces are sufficiently short ranged so that practically the entire potential energy of the system results from interactions between nearest neighbors. The thermodynamic properties of a solid with respect to a given coordinate, α, (for example, in a ferromagnetic system α might represent the excess unpaired electron spin at a given lattice point; or in a substitutional binary alloy α might denote which of the two possible kinds of atoms are at a given lattice point) can be found from the factor of the partition function which averages over all possible configurations of α at all lattice points.

Here the evaluation of such a factor of the partition function is reduced to the calculation of the largest characteristic value of a linear homogeneous operator equation involving the potential energy between two adjacent layers of lattice points in the solid. By assuming that all possible configurations of a layer are equally probable, a lower bound for the partition function for a simple cubic lattice is found in terms of the partition function of a cube of eight molecules.

The operator equation for a real crystal becomes quite complex, but in some problems it is possible to obtain characteristic vectors and characteristic values (and thus the partition function) at high and low temperatures. For intermediate temperatures a theory of resonance between the low temperature "almost ordered" characteristic vectors and the high temperature "almost disordered" characteristic vectors is developed. In cases where the operator equation can be solved for microcrystals a few layers thick, a perturbation method is discussed in which interactions between the individual microcrystals are treated as perturbations.

Some remarks are made concerning phase transitions and finally the general theory is applied to a superficial treatment of two-dimensional ferromagnetic plates.

IN many physical systems containing a large number of molecules, the intermolecular forces are sufficiently short ranged to permit the total potential energy of the system to be represented by the sum of the interactions of each molecule with its nearest neighbors. Much research has been devoted to applying the "nearest neighbor approximation" to the study of normal solids,[1] order-disorder phenomenon[2] in substituted binary alloys, hindered rotation,[3] ferromagnetism[4] and related topics; but no general mathematical technique for the handling of these problems (which are abstractly alike) has been developed. Usually the partition function of the system in question is not found directly, but is expressed as a function of a parameter which is so chosen to minimize the free energy of the system, and often correlations (which arise not through direct interaction but indirectly through cooperational effects of intermediate lattice points) between distant neighbors are neglected.

It is the purpose of this paper to introduce a method of reducing the evaluation of the partition function of nearest neighbor systems to the solution of linear homogeneous operator equations with the hope that the vast store of knowledge concerning these equations will be helpful in analyzing some of the elusive problems of statistical mechanics. The general theory proposed in the first part of the paper will be applied in the second part to a superficial study of two-dimensional ferromagnetic materials.

I. General Theory

1. Characteristic value theory of the partition function

Suppose a system can be divided into $L \times M \times N$ cells as is done in Fig. 1, so that there will be L layers each composed of $N \times M$ cells[5] and each layer will have the same average behavior as any other layer. The molecules in each cell may have several or even a continuum of possible configurations. Since the same is true of

* Sterling Research Fellow in Chemistry.

[1] Cf. Born and von Kármán, Physik. Zeits. **13**, 297 (1912). Blackman, Proc. Roy. Soc. **148**, 365, 384 (1934); **149**, 117, 126 (1935).

[2] For review of this subject see Nix and Shockley, Rev. Mod. Phys. **10**, 1 (1938).

[3] Cf. Kirkwood, J. Chem. Phys. **8**, 205 (1940).

[4] Ising, Zeits. f. Physik **31**, 253 (1925).

[5] In a simple cubic lattice each cell would contain one molecule and each layer, $M \times N$ molecules. This is not necessarily so in more complicated lattices.

each layer, one can define a set $\{\alpha_i\}$ of all those configurations available to a physical coordinate, α, of a layer. For example, in a binary substitutional alloy α_i might correspond to an ith arrangement of the two kinds of atoms in a layer; or in a normal solid α_i might be one of the continuum of simultaneous positions of all the molecules of a layer.

If $v(\alpha_m)$ is the total potential energy with respect to a coordinate α between all neighboring cells of a layer in the mth configuration, and if $v(\alpha_m, \alpha_n)$ is the total potential energy of interaction between cells of one layer in the mth configuration with their nearest neighbors of an adjacent layer in the nth configuration, the potential energy factor of the partition function with respect to the coordinate[6] α is

$$Z=\sum_{\{\alpha_1\}}\cdots\sum_{\{\alpha_L\}}\exp -[v(\alpha_1)+\cdots+v(\alpha_L)+v(\alpha_1,\alpha_2)+\cdots+v(\alpha_{L-1},\alpha_L)]/kT. \quad (1)$$

Making the substitution

$$V(\alpha_i,\alpha_j)=v(\alpha_i)/2+v(\alpha_i,\alpha_j)+v(\alpha_j)/2, \quad (2)$$

(1) becomes

$$Z=\sum_{\{\alpha_1\}}\cdots\sum_{\{\alpha_L\}}\{\prod_{i=1}^{L-1}\exp[-V(\alpha_i,\alpha_{i+1})/kT]\}\times\exp(-[v(\alpha_1)+v(\alpha_L)]/2kT). \quad (3)$$

Since $v(\alpha_1)+v(\alpha_L)/2$ is one-half the total potential energy of the top and bottom layers of the system and can be neglected when the total number of layers is large,

$$Z=\sum\cdots\sum\{\prod\exp[-V(\alpha_i,\alpha_{i+1})/kT]\}. \quad (4)$$

To simplify this expression let us expand each factor as a bilinear combination of the components of a set of linearly independent orthonormal vectors $\{\psi_n\}$. If each cell has ν possible

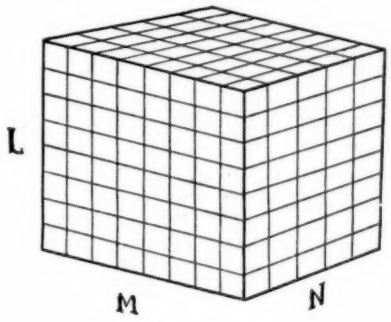

FIG. 1.

configurations, each layer has ν^{MN} possible configurations and each vector would have ν^{MN} components. Writing

$$\psi_n=\begin{pmatrix}\psi_n(1)\\ \cdot\\ \cdot\\ \cdot\\ \psi_n(\nu^{MN})\end{pmatrix};$$

$$\psi^*{}_n=(\psi_n(1),\psi_n(2),\cdots,\psi(\nu^{MN})), \quad (5)$$

the orthonormality of the ψ's demands that

$$\psi^*{}_m\cdot\psi_n=\sum_{\alpha_i=1}^{\nu^{MN}}\psi_m(\alpha_i)\psi_n(\alpha_i)=\delta_{mn}. \quad (6)$$

The desired expansion is

$$\exp -V(\alpha_i,\alpha_j)/kT=\sum_{m=1}^{\nu^{MN}}\sum_{n=1}^{\nu^{MN}}a_{mn}\psi_m(\alpha_i)\psi_n(\alpha_j), \quad (7)$$

where the coefficients, a_{kh}, result from multiplication of both sides of (7) by $\psi_k(\alpha_i)\psi_h(\alpha_j)$, summing over all elements of the sets $\{\alpha_i\}$ and $\{\alpha_j\}$, and using the orthonormality conditions:

$$a_{kh}=\sum_{\alpha_i=1}^{\nu^{MN}}\sum_{\alpha_j=1}^{\nu^{MN}}\psi_k(\alpha_i)\exp[-V(\alpha_i,\alpha_j)/kT]\psi_h(\alpha_j), \quad (8a)$$

or in matrix form

$$\psi^*{}_k\,\mathbf{exp}\,(-\mathbf{V/kT})\psi_h=a_{kh}, \quad (8b)$$

with

$$\mathbf{exp}\,(-\mathbf{V/kT})=\begin{bmatrix}\exp[-V(\alpha_1,\alpha_1)/kT] & \exp[-V(\alpha_1,\alpha_2)/kT] & \cdots\\ \exp[-V(\alpha_2,\alpha_1)/kT] & \exp[-V(\alpha_2,\alpha_2)/kT] & \cdots\\ \cdot & \cdot & \cdot\\ \cdot & \cdot & \cdot\end{bmatrix}.$$

One might now ask if it is possible to select the set $\{\psi_n\}$ so that a_{hk} is zero when $h\neq k$. When $\mathbf{exp}\,(-\mathbf{V/kT})$ is a symmetrical matrix the answer is yes, for if the ψ's are the characteristic vector of the matrix equation

$$\lambda\psi=\mathbf{exp}\,(-\mathbf{V/kT})\psi, \quad (9)$$

then,

$$\psi^*{}_k\,\mathbf{exp}\,(-\mathbf{V/kT})\psi_h=\psi^*{}_k\lambda_h\psi_h=\lambda_h\delta_{hk}$$

and

$$a_{hk}=\lambda_h\delta_{hk}. \quad (10)$$

[6] Note the implicit assumption of independence of the various kinds of coordinates; for example, in a ferromagnetic system this would be equivalent to the assertion that spin orientations are independent of lattice vibrations.

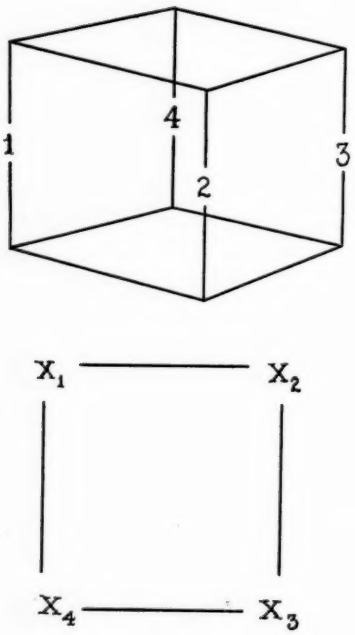

FIG. 2.

It is with this symmetrical case that we shall be concerned. The diagonalized expansion of $\exp[-V(\alpha_i, \alpha_j)/kT]$ becomes

$$\exp -V(\alpha_i, \alpha_j)/kT = \sum_k \lambda_k \psi_k(\alpha_i)\psi_k(\alpha_j). \quad (11)$$

Substituting[7] (11) in (4) and applying the orthonormality conditions

$$Z = \sum_{k=1}^{\nu^{MN}} \lambda_k^{L-1} \{ \sum_{\{\alpha_1\}} \sum_{\{\alpha_L\}} \psi_k(\alpha_1)\psi_k(\alpha_L) \}$$

$$= \sum_k \lambda_k^{L-1} \{ \sum_{\alpha_1=1}^{\nu^{MN}} \psi_k(\alpha_1) \}^2. \quad (12)$$

Schwarz's inequality implies that

$$|\sum_{\alpha_1=1}^{\nu^{MN}} \psi_k(\alpha_1)|^2 \leq (\sum_{\alpha_1=1}^{\nu^{MN}} \psi_k^2(\alpha_1))(\sum_{\alpha_1=1}^{\nu^{MN}} 1) = \nu^{MN}. \quad (13)$$

Equation (12) has reduced the evaluation of Z to solving a characteristic value problem, and, moreover, since in a real crystal the number of layers, L, is very large, one need only find the largest characteristic value λ_{max} of (9). Thus[8]

$$Z = \lambda_{max}^{L-1} [\sum_{\{\alpha_1\}} \psi_{max}(\alpha_1)]^2. \quad (14)$$

Physically $|\psi_{max}(\alpha_i)|^2$ can be interpreted as the relative probability of any layer in the system being in the ith configuration. It is apparent that at absolute zero the components of ψ_{max} corresponding to the completely ordered state have the value $1/\sqrt{n_0}$ where n_0 is the number of configurations corresponding to complete order—the other components are zero. At temperatures sufficiently high for thermal agitation to cause complete disorder, all configurations are equally probable and

$$\psi_{max} \to (1, 1, \cdots, 1)/\sqrt{\nu^{MN}}.$$

Before investigating the implications and technicalities of the results up to this point, let us linger a moment to note the formal changes required in those problems that permit the configuration of each cell (or layer) to achieve any one of a continuum of energy configurations. In the partition function all summation operations must be replaced by integrations

$$Z = \int_{\alpha_1} \cdots \int_{\alpha_L} \exp -[v(\alpha_1) + \cdots + v(\alpha_{L-1}, \alpha_L)]/kT \times d\{\alpha_1\} \cdots d\{\alpha_L\}. \quad (1')$$

$d\{\alpha_i\}$ is the volume element in $\{\alpha_i\}$ space; for example, if $\{\alpha_i\}$ is the set of possible simultaneous positions of the molecules in the ith layer,

$$d\{\alpha_i\} = (dx_1^i dy_1^i dz_1^i) \cdots (dx_{MN}^i dy_{MN}^i dz_{MN}^i).$$

All expansions of the potential energy exponentials must be expressed in terms of the characteristic functions of the integral equation:

$$\lambda\psi(\alpha_i) = \int_{\{\alpha_j\}} \psi(\alpha_j) \exp[-V(\alpha_i, \alpha_j)/kT] d\{\alpha_j\}. \quad (9')$$

2. A lower bound to the partition function

Since ψ_{max} is the vector which maximizes

$$\psi^* \exp(-\mathbf{V}/\mathbf{kT})\psi/\psi^*\psi = \lambda, \quad (15)$$

any arbitrary ψ corresponds to a λ that is $\leq \lambda_{max}$

[7] An abstractly equivalent process has been used to evaluate some of the multiple integrals occurring in the theory of imperfect gases. See Montroll and Mayer, J. Chem. Phys., in press.

[8] Since $\log \lambda^{L-1} = O(LMN)$ and $\log \nu^{MN} = O(MN)$, in taking logarithms to calculate physical properties one can neglect the second factor in (14).

and therefore would give a lower bound to Z. A ψ which permits the calculation of a $\lambda \leq \lambda_{max}$ without any special appeal to the problem concerned until the end of the calculation is

$$\psi_0 = (1, 1, 1, \cdots, 1)/\sqrt{\nu^{MN}},$$

for in that case

$$\lambda_0 = \frac{1}{\nu^{NM}} \sum_{\alpha_1} \sum_{\alpha_2} \exp - V(\alpha_1, \alpha_2)/kT.$$

Now $\lambda_0 \nu^{MN}$ is exactly the partition function of a two layer system in which the interactions between cells of the same layer is one-half that between those of different layers. By standing the system on end so that it becomes a system of $M2\times N$ layers, the repetition of the "compressing operation" (this time with a ν^{2N}-dimensional vector) reduces the system to one of $N2\times 2$ layers. Finally, compression of the $2\times 2\times N$ system in the N direction, one obtains

$$\lambda_{max} \geq \omega^{(L-1)(M-1)(N-1)} \times \nu^{-3LMN+4(LM+LN+MN)+4(1-L-M-N)}, \quad (16)$$

where $\omega\nu^4$ is the partition function of a system of $2\times 2\times 2$ cells in which the interaction energy between a pair of adjacent cells is only one-fourth that in the original system.

The evaluation of ω can be simplified by picturing its $2\times 2\times 2$ cells (Fig. 2) as a square with each numbered pair $\bullet\!-\!i\!-\!\bullet$ in the cube replaced by an X_i in the square. If σ_i is the configuration of the ith corner of the square, and if $W(\sigma_i, \sigma_j)$ is the mutual potential energy between the ith corner of the square with its neighboring jth corner (remembering that all interactions are only one-fourth their value in the original $L\times M\times N$ system)

$$\omega\nu^4 = \sum_{\sigma_1=1}^{\nu^2} \cdots \sum_{\sigma_4=1}^{\nu^2} \exp -[W(\sigma_1, \sigma_2) + W(\sigma_2, \sigma_3) + W(\sigma_3, \sigma_4) + W(\sigma_4, \sigma_1)/kT]. \quad (17)$$

Developing $\exp - W(\sigma_i, \sigma_j)/kT$ in terms of its ν^2 orthonormal characteristic vectors ϕ_i (each with ν^2 components), i.e., the characteristic vectors of

$$\mu\varphi(\sigma_1) = \sum_{\sigma_2=1}^{\nu^2} \varphi(\sigma_2) \exp [-W(\sigma_1, \sigma_2)/kT] \qquad (\sigma_1 = 1, 2, \cdots, \nu^2)$$

and substituting the resulting expressions in (17), one obtains

$$\omega\nu^4 = \sum_{k=1}^{\nu^2} \mu_k^4 \qquad (\mu_k = \phi^*{}_k \exp [-\mathbf{W}/\mathbf{kT}]\phi_k/\phi^*{}_k\phi_k).$$

In special problems involving a specific knowledge of $V(\alpha_i, \alpha_j)$, it is often possible to guess a better λ than λ_0 (usually it is desirable to choose one with an arbitrary parameter so that the variational principle can be applied) and thus find a better lower bound for Z. This procedure is being applied by Professor Onsager to the calculation of residual entropies of crystals of polar molecules.

3. Resonance between "almost ordered" and "almost disordered" states

As has been mentioned before, at a temperature of absolute zero where a system is completely ordered, its characteristic vector (unnormalized) has a unit component for every ordered configuration and a zero component for all others. Then λ_{max} in the ordered state is

$$\lambda_{or} = \exp (-V(\text{or})/kT), \quad (18)$$

where $V(\text{or})$ is the total $V(\alpha_i, \alpha_j)$ in the ordered state. At temperatures above absolute zero it is possible by the method of successive approximations to be described in Part II to express the non-ordered components of ψ_{max} as sums of exponential functions of $(-1/kT)$ and to write

$$\lambda_{max} = \exp [-V(\text{or})/kT] \times [1 + \textstyle\sum_n a_n (\exp [-b_n/kT])]. \quad (18')$$

The characteristic vectors and values at low temperatures that are expressed in this manner will henceforth be written as ψ_{ao} and λ_{ao} and will be said to represent the "almost ordered" state.

At very high temperatures a system will approach complete disorder and all its configurations will have an equal probability of existence causing $\psi_{max} \to (1, 1, \cdots, 1)/\sqrt{\nu^{MN}}$, and $\lambda_{max} \to \nu^{MN}$. Any decrease in temperature induces the components of ψ to become linear combinations[9] of inverse powers of kT and

$$\lambda_{max} = \nu^{MN}(1 + \textstyle\sum c_n (1/kT)^n). \quad (19)$$

[9] This point will be discussed in more detail in Part II.

These high temperature characteristic vectors and characteristic values which will henceforth be represented by ψ_{ad} and λ_{ad} will be called representations of the "almost disordered" state.

In a given problem calculations from the ao and ad states are valid for quite large temperature ranges in the neighborhood of the extreme cases, but in the intermediate range (which usually includes that of a phase transition if there be one) neither the ao nor the ad vectors give exact results. However it is quite possible that a linear combination of these vectors, which physically is analogous to resonance between the ao and ad states (in the manner that resonance enters the theory of chemical binding and molecular structure[10]) gives a more exact characteristic value than either of the individual ones. More explicitly stated, there exist functions $A(T)$ and $B(T)$ such that

$$\psi = A(T)\psi_{ao} + B(T)\psi_{ad}. \tag{20}$$

By combining (20) and (15), the desired A and B are those which make

$$\frac{A^2\lambda_{ao} + 2ABa_{12} + B^2\lambda_{ad}}{A^2 + 2ABb + B^2} = \lambda = \max,$$

where

$$a_{12} = \psi^*_{ad}\,\mathbf{exp}\,(-\mathbf{V}/\mathbf{kT})\psi_{ao} = \psi^*_{ao}\,\mathbf{exp}\,(-\mathbf{V}/\mathbf{kT})\psi_{ad},$$

$$b = \psi^*_{ad}\psi_{ao}.$$

That is

$$F(A, B) = A^2\lambda_{ao} + 2ABa_{12} + B^2\lambda_{ad} - \lambda(A^2 + 2ABb + B^2) = \max.$$

As is well known from calculus of variations, A and B must satisfy

$$\tfrac{1}{2}\frac{\partial F}{\partial A} = A(\lambda_{ao} - \lambda) + B(a_{12} - \lambda b) = 0,$$

$$\tfrac{1}{2}\frac{\partial F}{\partial B} = A(a_{12} - \lambda b) + B(\lambda_{ad} - \lambda) = 0.$$

But solutions to these equations exist only when λ is a root of

$$\begin{vmatrix} \lambda_{ao} - \lambda & a_{12} - \lambda b \\ a_{12} - \lambda b & \lambda_{ad} - \lambda \end{vmatrix} = 0.$$

The largest root of this equation is the characteristic value corresponding to the resonance state and has the value

$$\lambda = \frac{\left[\frac{\lambda_{ad} + \lambda_{ao}}{2} - ba_{12}\right] + \left\{\left[\frac{\lambda_{ad} + \lambda_{ao}}{2} - ba_{12}\right] + (1 - b^2)(a_{12}^2 - \lambda_{ao}\lambda_{ad})\right\}^{\frac{1}{2}}}{(1 - b^2)}. \tag{21}$$

If A and B are chosen so that ψ is normalized

$$A^2 + 2ABb + B^2 = 1$$

and

$$A^2 = \frac{(\lambda_{ad} - \lambda)^2}{(a_{12} - \lambda b)^2 - 2b(a_{12} - \lambda b)(\lambda_{ad} - \lambda) + (\lambda_{ad} - \lambda)^2},$$

$$B^2 = \frac{(\lambda_{ao} - \lambda)^2}{(a_{12} - \lambda b)^2 - 2b(a_{12} - \lambda b)(\lambda_{ao} - \lambda) + (\lambda_{ao} - \lambda)^2}. \tag{22}$$

The ratio $A/(A+B)$ gives an indication of the degree of order of a system, and in the neighborhood of a phase transition one would expect it to vary rapidly with a small variation in temperature.

4. Remarks on phase transitions

As one raises the temperature of a physical system (containing a large number of molecules) in a given state there often exist temperatures at which the system undergoes a radical change in state. For example, in a solid with a definite crystal structure the lattice is sharply disrupted at a temperature called the melting point, and above this temperature the liquid state exists. There is a temperature at which a ferromagnetic material sharply loses its magnetic properties. Such changes in state are called phase changes or phase transitions. At the transition temperature both states are equally probable and can coexist

[10] Cf. Pauling, *Nature of the Chemical Bond* (Ithaca, 1940), p. 8.

at equilibrium in any proportion. These qualitative properties of phase changes can be translated into the language of characteristic value problems by ascribing a characteristic vector ψ_1 to the state below the transition temperature and another, ψ_2, to that above it. Obviously $\lambda_1>\lambda_2$ if $T<T_{\text{trans}}$ and $\lambda_2>\lambda_1$ if $T>T_{\text{trans}}$, for otherwise the two would be interchanged (or one would not be a $\psi_{\max}$ at any temperature). Since both states are equally probable at T_{trans}, the ψ's corresponding to both states must have the same characteristic value at $T=T_{\text{trans}}$ and the criterion for a sharp phase transition is

$$\lambda_1=\lambda_2 \quad \text{at} \quad T=T_{\text{trans}}$$
$$\lambda_1>\lambda_2 \quad \text{if} \quad T<T_{\text{trans}}$$
$$\lambda_1<\lambda_2 \quad \text{if} \quad T>T_{\text{trans}}.$$

(i.e., $\lambda_{\max}$ is doubly degenerate at T_{trans}).

When M and N are finite in a solid whose cells are limited to a finite number ν of configurations, $|V(\alpha_i, \alpha_j)|$ is always finite and only as either M or N becomes infinite can $|V(\alpha_i, \alpha_j)|\to\infty$. Therefore the elements of the **exp** $(-\mathbf{V}/\mathbf{kT})$ matrix of a crystal with finite layers are all positive. Frobenius[11] proved that if all the elements of a finite matrix are >0, the largest characteristic value $\lambda_{\max}$ is positive and simple (i.e., nondegenerate). This theorem implies that $\lambda_{\max}$ of a finite crystal with a finite number of configurations per lattice point can at no finite temperature be degenerate, and therefore sharp phase transitions are impossible. If the crystal is infinite in one direction, this can be chosen as the "L" direction and the elements of the **exp** $(-\mathbf{V}/\mathbf{kT})$ matrix would still be >0. However, if the crystal is infinite in two directions some of the matrix elements can be zero and a phase transition can occur. That is, a necessary condition for the existence of a sharp phase transition is that the crystal be infinite in at least two directions. By the same reasoning a necessary condition for the existence of a sharp phase transition in a two-dimensional square lattice is that it be infinite in both directions; and no sharp phase transition is possible in a one-dimensional nearest neighbor system, finite or infinite.

Although real crystals are finite they have for all practical purposes an infinite number of lattice points per direction—or more exactly, the number of lattice points per direction is sufficiently large to produce configurations that cause some elements in **exp** $(-\mathbf{V}/\mathbf{kT})$ to be as close to zero as an experimenter can measure the sharpness of a transition. Thus our condition of necessity does not prevent the occurrence of a phase transition, but merely serves as a warning signal to be careful about expecting calculations on "small" crystals to give a correct picture of a phase transition, and to remember that the properties of a two- or three-dimensional system are not always deducible from the study of a one-dimensional one.[12]

5. Perturbation theory of the partition function

It is apparent that in a real crystal the order of the **exp** $(-\mathbf{V}/\mathbf{kT})$ matrix is so large that the direct calculation of its characteristic values is difficult if not impossible. However, one may be able to solve analytically (at least at high and low temperatures) the characteristic value problems associated with crystals that are only a few layers thick. This immediately suggests the use of a perturbation method for the solution of the real crystal problem, for physically a real crystal can be considered as a pile of microcrystals with the interactions between neighboring microcrystals as perturbations. Thus if the partition function of a crystal s layers thick can be evaluated, that of a real crystal (the subscript on Z in this discussion will denote the number of layers in the Z under consideration) can usefully be written

$$Z_L=\sum_{\alpha_1}\cdots\sum_{\alpha_L}\prod_{i=1}^{[L/s]}\exp-[V(\alpha_{(i-1)s+1},\alpha_{(i-1)s+2})+\cdots+V(\alpha_{is-1},\alpha_{is})]/kT\times\exp(-\theta(s)/kT), \quad (23)$$

where

$$\theta(s)=V(\alpha_s,\alpha_{s+1})+V(\alpha_{2s},\alpha_{2s+1})+\cdots+V(\alpha_{L-s},\alpha_{L-s+1}).$$

[11] S. B. Frobenius, Preuss. Akad. Wiss., 514–518 (1909). See also R. Oldenburger, Duke Math. J. **6**, 357 (1940). The author is indebted to Professor Onsager for pointing out this theorem and its implications.

[12] This has been observed before in special cases; for example, a one-dimensional gas does not have a sharp condensation point. Herzfeld and Goeppert-Mayer, J. Chem. Phys. **2**, 28 (1934).

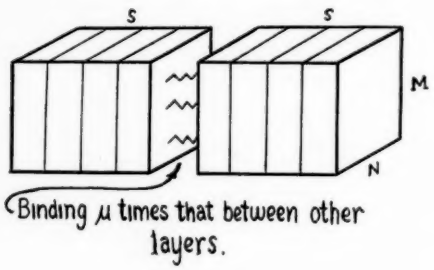

FIG. 3.

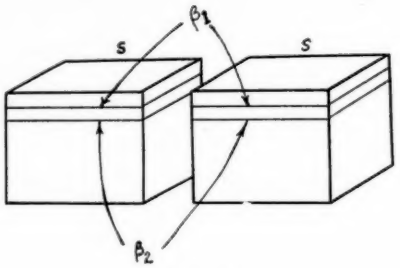

FIG. 4.

Using the high temperature expansion of $\exp -\theta(s)/kT$

$$Z_L=\sum_{\alpha_1}\cdots\sum_{\alpha_L}\prod_{i=1}^{[L/s]}(1-\theta(s)/kT+\theta^2(s)/2(kT)^2-\cdots)\times\exp-[V(\alpha_{(i-1)s+1},\alpha_{(i-1)s+2})+\cdots+V(\alpha_{is-1},\alpha_{is})]/kT$$

$$=Z_s^{L/s}-\frac{(L/s-1)}{kT}Z_s^{(L/s-2)}\langle V_{s,s+1}\rangle_{Av}+\frac{Z_s^{(L/s-4)}}{2(kT)^2}[Z_s^2(L/s-1)\langle V_{s,s+1}^2\rangle_{Av}+2(L/s-2)\langle V_{s,s+1}V_{2s,2s+1}\rangle_{Av}+(L/s-1)(L/s-2)\langle V_{s,s+1}\rangle_{Av}^2]+\cdots, \quad (24)$$

where

$$\left\langle\prod_{n=1}^{k}V_{ns,ns+1}^{p_n}\right\rangle_{Av}=\sum_{\alpha_1}\cdots\sum_{\alpha_{(k+1)s}}\prod_{n=1}^{k+1}V^{p_n}(\alpha_{ns}\,\alpha_{ns+1})\exp[-V(\alpha_{(n-1)s+1}\,\alpha_{(n-1)s+2})+\cdots+V(\alpha_{ns-1}\,\alpha_{ns})]/kT$$

$$=\lim_{\substack{\mu_1\to 0\\ \vdots\\ \mu_k\to 0}}(-kT)^{\sum_{n=1}^{k}p_n}\frac{\partial^{p_1+\cdots+p_k}}{\partial\mu_1^{p_1}\partial\mu_2^{p_2}\cdots\partial\mu_k^{p_k}}\sum_{\alpha}\cdots\sum_{\alpha_{(k+1)s}}\prod_{n=1}^{k+1}\times\exp\{-[V(\alpha_{(n-1)s+1},\alpha_{(n-1)s+1})+\cdots+V(\alpha_{ns-1},\alpha_{ns})+\mu V(\alpha_{ns},\alpha_{ns+1})]/kT\}. \quad (25)$$

$$(\mu_{k+1}=0)$$

We shall not exhibit a general expression for these averages, but the method of calculating a particular one will be apparent from a discussion of $\langle V_{s,s+1}\rangle_{Av}$. Here we must study

$$Z_2'=\sum_{\alpha_1}\cdots\sum_{\alpha_{2s}}\exp-[V(\alpha_1\alpha_2)+\cdots+V(\alpha_{s-1},\alpha_s)+\mu V(\alpha_s,\alpha_{s+1})+V(\alpha_{s+1},\alpha_{s+2})+\cdots+V(\alpha_{2s-1},\alpha_{2s})]/kT,$$

which is the partition function of the system in Fig. 3. Now Z_2' can equally well be calculated on the basis of the system being a pile of M layers of $2s\times N$ cells with an anemic interaction between the sth and the $(s+1)$st row in each layer:

$$Z_2'=\sum_{\beta_1}\cdots\sum_{\beta_n}\exp\{-[V(\beta_1,\beta_2)+\cdots+V(\beta_{M-1},\beta_M)]/kT\}.$$

$V(\beta_1,\beta_2)$ is the reduced double layer potential (of Eq. 2) between one layer in configuration 1 and the other in configuration 2. Proceeding in the manner discussed in Section 1:

$$Z_2'=\lambda_{\max}^{M-1}\{\sum_{\beta}\psi_{\max}(\beta)\}^2,$$

where $\lambda_{\max}$ is the greatest characteristic value and $\psi_{\max}$ its corresponding characteristic vector of

$$\exp(-\mathbf{V}_\beta/\mathbf{kT})=\begin{pmatrix}\exp[-V(\beta_1,\beta_1)/kT] & \exp[-V(\beta_1,\beta_2)/kT] & \cdots\\ \exp[-V(\beta_2,\beta_1)/kT] & \exp[-V(\beta_2,\beta_2)/kT] & \cdots\\ \cdots & \cdots & \cdots\end{pmatrix}.$$

It is at this point that the perturbation theory is useful, for we can express our characteristic value problem as

$$\lambda\psi(\beta_1)=\sum_{\beta_2}\psi(\beta_2)\exp\{-[V_0(\beta_1\beta_2)+\mu V_1(\beta_1\beta_2)]/kT\} \tag{26a}$$

or

$$\lambda\psi(\beta_1)=\sum_{\beta_2}\psi(\beta_2)\exp[-V_0(\beta_1\beta_2)/kT](1-\mu V_1(\beta_1\beta_2)/kT+\cdots). \tag{26b}$$

$V_0(\beta_1\beta_2)$ is the reduced potential energy function for two adjacent layers in the two independent systems, and $\mu V(\beta_1\beta_2)$ is the weak perturbation resulting from interactions between a pair of layers in the left system with the corresponding pair in the system on the right (Fig. 4). As is customary in perturbation theory we assume that

$$\lambda=\lambda_0+\mu\lambda_1+\mu^2\lambda_2+\cdots,\quad \psi=\psi_0+\mu\psi_1+\mu^2\psi_2+\cdots, \tag{27}$$

where λ_0 and ψ_0 satisfy the equation

$$\lambda_0\psi_0=\mathbf{exp}\,(-\mathbf{V}_0/\mathbf{kT})\psi_0. \tag{28}$$

Since we assumed that the s layer problem has already been solved, λ_0 and ψ_0 are known and Eq. (26b) becomes (neglecting all terms of $0(\mu^2)$ and higher):

$$(\lambda_0+\mu\lambda_1)(\psi_0+\mu\psi_1)=\mathbf{exp}\,(-\mathbf{V}_0/\mathbf{kT})(1-\mu\mathbf{V}_1/kT)(\psi_0+\mu\psi_1)$$

or

$$\lambda_0\psi_0+\lambda_0\mu\psi_1+\mu\lambda_1\psi_0=\mathbf{exp}\,(-\mathbf{V}_0/\mathbf{kT})(\psi_0-\mu\mathbf{V}_1\psi_0/kT+\mu\psi_1).$$

Multiplying by ψ^*_0 and remembering (28)

$$\begin{aligned}\lambda_1&=-\psi^*_0\,\mathbf{exp}\,(-\mathbf{V}_0/\mathbf{kT})\mathbf{V}_1\psi_0/kT\\&=-\sum_{\beta_1}\sum_{\beta_2}\psi_0(\beta_1)\exp[-V_0(\beta_1\beta_2)/kT]V_1(\beta_1\beta_2)\psi_0(\beta_2)/kT.\end{aligned} \tag{29}$$

Therefore, correct to terms of order μ:

$$\lambda=\psi^*_0[\mathbf{exp}\,(-\mathbf{V}_0/\mathbf{kT})(1-\mu\mathbf{V}_1/kT)]\psi_0. \tag{30}$$

For details necessary in the calculation of ψ_1 the reader is referred to the chapter on perturbation theory in any of the standard quantum mechanics texts.

The higher order V averages are found by essentially the same method, and $\langle V_{s,s+1}\rangle_{Av}$ can be better approximated by taking second perturbations.

In the low temperature region it seems advisable to handle the perturbations by expanding the exponential $\exp[-\theta(s)/kT]$ as

$$e^{-\theta(s)/kT}=e^{-V(\mathrm{or})/kT}\Big(1-\sum_{n=1}^{[L/s]}f_{ns,\,ns+1}+\cdots\Big),$$

where $V(\mathrm{or})$ is the reduced potential energy of the perturbing interactions between adjacent microcrystals when they are in a completely ordered state, and

$$f_{ij}=\exp\left\{-\left[V(\alpha_{ij})-\frac{s}{L}V(\mathrm{or})\right]/kT\right\}-1.$$

The development would then proceed by combining the high temperature formalism with that of Mayer's treatment of imperfect gases.[13]

II. Application to Two-Dimensional Ferromagnetic Nets

1. General remarks

A problem well suited as an example for the application of the general theory of Part I is the statistics of a two-dimensional ferromagnetic net. Here we shall not be so much concerned with the physics or complete solution of the problem as we shall be in using it as a medium of demonstration.

[13] Mayer and Mayer, *Statistical Mechanics* (New York, 1940), p. 277.

Wannier and Kramers have studied ferromagnetic nets in detail by a method somewhat similar to that described here. They first show that the partition function is the largest characteristic value of a set of linear difference equations that are derived by considering the change in the configuration of the lattice points of the system by the addition of one more molecule. Their final characteristic value problem[14] resembles ours rather closely.

The seat of magnetic properties of a ferromagnetic crystal is the unpaired electron spins in the d shells of the atoms at each lattice point in the crystal.[15] We shall let $-\epsilon$ be the energy of interaction of two neighboring atoms whose unpaired spins are parallel and $+\epsilon$ that when they are antiparallel. Also we shall write $J=\epsilon/kT$ and in the operator equation[16] $\mathbf{exp}\,(-\mathbf{V}/\mathbf{kT})\psi=\lambda\psi$, the matrix elements will be abbreviated

$$\exp\,[-V(\alpha_i\alpha_j)/kT]=[\alpha_i,\,\alpha_j].$$

In a system in which two possible configurations are available to each lattice point a "0" may be used to represent one configuration and a "1" the other. Then there exists a unique number n in the binary system ($n\leq 2^N-1$ if there are N lattice points per row) that corresponds to a given configuration of a row:

$$\begin{aligned}
&\alpha=0\sim 0000\cdots 00\\
&\alpha=1\sim 0000\cdots 01\\
&\alpha=2\sim 0000\cdots 10\\
&\quad\cdots\cdots\cdots\\
&\alpha=2^N-1\sim 1111\cdots 11
\end{aligned}$$

Ferromagnetically speaking a "0" will represent a lattice point with a + excess spin and a "1" will represent a − excess spin. If $v(\sigma_1\sigma_2)$ is the potential energy between a lattice point with excess spin σ_1 and a nearest neighbor with excess spin σ_2

$$v(1,\,1)=v(0,\,0),\quad v(1,\,0)=v(0,\,1).$$

This symmetry implies the invariance of all potential energy functions with respect to interchanges of 0's with 1's. A configuration will be called complementary to another if the replacement of 0's by 1's and vice versa makes the second configuration identical with the first. In the binary number system the exchange of 0's and 1's changes a number α to $2^N-1-\alpha$ because the sum of a number and complement is always

$$1111\cdots 11=2^N-1.$$

The $\mathbf{exp}\,(-\mathbf{V}/\mathbf{kT})$ matrix can be constructed in the symmetrical form

$$\mathbf{exp}\,(-\mathbf{V}/\mathbf{kT})$$

$$\sim\left(\begin{array}{ccc|ccc}
[0,\,0][0,\,1] & \cdots & [0,\,2^{N-1}-1] & [0,\,2^N-1] & \cdots & [0,\,2^{N-1}]\\
[1,\,0][1,\,1] & \cdots & [1,\,2^{N-1}-1] & [1,\,2^N-1] & \cdots & [1,\,2^{N-1}]\\
\cdots & \cdots & \cdots & \cdots & \cdots & \cdots\\
[2^{N-1}-1,\,0] & \cdots & [2^{N-1}-1,\,2^{N-1}-1] & [2^{N-1}-1,\,2^N-1] & \cdots & [2^{N-1}-1,\,2^{N-1}]\\
\hline
[2^N-1,\,0][2^N-1,\,1] & \cdots & [2^N-1,\,2^N-1] & [2^N-1,\,2^N-1] & \cdots & [2^N-1,\,2^{N-1}]\\
\cdots & \cdots & \cdots & \cdots & \cdots & \cdots\\
[2^{N-1},\,0] & \cdots & [2^{N-1},\,2^{N-1}-1] & [2^{N-1},\,2^N-1] & \cdots & [2^{N-1},\,2^{N-1}]
\end{array}\right)\qquad(31)$$

[14] Unfortunately the present state of world affairs has delayed publication of this work. However, it is abstracted in the Proceedings of the Boston Meeting of the American Physical Society, Feb. 1941. See Phys. Rev. **59**, 683A (1941). The author is greatly indebted to Dr. Wannier for a discussion of his unpublished work; indeed to a large degree it was this discussion that inspired the writing of the present paper.

[15] For reviews of research in this field see Bitter, *Introduction to Ferromagnetism*, (McGraw-Hill, New York, 1937), Chap. V; and Van Vleck, *The Theory of Electric and Magnetic Susceptibilities* (Oxford University Press, 1932), Chap. XII.

[16] Note that in two-dimensional problems the word "layer" used so frequently in Part I is to be replaced by the word "row."

with the upper left quadrant identical to the lower right and the upper right identical with the lower left. This quadrant symmetry follows from the observation that the element in the ith row and jth column in the upper left quadrant is $[i, j]$ and that in the lower right quadrant is $[2^N-1-i, 2^N-1-j]$. Since the configurations yielding these matrix elements are complementary, the elements are equal (the same sort of reasoning applies in the proof of upper right, lower left symmetry). Thus

$$\mathbf{exp}\,(-\mathbf{V}/\mathbf{kT})=\begin{pmatrix}P & Q\\ Q & P\end{pmatrix},$$

where

$$P=\begin{pmatrix}[0,0] & \cdots & [0,2^{N-1}-1]\\ \vdots & \vdots & \vdots\\ [2^{N-1},0] & \cdots & [2^{N-1}-1,2^{N-1}-1]\end{pmatrix} \tag{32b}$$

and

$$Q=\begin{pmatrix}[0,2^N-1] & \cdots & [0,2^{N-1}]\\ [1,2^N-1] & \cdots & [1,2^{N-1}]\\ \vdots & \vdots & \vdots\\ [2^{N-1}-1,2^N-1] & \cdots & [2^{N-1}-1,2^{N-1}]\end{pmatrix} \tag{32c}$$

$$=\begin{pmatrix}[0,2^N-1] & \cdots & [0,2^{N-1}]\\ \vdots & \vdots & \vdots\\ [0,2^{N-1}] & \cdots & [2^{N-1}-1,2^{N-1}]\end{pmatrix}.$$

The latter equality is the result of the property

$$[i,2^N-1-j]=[2^N-1-i,2^N-1-2^N+j]=[2^{N-1}-1-i,j].$$

Our operator Eq. (9) now becomes

$$\begin{pmatrix}P & Q\\ Q & P\end{pmatrix}\psi=\lambda\psi. \tag{33}$$

Transforming to a new vector ϕ by letting

$$\psi=\frac{1}{\sqrt{2}}\begin{pmatrix}(1) & (1)\\ (1) & (-1)\end{pmatrix}\phi=\mathbf{R}\phi;\quad \mathbf{R}=\mathbf{R}^{-1}$$

with

$$(1)=\begin{pmatrix}1 & 0 & \cdots & 0\\ 0 & 1 & \cdots & 0\\ \vdots & \vdots & \vdots & \vdots\\ 0 & 0 & \cdots & 1\end{pmatrix},\quad (-1)=\begin{pmatrix}-1 & 0 & \cdots & 0\\ 0 & -1 & \cdots & 0\\ \vdots & \vdots & \vdots & \vdots\\ 0 & 0 & \cdots & -1\end{pmatrix},$$

we have

$$\begin{pmatrix}P+Q & 0\\ 0 & P-Q\end{pmatrix}\phi=\lambda\phi$$

and the largest characteristic value of (33) is the largest root of the secular equation

$$|P+Q-\lambda|=0. \tag{35}$$

The $(P-Q)$ portion of the reduced matrix yields smaller characteristic values and may be ignored; so, if $\{\tilde{\phi}_i\}$ is a set of orthonormal vectors in the reduced manifold of ϕ we need only study

$$(P+Q)\tilde{\phi}=\lambda\tilde{\phi}. \tag{36}$$

The $(P+Q)$ matrix is still reducible, but its reduction is not a very great simplification and will not be performed here.

2. Calculation of the partition function for some narrow strips*

Using a strictly scalar model of spin interactions, we have the following partition function calculations.

(*a*) *Linear chains.*—A linear ferromagnetic chain of N equally spaced lattice points has an easily calculated partition function. Its $\mathbf{exp}\,(-\mathbf{V}/\mathbf{kT})$ matrix is

$$\mathbf{exp}\,(-\mathbf{V}/\mathbf{kT})=\begin{pmatrix} e^{J} & e^{-J} \\ e^{-J} & e^{J} \end{pmatrix}$$

and the secular equation of this operator shows the largest characteristic value to be $\lambda_{\max}=e^{J}+e^{-J}$. The corresponding characteristic vector is $\psi_{\max}=(1,1)/\sqrt{2}$. Therefore

$$Z_{N,1}=2^{N}\cosh^{N-1}J. \tag{37}$$

(*b*) $2\times N$ *strip.*—Every spin configuration of a row of a $2\times N$ ferromagnetic strip corresponds to a two-digit number in the binary system, and in the notation of Section 1 of this part, the secular equation for this problem is

$$|P+Q-\lambda|=\begin{vmatrix} [0,0]+[0,3]-\lambda & 2[0,1] \\ 2[1,0] & [1,1]+[1,2]-\lambda \end{vmatrix}$$
$$=\begin{vmatrix} e^{-J}+e^{3J}-\lambda & 2 \\ 2 & e^{J}+e^{-3J}-\lambda \end{vmatrix}=0.$$

Simple algebra shows the largest root of this equation to be

$$\lambda_{\max}=\tfrac{1}{2}\left[\frac{\sinh 4J}{\sinh J}+\Delta\right]=\tfrac{1}{2}[(\Delta^{2}-16)\coth J+\Delta], \tag{38}$$

where

$$\Delta^{2}=16+(e^{3J}-e^{J}+e^{-J}-e^{-3J})^{2}=16+(\sinh 4J/\cosh J)^{2}$$

and

$$\psi^{*}_{\max}=(a,b,a,b)/\sqrt{2}$$

with

$$a^{2}=8/(\Delta^{2}-\Delta[\Delta^{2}-16]^{\frac{1}{2}}),\quad b^{2}=8/(\Delta^{2}+\Delta[\Delta^{2}-16]^{\frac{1}{2}}).$$

Thus

$$[\textstyle\sum_{\alpha}\psi(\alpha)]^{2}=(2a+2b)^{2}/2=2(1+4/\Delta)$$

and

$$Z_{N,2}=2\left[\frac{\sinh 4J}{2\sinh J}+\frac{\Delta}{2}\right]^{N-1}(1+4/\Delta). \tag{39}$$

(*c*) $3\times N$ *strips.*—The secular equation of a $3\times N$ strip

$$|P+Q-\lambda|=\begin{vmatrix} e^{5J}+e^{-J}-\lambda & e^{2J}+1 & e^{2J}+1 & e^{J}+e^{-J} \\ e^{2J}+1 & e^{3J}+e^{-3J}-\lambda & e^{J}+e^{-J} & e^{-2J}+1 \\ 1+e^{2J} & e^{J}+e^{-J} & e^{3J}+e^{-3J}-\lambda & 1+e^{-2J} \\ e^{J}+e^{-J} & 1+e^{-2J} & 1+e^{-2J} & e^{J}+e^{-5J}-\lambda \end{vmatrix}$$

(and that of wider strips) is of too great a degree to be solved in a direct analytical manner, so one must resort to numerical or approximation methods. Fortunately the method of successive approximations is ideally suited to the high and low temperature evaluations of $\lambda_{\max}$. Here one guesses a reasonable vector $\tilde{\varphi}_{0}$ and calculates

$$(P+Q)\tilde{\phi}_{0}=\lambda_{0}\tilde{\phi}_{1}, \tag{40}$$

* The results of this section are not new, having been obtained by Wannier and Kramers; however, the approach, especially that in $c-e$, is new.

where the first component of $\tilde{\phi}_i$ is factored into $\lambda_0\tilde{\varphi}_0(1)$. This process is continued according to the general scheme

$$(P+Q)\tilde{\phi}_i=\lambda_i\tilde{\phi}_{i+1} \quad (\tilde{\varphi}_i(1)=\tilde{\varphi}_{i+1}(1)), \tag{41}$$

until the difference between $\tilde{\phi}_i$ and $\tilde{\phi}_{i+1}$ is as small as one desires. The largest characteristic value of $(P+Q)$ to the same accuracy is[17] λ_i. In the completely ordered state the characteristic vector $\tilde{\phi}_{\max}$ of $(\mathbf{P}+\mathbf{Q})$ is (0, 0, 0, 1) so for low temperature (large $-J$ values) calculations of λ we assume $\tilde{\phi}_0^*=(0, 0, 0, 1)$ (note that no attention will be paid to normalization until the end of our calculations and that at each step higher powers of e^{+J} are neglected) and proceed by the method discussed above.

$$(P+Q)\tilde{\varphi}_0=\begin{pmatrix} e^{5J}+e^{-J} & e^{2J}+1 & e^{2J}+1 & e^{J}+e^{-J} \\ e^{2J}+1 & e^{3J}+e^{-3J} & e^{-J}+e^{J} & e^{-2J}+1 \\ 1+e^{2J} & e^{J}+e^{-J} & e^{3J}+e^{-3J} & 1+e^{-2J} \\ e^{J}+e^{-J} & 1+e^{-2J} & 1+e^{-2J} & e^{J}+e^{-5J} \end{pmatrix}\begin{pmatrix} 0 \\ 0 \\ 0 \\ 1 \end{pmatrix}=e^{-5J}\begin{pmatrix} e^{4J} \\ e^{3J} \\ e^{3J} \\ 1 \end{pmatrix}$$

$$=\begin{pmatrix} e^{5J}+e^{-J} & e^{2J}+1 & e^{2J}+1 & e^{J}+e^{-J} \\ e^{2J}+1 & e^{3J}+e^{-3J} & e^{-J}+e^{J} & e^{-2J}+1 \\ 1+e^{2J} & e^{J}+e^{-J} & e^{3J}+e^{-3J} & 1+e^{-2J} \\ e^{J}+e^{-J} & 1+e^{-2J} & 1+e^{-2J} & e^{J}+e^{-5J} \end{pmatrix}\begin{pmatrix} e^{4J} \\ e^{3J} \\ e^{3J} \\ 1 \end{pmatrix}=(e^{-5J}+3e^{+J})\begin{pmatrix} e^{4J}+e^{6J} \\ e^{3J}+2e^{5J} \\ e^{3J}+2e^{5J} \\ 1 \end{pmatrix},$$

until

$$\lambda_{\max}=e^{-5J}+3e^{+J}+7e^{3J}+0(e^{5J}) \tag{42}$$

and

$$\tilde{\phi}_{a0}=\frac{1}{(1+2e^{6J}+9e^{8J}+22e^{10J})^{\frac{1}{2}}}\begin{pmatrix} e^{4J}+e^{6J}+3e^{8J} \\ e^{3J}+2e^{5J}+3e^{7J} \\ e^{3J}+2e^{5J}+3e^{7J} \\ 1 \end{pmatrix}.$$

The characteristic vector of the $P+Q$ matrix in the disordered state (unnormalized), $\tilde{\varphi}^*=(1, 1, 1, 1)$ will provide the first approximation at high temperatures. In this range it would be desirable to express the partition function in ascending powers of $1/kT$ (i.e., in powers of J) so the elements of the $(\mathbf{P}+\mathbf{Q})$ matrix will be written as power series in J.

$$(\mathbf{P}+\mathbf{Q})\tilde{\phi}_0=\begin{pmatrix} 2+4J & 2+2J & 2+2J & 2 \\ 2+2J & 2 & 2 & 2-2J \\ 2+2J & 2 & 2 & 2-2J \\ 2 & 2-2J & 2-2J & 2-4J \end{pmatrix}\begin{pmatrix} 1 \\ 1 \\ 1 \\ 1 \end{pmatrix}=(8+8J)\begin{pmatrix} 1 \\ 1-J \\ 1-J \\ 1-2J \end{pmatrix}$$

$$=\begin{pmatrix} 2+4J & 2+2J & 2+2J & 2 \\ 2+2J & 2 & 2 & 2-2J \\ 2+2J & 2 & 2 & 2-2J \\ 2 & 2-2J & 2-2J & 2-4J \end{pmatrix}\begin{pmatrix} 1 \\ 1-J \\ 1-J \\ 1-2J \end{pmatrix}=(8+0(J^2))\begin{pmatrix} 1 \\ 1-J+0(J^2) \\ 1-J+0(J^2) \\ 1-2J+0(J^2) \end{pmatrix}$$

$$=\begin{pmatrix} 2+4J+13J^2 & 2+2J+2J^2 & 2+2J+2J^2 & 2+J^2 \\ 2+2J+2J^2 & 2+9J^2 & 2+J^2 & 2-2J+2J^2 \\ 2+2J+2J^2 & 2+J^2 & 2+9J^2 & 2-2J+2J^2 \\ 2+J^2 & 2-2J+2J^2 & 2-2J+2J^2 & 2-4J+13J^2 \end{pmatrix}\begin{pmatrix} 1 \\ 1-J \\ 1-J \\ 1-2J \end{pmatrix}=(8+14J^2)\begin{pmatrix} 1 \\ 1-J+J^2/2 \\ 1-J+J^2/2 \\ 1-2J+2J^2 \end{pmatrix},$$

until

$$\lambda_{\max}\sim 8+20J^2+113J^4/3+0(J^6)$$

[17] For a detailed discussion of this method see Frazier, Duncan, and Collar, *Elementary Matrices* (University Press Cambridge, 1938), p. 140.

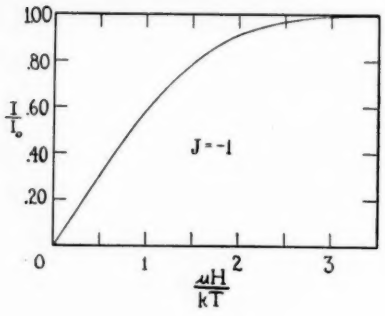

FIG. 5.

TABLE I.

$-J=-\epsilon/kT$	λ_{ad}	λ_{ao}	λ_{exact}
0	8.000		8.000
0.1	8.204		8.204
.2	8.861		8.864
.3	10.090		10.098
.4	12.41		12.44
.5		16.43	16.47
.6		23.57	23.58
.7		35.92	35.92
.8		56.86	56.86

and $\tilde{\varphi}_{max}$ (normalized) is

$$\tilde{\phi}_{ad}=\begin{pmatrix}1\\ 1-J+(J^2/2)-13/6J^3+J^4/24\\ 1-J+(J^2/2)-13/6J^3+J^4/24\\ 1-2J+2J^2-16/3J^3+26/3J^4\end{pmatrix}\frac{1}{[4-8J+12J^2-88/3J^3+52J^4]^{\frac{1}{2}}}.$$

In Table I the exact values of λ_{max} as computed numerically are compared with those given by the vectors $\tilde{\phi}_{ao}$ and $\tilde{\phi}_{ad}$.

$$\lambda_{ao}=\tilde{\phi}^*_{ao}\,\mathbf{exp}\,(-\mathbf{V/kT})\tilde{\phi}_{ao};\quad \lambda_{ad}=\tilde{\phi}^*_{ad}\,\mathbf{exp}\,(-\mathbf{V/kT})\tilde{\phi}^*_{ad}.$$

(*d*) $2\times N$ *strip by perturbation method.*—Since the application of the perturbation method to wide strips requires much space, and since at the present we are only interested in principles, we shall be satisfied in discussing this method in connection with $2\times N$ strips. These strips can be imagined as two linear chains whose interaction is a perturbation. At high temperatures

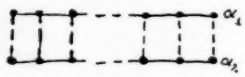

$$Z_2=\sum_{\alpha_1}\sum_{\alpha_2}\exp\{-[v(\alpha_1)+v(\alpha_2)]/kT\}\exp[-v(\alpha_1\alpha_2)/kT]$$
$$=\sum_{\alpha_1}\sum_{\alpha_2}\exp\{-[v(\alpha_1)+v(\alpha_2)]/kT\}\left(1-\frac{v(\alpha_1\alpha_2)}{kT}+\frac{v^2(\alpha_1\alpha_2)}{2(kT)^2}-\cdots\right)$$
$$=Z_1{}^2-\frac{\langle v(\alpha_1\alpha_2)\rangle_{Av}}{kT}+\frac{\langle v^2(\alpha_1\alpha_2)\rangle_{Av}}{2(kT)^2}-\cdots,$$

where

$$\langle v^n(\alpha_1\alpha_2)\rangle_{Av}=\sum_{\alpha_1}\sum_{\alpha_2}v^n(\alpha_1\alpha_2)\exp\{-[v(\alpha_1)+v(\alpha_2)]/kT\}$$
$$=\lim_{\mu\to 0}(-kT)^n(\partial^n/\partial\mu^n)\sum_{\alpha_1}\sum_{\alpha_2}\exp\{-[v(\alpha_1)+\mu v(\alpha_1\alpha_2)+v(\alpha_2)]/kT\}.$$

The quantity

$$Z_2'(\mu)=\sum_{\alpha_1}\sum_{\alpha_2}\exp\{-[v(\alpha_1)+v(\alpha_2)+\mu v(\alpha_1\alpha_2)]/kT\}$$

can equally well be written

$$=\sum_{\beta_1}\sum_{\beta_2}\exp[-V(\beta_1\beta_2)/kT]=\lambda_{max}^{N-1}\{\sum_\beta\psi(\beta)\}^2$$

with the β's referring to the configuration and

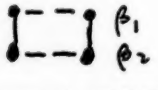

$$\lambda\psi=\exp(-V/kT)\psi.$$

Introduction of the transformation of Eq. (34) yields

$$\lambda\tilde{\phi}=(\mathbf{P}+\mathbf{Q})\tilde{\phi},$$

$$(\mathbf{P}+\mathbf{Q})=\begin{pmatrix} e^{\mu J}(e^{2J}+e^{-2J}) & 2 \\ 2 & e^{-\mu J}(e^{2J}+e^{-2J}) \end{pmatrix}.$$

In the unperturbed system, $\mu=0$ and

$$\lambda^0\tilde{\phi}^0=\begin{pmatrix} e^{2J}+e^{-2J} & 2 \\ 2 & e^{2J}+e^{-2J} \end{pmatrix}\tilde{\phi}^0.$$

Now let

$$\tilde{\phi}^0=\frac{1}{\sqrt{2}}\begin{pmatrix} 1 & 1 \\ 1 & -1 \end{pmatrix}\vartheta^0.$$

Then

$$\lambda^0\vartheta^0=\begin{pmatrix} (e^J+e^{-J})^2 & 0 \\ 0 & (e^J-e^{-J})^2 \end{pmatrix}\vartheta^0.$$

The characteristic values and characteristic vectors are then

$$\lambda_1^0=(e^J+e^{-J})^2;\quad \vartheta_1^{0*}=(1,0)\quad \text{or}\quad \tilde{\phi}_1^{0*}=(1,1)/\sqrt{2}$$

$$\lambda_2^0=(e^J-e^{-J})^2;\quad \vartheta_2^{0*}=(0,1)\quad \text{or}\quad \tilde{\phi}_2^{0*}=(1,-1)/\sqrt{2}.$$

Note that $\tilde{\phi}_1^{0*}$ and $\tilde{\phi}_2^{0*}$ are the characteristic vectors and λ_1^0 and λ_2^0 the characteristic values of the linear chain matrices, as they must be because we have a linear chain problem when $\mu=0$.

The assumption that

$$\lambda=\lambda^0+\lambda^{(1)}\mu+\lambda^{(2)}\mu^2+\cdots,\quad \tilde{\phi}=\tilde{\phi}^0+\tilde{\phi}^{(1)}\mu+\tilde{\phi}^{(2)}\mu^2+\cdots$$

leads to [see Eq. (29)]

$$\lambda_1^{(1)}=\tfrac{1}{2}(1,1)\begin{pmatrix} J(e^{2J}+e^{-2J}) & 0 \\ 0 & -J(e^{2J}+e^{-2J}) \end{pmatrix}\begin{pmatrix} 1 \\ 1 \end{pmatrix}=0$$

$$\lambda_{1,2}=\tfrac{1}{2}(1,1)\begin{pmatrix} J(e^{2J}+e^{-2J}) & 0 \\ 0 & -J(e^{2J}+e^{-2J}) \end{pmatrix}\begin{pmatrix} 1 \\ 1 \end{pmatrix}=J(e^{2J}+e^{-2J}).$$

Since[18]

$$\tilde{\phi}_1^{(1)}=\tilde{\phi}_1^0-\mu\frac{\lambda_{1,2}}{\lambda_2^0-\lambda_1^0}\tilde{\phi}_2^0,\quad \tilde{\varphi}_1^{(1)}\backsimeq\frac{1}{\sqrt{2}}\begin{pmatrix} 1+\mu J/2 \\ 1-\mu J/2 \end{pmatrix}$$

at high temperatures. The normalized $\varphi_1^{(1)}$ when $\mu=1$ can be written

$$\frac{1}{[4+0(J^2)]^{\frac{1}{2}}}\begin{pmatrix} 1 \\ 1-J \end{pmatrix},$$

which checks with the corresponding vector as found by the method described in Section (*c*). Inasmuch as $\lambda^{(1)}$ is independent of μ,

$$\langle v(\alpha_1\alpha_2)\rangle_{Av}=0$$

and

$$Z_2=2^{2N}+0(J^2).$$

Second perturbations give the term of $0(J^2)$.

(*e*) *Introduction of external fields.*—Certain types of external fields do not invalidate the formal developments of Part I. For example, let us consider a linear ferromagnetic chain of N equally spaced

[18] Cf. Pauling and Wilson, *Introduction to Quantum Mechanics* (McGraw-Hill, New York, 1935), p. 160.

lattice points in a magnetic field H whose direction is parallel to the chain. The interaction between field and spin when the chain is in a configuration with n_+ "+" spins and n_- "−" spins, is

$$-\mu(n_+-n_-)H=-\mu H\sum_{i=1}^{N}[n_+(\alpha_i)-n_-(\alpha_i)].$$

μ = magnetic moment at each lattice point.
$n_+(\alpha_i)$ = number of "+" spins at the ith lattice point when it is in configuration α_i.
$n_-(\alpha_i)$ = same with "−" spins.

Then letting

$$V(\alpha_i\alpha_j)=v(\alpha_i\alpha_j)-\frac{\mu H}{2}\{[n_+(\alpha_i)+n_+(\alpha_j)]-[n_-(\alpha_i)+n_-(\alpha_j)]\},$$

$$Z_{N,1}(H)=\sum_{\alpha_1}\cdots\sum_{\alpha_N}\exp\{-[V(\alpha_1\alpha_2)+\cdots+V(\alpha_{N-1}\alpha_N)]/kT\}$$

$$=\lambda_{\max}^{N-1}\{\sum_\alpha \psi_{\max}(\alpha)\}^2.$$

The $e^{-V/kT}$ matrix is

$$e^{-V/kT}=\begin{pmatrix} e^{J-\mu H/kT} & e^{-J} \\ e^{-J} & e^{J+\mu H/kT}\end{pmatrix}.$$

If $\psi^*_{\max}=(a,b)$; $a^2+b^2=1$, then

$$a(e^{J-\mu H/kT}-\lambda)+\quad be^{-J}\quad=0,$$

$$ae^{-J}\quad+b(e^{J+\mu H/kT}-\lambda)=0$$

and

$$\lambda_{\max}=e^J\cosh\mu H/kT+(e^{2J}\sinh^2\mu H/kT+e^{-2J})^{\frac{1}{2}},$$

$$(\textstyle\sum_\alpha\psi_{\max}(\alpha))^2=a^2+b^2+2ab=1+2ab$$

$$=1+1/(1+e^{4J}\sinh\mu H/kT)^{\frac{1}{2}}.$$

Therefore

$$Z_{N,1}(H)=[e^J\cosh\mu H/kT+(e^{2J}\sinh^2\mu H/kT+e^{-2J})^{\frac{1}{2}}]^{N-1}[1+1/(1+e^{4J}\sinh\mu H/kT)^{\frac{1}{2}}].$$

The magnetic moment of the chain is

$$I=\frac{\partial\log Z}{\partial[H\mu/kT]}$$

and that at saturation is $I_0=\mu N$. Therefore

$$\frac{I}{I_0}=\frac{\sinh\mu H/kT}{(\sinh^2\mu H/kT+e^{-4J})^{\frac{1}{2}}}.$$

This function is plotted in Fig. 5.

3. Spin contributions to specific heat

The well-known formulae

$$\bar{E}=\frac{d\log Z}{d(-1/kT)},\quad C_v=\left(\frac{\partial E}{\partial T}\right)_v$$

give the average energy and specific heat contribution of spin in terms of the partition function. They will be used in the following calculations.

(*a*) *Linear chain.*—

$$Z_{N,1}=2^N\cosh^{N-1}J;\quad\frac{dJ}{d(-1/kT)}=-\epsilon.$$

Therefore[19]

$$\bar{E}/N = -\epsilon \frac{\partial \log Z_{N,1}}{dJ} = -\epsilon \tanh J$$

and

$$C_v/Nk = J^2 \operatorname{sech}^2 J.$$

(*b*) $2 \times N$ *strip.*—Here the calculations are more tedious. They seem to be most easily performed by using the function Δ defined in Eq. 38.

$$Z_{N,2} = (\cosh 3J + \cosh J + \Delta/2)^{n-1}(1 + 4/\Delta).$$

From the equation for the average energy given at the beginning of this section (neglecting terms of $0(1/N)$, the average internal spin energy per lattice point is

$$\bar{E}/2N = -\frac{\epsilon}{2} \frac{(3 \sinh 3J + \sinh J + \Delta'/2)}{(\cosh 3J + \cosh J + \Delta/2)},$$

$$C_v/2Nk = [10 + 10 \cosh J \cosh 3J - 6 \sinh 3J \sinh J + (\Delta\Delta'' - \Delta'^2)/4 + (\cosh 3J)(\Delta'' + 9\Delta)/2 + (\cosh J)(\Delta'' + \Delta)/2 + (3 \sinh 3J + \sinh J)]J^2/2(\cosh 3J + \cosh J + \Delta/2)^2.$$

At low temperatures

$$C_v/2Nk \sim 8J^2 e^{4J}(1 + 9e^{2J} + 14e^{4J} + \cdots)$$

and at high temperatures

$$C_v/2Nk \sim J^2(3 + 9J^2 + \cdots)/2.$$

Wannier[14] has pointed out that the peak in the specific heat curve of plates $N \times \infty$ is of order $\log N$.

The author hopes to treat some of the other nearest neighbor problems mentioned at the beginning of this paper at some later date; and in conclusion he would like to thank Professor Onsager for his interesting discussions and for the numerous suggestions made throughout the course of this research.

[19] These results differ somewhat in form from those of Ising (see reference 4 or Bitter's book, p. 145) because if one interprets his directed dipoles as spin orientations, the interaction between parallel spins would be zero.

Raman Spectrum of Di-Tertiary-Butyl Ether

FORREST F. CLEVELAND
Department of Physics, Illinois Institute of Technology, Chicago, Illinois
(Received July 28, 1941)

Raman displacements, estimated intensities and depolarization factors are listed for di-tertiary-butyl ether, $(CH_3)_3COC(CH_3)_3$, in the liquid state and the results are compared with previous data for di-normal-butyl and di-isobutyl ethers. A tentative assignment of the observed lines to frequencies of the di-tertiary-butyl ether molecule is made.

INTRODUCTION

ERICKSON and Ashton[1] have recently carried out the first successful synthesis of di-tertiary-butyl ether, $(CH_3)_3COC(CH_3)_3$, and have kindly supplied the author with a sample of this material for use in a study of its Raman spectrum. The results of this investigation are given below.

EXPERIMENTAL

The spectrograph and the experimental technique have been described previously.[2] The Raman spectrum was obtained in the liquid state, with excitation by Hg 4358A. The boiling point of the liquid was 106.5–107.0°C, d_4^{20} was 0.7658 and n_D^{20} was 1.3949. Additional properties are listed elsewhere[1] and will not be repeated here. The sample was used as received from Professor Erickson, without redistillation. Only slight continuous background was obtained, even upon long exposure. The film used was Agfa Super Plenachrome Press and development was in Agfa 47 developer for six minutes at 18°C. The depolarization factors were obtained by the method previously described,[3] except that now the Polaroid disk has been replaced by a Nicol prism, on account of the rather strong absorption of light by the Polaroid. It is estimated that this change approximately doubles the amount of transmitted light.

[1] J. L. E. Erickson and W. H. Ashton, J. Am. Chem. Soc. **63**, 1769 (1941).
[2] Forrest F. Cleveland, M. J. Murray, H. H. Haney and Julia Shackelford, J. Chem. Phys. **8**, 153 (1940).
[3] Forrest F. Cleveland and M. J. Murray, J. Chem. Phys. **7**, 396 (1939).

RESULTS

The results are given in the columns at the left of Table I, in which $\Delta\nu$ represents the Raman displacement in cm^{-1}, I represents the estimated intensity and ρ represents the depolarization factor. Unusually sharp or broad lines are designated by the symbols s and b, respectively. Data in regard to which there is some question are enclosed in brackets. The brace joins lines that were unresolved on the polarization spectrograms. The symbol P means that the line was somewhat polarized, but that an estimate of the numerical value of the depolarization factor could not be made.

COMPARISON OF THE SPECTRA OF THE BUTYL ETHERS

The results previously obtained[2] for di-*n*-butyl and di-isobutyl ethers are included in Table I to facilitate comparison of these spectra with the present results for di-*t*-butyl ether. According to this table, it will be seen that the spectrum of di-*t*-butyl ether contains strong, polarized lines at 327, 567 and 701 and strong, depolarized lines at 298 and 902. All of these lines are absent or appear with low intensity in the spectra of the di-isobutyl and di-*n*-butyl ethers. Also, the tertiary ether has more lines in the 1200–1265 cm^{-1} region and fewer lines in the 1400–1500 and 2700–3000 cm^{-1} regions than the di-isobutyl and di-*n*-butyl ethers.

Di-isobutyl ether is distinguished by the group of three lines near 450 cm^{-1} and the fairly strong lines at 810, 1249 and 1339, while di-*n*-butyl ether differs from the other two by the group of three lines near the 844 line and by the line at 1228 cm^{-1}. The strong, polarized line at 840 appears in

all three ethers. The C-H frequencies above 1400 cm^{-1} are quite similar for the di-isobutyl and di-*n*-butyl ethers, but are quite different in the case of di-*t*-butyl ether. It is interesting to note that the spectrum of tertiary-butyl alcohol[4] above 1400 cm^{-1} is practically the same as that obtained for the di-*t*-butyl ether, but that below 1400 cm^{-1} the two spectra, while similar in some respects, are by no means identical.

Origin of the Di-*T*-Butyl Ether Lines

It is not possible with the information at present available to make a complete assignment of the Raman lines to definite vibrations of the $(CH_3)_3COC(CH_3)_3$ molecule. A rough approach to this problem may, however, be made by considering the frequencies to be expected from smaller groups within the molecule. The groups that make up the molecule may be considered to be a pyramidal CH_3 group, a pyramidal CC_3 group (neglecting the hydrogen atoms) and a non-linear R–O–R group, where R represents the rigid $(CH_3)_3C$ group. Obviously, this is only a very crude approximation, but if it be accepted for the moment, one may then investigate what frequencies would be expected for such groups.

The types of frequencies to be expected for such groups are listed in Table II. In the last column of this table are listed the values of the frequencies[5] for certain well-known molecules or ions which have the same symmetry as the groups under consideration. Using this table as a guide, one may then choose frequencies of the complicated molecule which correspond approximately to these group frequencies. The fundamentals so chosen are designated by the symbols ν_a, ν_b, etc. in Table III. The frequencies ν_d, ν_b, ν_f and ν_a have been selected as corresponding approximately to the frequencies ν_1, ν_2, ν_3 and ν_4 of the CC_3 group; ν_e, ν_c and ν_h to the frequencies ν_1, ν_2 and ν_3 of the COC group; and ν_l, ν_i, ν_m and ν_j, ν_k to the frequencies ν_1, ν_2, ν_3 and ν_4 of the CH_3 group. Apparently the doubly degenerate frequency ν_4 of the CH_3 group splits into the frequencies ν_j and ν_k in the complicated molecule. There is some evidence for a similar effect in the corresponding frequency of the CC_3 group, since the frequency ν_a, while not resolved into two components, is broader than usual on the spectrogram.

Three lines were observed near the frequency chosen as ν_h, perhaps due to Fermi resonance interactions with some of the combination fre-

Table I. *Raman spectra of butyl ethers.*

Present Results			Cleveland, Murray, Haney, Shackelford*					
Di-Tertiary			Di-Iso			Di-Normal		
$\Delta\nu$	I	ρ	$\Delta\nu$	I	ρ	$\Delta\nu$	I	ρ
203	¼							
			263	4	0.5	262	2	
						276	2	
298	3*b*	0.9	299	1		294	2	
						319	2	
327	3	0.4						
						346	1	
369	½		362	2				
						398	1	
424	½		418	3				
			450	1				
			467	1				
567	3	0.4						
701	9*s*	0.1						
			789	½				
			810	2				
						820	2	
841	7*s*	0.5	836	6	0.2	844	4	0.4
						882	1	
902	5	0.9				900	1	
			930	½				
			958	4	0.7	961	3	0.9
						979	2	
994	1	0.9	1001	1				
1026	2	0.9				1026	1	
						1068	4	0.7
			1123	3	0.7	1120	3	
			1137	3		1137	3	0.8
[1166]	½		1168	3	0.7	1156	3	
			1181	3				
1210	4	0.9						
1226	4	0.9				1228	2	
			1249	4	0.8			
1261	2	0.8						
			1294	2	0.8	1300	5	0.8
			1339	4	0.8			
1392	1	*P*						
1445	5	0.9	1448	7		1439	6	0.7
1461	3	0.9	1461	3	0.8	1459	6	
			1478	2		1484	3	0.7
2709	2	0.3	2718	3	0.4	2732	2	0.5
			2793	3	0.4	2798	3	0.5
			2837	3		2849	3	
2868	2	0.3	2866	10	0.2	2864	10	0.2
						2876	10	
			[2891]	1				
2924	10	0.2	2905	3	0.4	2912	8	0.3
			2952	1		2941	8	
2982	10	0.9	2963	4	0.8	2967	6	0.9
			2975	3				

* See reference 2 in text.

[4] M. Magat, *Tables Annuelles de Constantes et Données Numériques, Effet Raman* (Hermann and Company, Paris, 1937), Vol. 12, p. 32.

[5] Data taken from T. Y. Mu, *Vibrational Spectra and Structure of Polyatomic Molecules* (National University of Peking, Kun-ming, China, 1939), pp. 171, 203 and 238.

TABLE II. *Classification of the Raman frequencies.*

GROUP	SYMMETRY	FREQUENCY DESIGNATION	SYMMETRY CLASS	SELECTION[a] RULE	MOLECULE OR ION	FREQUENCY $\Delta\nu$	ρ
CH_3	C_{3v}	ν_1	A_1	P	CH_3Cl[b]	2955	0.05
		ν_2	A_1	P		1357	P
		ν_3	E	D		3024	0.86
		ν_4	E	D		1450	D
CC_3	C_{3v}	ν_1	A_1	P	IO_3^-	779	0.43
		ν_2	A_1	P		390	—
		ν_3	E	D		826	0.67
		ν_4	E	D		330	6/7
COC	C_{2v}	ν_1	A_1	P	SO_2	1151	P(gas)
		ν_2	A_1	P		525	P(liq.)
		ν_3	B_1	D		1366	D(liq.)

[a] P = polarized, D = depolarized.
[b] Only the frequencies which relate chiefly to the CH_3 group are listed here. There are two other frequencies ν_5 and ν_6 in which the Cl atom is more directly involved.

quencies $\nu_f+\nu_a$, $\nu_f+\nu_b$ and $\nu_d+\nu_e$. Fermi resonance also seems to exist between the fundamental ν_l and some of the overtones $2\nu_i$, $2\nu_j$ and $2\nu_k$.[6] The frequency ν_g is considered to be analogous to the frequency ν_6 in the methyl halides, in which the nucleus of the carbon atom and the center of gravity of the hydrogen nuclei in the methyl group are displaced in opposite directions, perpendicular to the symmetry axis of the methyl group. It is the motion of the methyl group which would correspond to rotation if the group were free. The frequency ν_6 is doubly degenerate and

[6] It should be remarked that the 2924 line excited by Hg 4347A would fall at 2867 cm^{-1}. However, it is believed that the intensity of the line observed at 2868 is too great to be accounted for by attributing it to this exciting line.

TABLE III. *Tentative assignment of di-t-butyl ether frequencies.*

ASSIGNMENT	FREQUENCY $\Delta\nu$	I	ρ	ASSIGNMENT	FREQUENCY $\Delta\nu$	I	ρ
$\nu_f-\nu_d$	203	$\frac{1}{4}$		$\nu_e+\nu_b$	[1166]	$\frac{1}{2}$	
ν_a	298	$3b$	0.9	$\nu_f+\nu_a$	1210	4	0.9
				ν_h			
ν_b	327	3	0.4	$\nu_f+\nu_b$	1226	4	0.9
$\nu_d-\nu_b$	369	$\frac{1}{2}$		$\nu_d+\nu_e$	1261	2	0.8
$\nu_d-\nu_a$	424	$\frac{1}{2}$		ν_i	1392	1	P
ν_e	567	3	0.4	ν_j	1445	5	0.9
ν_d	701	$9s$	0.1	ν_k	1461	3	0.9
ν_e	841	$7s$	0.5	$2\nu_i$	2709	2	0.3
				$2\nu_j$			
ν_f	902	5	0.9	$2\nu_k$	2868	2	0.3
$\nu_d+\nu_a$	994	1	0.9	ν_l	2924	10	0.2
ν_g							
$\nu_d+\nu_b$	1026	2	0.9	ν_m	2982	10	0.9

it is not clear whether the frequencies observed at 994 and 1026 result from the splitting of ν_6 into two frequencies in the large molecule or whether the two lines result from Fermi resonance interaction between ν_g and one of the combination frequencies $\nu_d+\nu_a$ or $\nu_d+\nu_b$.

The four remaining frequencies have only small intensities and may be ascribed to combination frequencies, as indicated in Table III. Some of them may, however, be fundamentals, since for the di-*t*-butyl ether molecule there should be $(3N-6)=75$ fundamentals and only thirteen (or fourteen, if both the frequencies 994 and 1026 are regarded as fundamentals) have been chosen above. It should again be emphasized that the above assignments are only tentative because of the very rough approximations made in arriving at them.

Letters to the Editor

THIS section will accept reports of new work, provided these are terse and contain few figures, and especially few halftone cuts. The Editorial Board will not hold itself responsible for opinions expressed by the correspondents. Contributions to this section should not exceed 600 words in length and must reach the office of the Managing Editor not later than the 15th of the month preceding that of the issue in which the letter is to appear. No proof will be sent to the authors. The usual publication charge ($3.00 per page) will not be made and no reprints will be furnished free.

Isotopic Exchange Between Carbon Tetrabromide and Bromine

J. H. HODGES AND A. S. MICELI
University of Michigan, Ann Arbor, Michigan
April 14, 1941

WEIGHED quantities of carbon tetrabromide and of bromine containing radioactive isotopes were allowed to react in Pyrex vessels of sufficient size to permit complete volatilization of the reactants. The radioactive bromine was obtained by exposing bromoform to neutrons from the cyclotron; it was allowed to age for periods of about 24 hr. to allow for decay of the two isotopes of shorter life.[1] The activity of the samples was measured with a Lauritsen electroscope. The rate of exchange of radioactive bromine could be determined conveniently over the temperature range 170° to 200°C. Molar concentrations of carbon tetrabromide and bromine were varied from a ratio of 10 : 1 to a ratio of 1 : 10. The reaction appears to be homogeneous, and the rate appears to be directly proportional to the concentration of the carbon tetrabromide and to the square root of the concentration of the bromine. This indicates a mechanism involving bromine atoms. If it is assumed that exchange occurs between a carbon tetrabromide molecule and a bromine atom, the energy of activation of this bimolecular process is zero. This is obtained by plotting log [(measured exchange rate)/$(CBr_4)(Br)$] against $1/T$. The value of (Br) is calculated from the equilibrium constant of the reaction $Br_2(g) \rightleftharpoons 2Br(g)$.

The same procedures were repeated using Pyrex capsules of small capacity in order to maintain the reactants in the liquid phase. The exchange rate was measured over the temperature range 107° to 160°C. The mechanism of the reaction seems to be the same as that in the gaseous phase. In this case, however, there is an energy of activation of about 3 kcal. The values of the activation energies for the reaction in the gaseous and liquid phases may be somewhat in error, first because of the extrapolation of the equilibrium constant expression to the rather low temperatures of our experiments, and second because of the inherent limits of accuracy in our experimental technique. An additional small error is involved in the use of this same equation in calculating the degree of dissociation in the liquid phase.

No parallelism can be detected between the intensity of the radioactivity of the bromine sample and the value of the specific reaction rate calculated for the runs. Furthermore, no exchange occurs at room temperature. These facts seem to indicate a thermal reaction and not one initiated by the energy of the nuclear decomposition.[2]

Calculation of theoretical rates on the basis of the collision theory, assuming a bimolecular reaction between carbon tetrabromide molecules and bromine atoms gives values in both the gaseous and liquid phases which are too large by a factor of between 10^4 and 10^5.

[1] Willard, J. Am. Chem. Soc. **62**, 256 (1940).
[2] Liberatore and Wiig, J. Chem. Phys. **8**, 165, 349 (1940); Libby, *ibid.* **8**, 348 (1940).

Infra-Red Absorption Spectrum of Acetone

DONNA PRICE
Mallinckrodt Chemical Laboratory, Harvard University, Cambridge, Massachusetts
July 29, 1941

THE infra-red spectrum, from 3–20μ, of gaseous acetone was obtained with a spectrometer[1] using fluorite, rocksalt, and KBr prisms. The acetone used was Mallinckrodt C.P. which had been refluxed and redistilled in this laboratory.

The spectra obtained for the three prisms are shown in Fig. 1. There is, though this is not evident in the figure, a shoulder on the low frequency side of the 1363 band. The frequencies and their qualitative intensities are given in

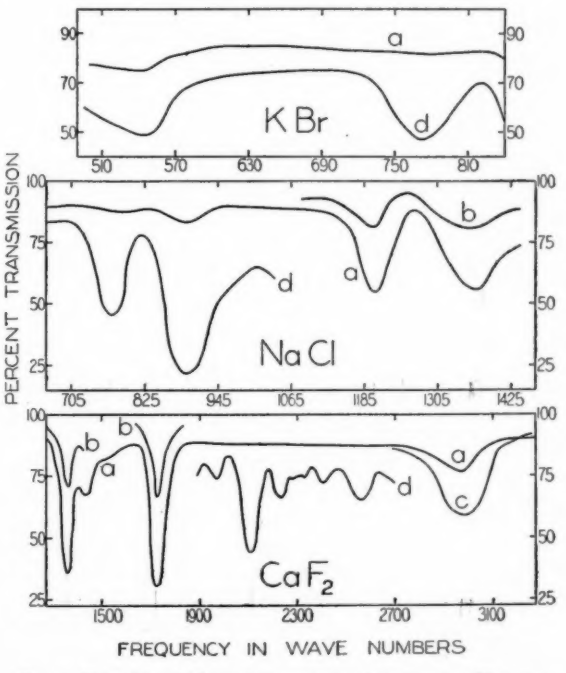

FIG. 1. The infra-red absorption spectrum of acetone gas. The transmission curves were taken in a 30-cm glass cell using NaCl windows with gas at the following pressures: *a*, 5 mm; *b*, 1.1 mm; *c*, 16 mm; *d*, 200 mm.

TABLE I. *The infra-red spectrum of acetone gas.*

FREQUENCY IN cm^{-1}	INTENSITY	FREQUENCY	INTENSITY
547	medium	1964	weak
774	medium	2109	medium
896	strong	2234	weak
1202	740 cm^{-1}	2418	weak
1363	1007 cm^{-1}	2554	weak
1430	strong	2984	strong
1725	1552 cm^{-1}		

Table I. By use of Wells' method,[2] the intensities of the three strongest bands were computed for $p=100$ mm. These results are the numerical values for the 1202, 1363, and 1725 bands given in Table I. It was assumed that acetone was at least as complicated as propylene, and hence no dilution with an inert gas was necessary. Moreover, the region 1.1–5 mm of the curve, ln (D_0/D) *vs.* p, was assumed practically a straight line. Wells' curves seem to justify this, but since only two points were taken and these determined by graphical integration, the values are given only as semi-quantitative approximations. Corrections were made for the blanks, but the stray effect was considered negligible in this region.

No other data are available for the vapor, but Coblentz obtained the infra-red absorption spectrum for liquid acetone, and Edsall and Wilson[3] have obtained the most recent Raman spectrum.

[1] H. Gershinowitz and E. B. Wilson, Jr., J. Chem. Phys. **6**, 197 (1938); E. B. Wilson, Jr., and A. J. Wells, J. Chem. Phys. **9**, 319 (1941).
[2] A. J. Wells, thesis, Harvard University, Cambridge, Massachusetts (1941); E. B. Wilson and A. J. Wells, J. Chem. Phys. **9**, 659 (1941).
[3] J. T. Edsall and E. B. Wilson, Jr., J. Chem. Phys. **6**, 124 (1938).

The Exchange Reaction Between Gaseous and Combined Nitrogen

T. H. NORRIS, S. RUBEN, AND M. D. KAMEN
Chemical Laboratory and Radiation Laboratory, University of California, Berkeley, California
August 13, 1941

USING radioactive nitrogen (N^{13}) as an indicator, Nishina, *et al.*[1] have reported that N_2 gas undergoes rapid exchange at room temperature with dilute (0.1–0.2M) solutions of $NaNO_3$, $NaNO_2$, $NH_2OH \cdot HCl$, etc. Moreover, according to these authors, the rate of exchange decreased with increasing concentration of nitrate or nitrite. Since these results are both unexpected and at variance with other investigations,[2,3] it has been considered desirable to repeat the experiments.

Charcoal was bombarded in a gas-tight chamber (containing 100 cc tank N_2) with 30μ of 8-Mev deuterons. Under these conditions ~30 percent of radioactive nitrogen formed[4] is present in gaseous state. An appreciable fraction of the gaseous activity is present as combined nitrogen[2] (formed by the recoiling N^{13} as a result of deuteron impact). Since the presence of combined nitrogen "impurity" can be construed as evidence for exchange, it is important to remove it from the labeled N_2. To this end the gaseous activity was pumped out of the target chamber and mixed with carrier (inactive) HCN and NO_2. The mixture was slowly pumped through a heated combustion tube containing CuO and was then passed through three glass spirals immersed in liquid air. By means of two Töpler pumps, one at each end of the train, the gas was forced back and forth several times through the CuO and cold traps.

After this treatment two portions of ~50 cc of the N_2* were vigorously shaken for ten minutes with 10 cc $NaNO_3$ and 10 cc $NaNO_2$ solution in separate (previously evacuated) vessels. The solutions were then gently boiled to drive off dissolved N_2 and were analyzed for radioactivity using methods described elsewhere.[5] The results are summarized in Table I.

TABLE I.

SUBSTANCE TESTED	CONCENTRATION (MOLES/LITER)	RADIOACTIVITY[a] (COUNTS/MINUTE)
$NaNO_3$	1.2	<4
	.1	<4
$NaNO_2$	1.3	<3
	.1	<5

[a] All figures are corrected for decay of N^{13} to the time of counting the first sample and are therefore comparable. The N_2* had an activity of 10^5 counts/minute.

It is apparent from Table I that <0.01 percent of the N_2* has exchanged with NO_3^- or NO_2^-. This is in agreement with the results of Burris and Miller[3] on N_2 fixation by *Azobacter* using heavy (N^{15}) nitrogen gas.

[1] Nishina, Iimori, Kubo, and Nakayama, J. Chem. Phys. **9**, 571 (1941).
[2] Ruben, Hassid, and Kamen, Science **91**, 578 (1940).
[3] Burris and Miller, Science **93**, 114 (1941).
[4] The remainder can be removed by completely burning the charcoal to carbon dioxide. This was not undertaken due to the short half-life of N^{13} (10.5 minutes).
[5] Ruben, Kamen, and Hassid, J. Am. Chem. Soc. **62**, 3443 (1940).

Measurement of Tension in Solutions

ARTHUR F. SCOTT AND G. MARSHALL POUND
Department of Chemistry, Reed College, Portland, Oregon
July 18, 1941

ALTHOUGH many properties of solutions have been studied, there appears to be no record of any systematic study of the maximum hydrostatic tension which solutions can withstand under varying conditions of temperature and concentration. With the publication of Vincent's ingenious method for measuring this tension such a study seemed possible and we have accordingly undertaken it in the hope of obtaining information of value to the problem of the structure of solutions. This letter is a preliminary report on the first experiments of this project.

Vincent's apparatus can be described briefly. It consists of a metallic bellows, closed by a needle valve, which contains the liquid under test. Inward leakage of air into the bellows is eliminated by surrounding the bellows and valve by the same liquid. With the bellows filled and the valve closed a gradually increasing load is applied to the bellows until the liquid breaks. The hydrostatic tension existing

TABLE I.

No.	PERCENT $Ca(NO_3)_2$	TEMP.	MAXIMUM TENSION atmos.
1	0	20	1.59
6	0	20	1.53
1	0	23.5	1.43
4	21	20	0.82
3	34	21	0.87
2	51	21	0.58
2	51	23	0.58
2	51	25	0.45
5	66	19	0.28

in the liquid prior to the breaking is then calculated from the load and the known effective area of the bellows. Our apparatus was constructed last winter from designs sent us by Vincent. When Vincent's complete paper was published[1] recently it was discovered that our procedure and experience with the apparatus were much the same as he described. Two exceptions, however, should be noted. First, in all but the first experiment we used an arrangement whereby the bellows could be filled under vacuum. Second, we could not detect bubbles escaping from the apparatus after breaking as Vincent observed with three organic liquids and we found no tendency for the maximum tension to increase on repeated breaks.

For our first measurements we chose aqueous solutions of calcium nitrate because they are known[2] to be stable to a high degree of supersaturation. The results of our measurements with these solutions and pure water are summarized in Table I.

In this table the number gives the chronological order in which the experiments were carried out. The fact that the first and last experiments yielded sensibly the same value for the tension of pure water and the fact that the results do not vary in the order in which they were obtained would seem to establish that no permanent distortion of the bellows took place. The recorded values for the tension are the means of at least four determinations of the force necessary to break the liquid in the bellows. These tension values were calculated as described by Vincent and might be uniformly in error by possibly ten percent because of an uncertainty in the effective cross section of the bellows.

The most significant fact revealed by these fragmentary data is that the maximum tension of solutions of calcium nitrate diminishes with increasing concentration. This would seem to indicate that the solute weakens rather than strengthens the bonds between the solvent molecules. It is of interest to note also that in a plot of the maximum tension values against values of the apparent molal volume of the solute at corresponding concentrations the plotted points fall closely on a straight line. Assuming this linear relationship and extrapolating to the hypothetical solution state at which the tension which the solution can withstand is zero, the value for the apparent molal volume at this hypothetical limit of the solution state is found to be 66 ml. This figure is of the order of magnitude of the volume of anhydrous calcium nitrate, measurements of which range from 67.5 ml to 73.4 ml. Finally, it may be pointed out that the maximum size of bubble which could withstand the observed maximum tension will increase with increasing concentration because in the case of this solution the surface tension increases while the tension and vapor pressure decrease with increasing concentration. This is noteworthy because Vincent calculated from his measurements that the radius of the maximum bubble for alcohol, ether, and mineral oil was approximately constant and of the order of 2.0×10^{-5} cm.

The authors are greatly indebted to Dr. Fred D. Ayres for invaluable help in building the apparatus and conducting the experiments.

[1] R. S. Vincent, Proc. Phys. Soc. **53**, 126 (1941).
[2] A. F. Scott and G. L. Bridger, J. Phys. Chem. **40**, 461 (1936).